

Alma Mater Studiorum – Università di Bologna

DOTTORATO DI RICERCA IN
Scienze Biomediche e Neuromotorie

Ciclo XXXV

Settore Concorsuale: 05/H1

Settore Scientifico Disciplinare: BIO/16

THE ROLE OF PHOSPHOLIPASES AS NOVEL POTENTIAL MODULATORS
OF AGGRESSIVENESS IN GLIOBLASTOMA

Presentata da: Maria Vittoria Marvi

Coordinatore Dottorato

Chiar.ma Prof.ssa Matilde Y. Follo

Supervisore

Chiar.mo Prof. Stefano Ratti

Esame finale anno 2022

Summary

Abstract	3
Introduction	4
1. <i>Brain tumors and gliomas</i>	4
Definition.....	4
World Health Organization (WHO) Classification ^{5,6} of Adult Primary Central Nervous System (CNS) Tumors.....	4
Classification of gliomas.....	6
Adult-type diffuse gliomas.....	7
Epidemiology.....	9
Clinical manifestations.....	9
Diagnosis.....	10
Prognosis, treatment and follow-up.....	13
2. <i>Phosphoinositides and Phospholipases</i>	15
Phosphoinositides.....	15
Structure and Activation of Phospholipases Implicated in Cancer.....	16
PLCs involvement in cancer.....	18
Role of PLCs in the nervous system.....	19
PLCs involvement in brain disorders.....	20
Aims	23
Notes	23
Materials and Methods	24
<i>In silico data</i>	24
<i>Collection of glioblastoma tumor samples for a retrospective study and collection of diffuse glioma tumor samples for a prospective study</i>	24
<i>DNA Mutation Analysis</i>	24
<i>DNA Methylation Analysis</i>	25
<i>Cell Cultures</i>	25
<i>Lentiviral Transduction for Immortalized cell lines and Human Astrocytes</i>	26
<i>TransIT Transfection for Glioma Stem cells</i>	26
<i>RNA extraction, reverse transcription, and real-time PCR for Immortalized Cell Lines and HA</i>	27
<i>RNA extraction, RNA sequencing and Differential Gene Analysis for GSCs</i>	27
<i>Protein extraction and western blot</i>	28
<i>Immunocytochemistry</i>	29
<i>Transwell migration and invasion assays</i>	29
<i>Wound Healing assay</i>	30
<i>Statistical analysis</i>	30
Results	31
1. <i>Histopathological and molecular characterization of Glioma samples</i>	31

Retrospective study and analysis of 50 Glioblastoma patients' samples.....	31
Prospective study and analysis of 23 Glioma patients' samples.....	32
2. <i>Study of the impact of PLCβ1 in Glioblastoma</i>	33
Glioblastoma is characterized by reduced PLC β 1 gene expression compared to both low-grade gliomas and healthy patients	33
PLC β 1 low expression is associated to a greater tendency to relapse.....	36
PLC β 1 silencing leads to an increase in the expression of mesenchymal markers and matrix metalloproteinases.....	37
Migration, Invasion and Proliferation abilities are increased in PLC β 1-silenced cells	40
PLC β 1 silencing enhances the activation of survival pathways.....	43
3. <i>Study of the impact of PLCγ1 in Glioblastoma</i>	46
PLC γ 1 gene expression correlates with the pathological grade of gliomas	46
Glioblastoma patients are characterized by higher PLC γ 1 gene expression compared to healthy individuals	46
Patients with mutated IDH1 have lower PLC γ 1 expression than patients with IDH1 WT	47
PLC γ 1 silencing leads to decreased cell migration and invasion in U87-MG.....	48
PLC γ 1 overexpression leads to increased cell migration and invasion in U87-MG	49
PLC γ 1 downregulation in GSCs affects the expression of some transcripts implicated in the mechanisms of tumor aggressiveness.....	50
Discussion	54
Conclusions	60
References	61

Abstract

Glioblastoma is the most malignant brain tumor in adults. The standard care of treatment is tumor resection, radiotherapy, and chemotherapy. Despite these invasive therapeutic approaches, glioblastoma prognosis remains unchanged. Therefore, a better understanding of the molecular mechanisms driving tumor transformation is needed to uncover novel therapeutic strategies. Several studies have shown the significance of lipid signaling and phospholipases (PLCs) in the regulation of different mechanisms in the central nervous system as well as in glioblastoma pathogenesis. This work suggests a potential role of PLC β 1 in the maintenance of a less aggressive phenotype of the tumor. Indeed, it was demonstrated that PLC β 1 gene was relatively less expressed in glioblastoma patients compared to their healthy/low-grade counterparts. Moreover, PLC β 1 silencing, in both immortalized and primary cell lines, led to increased cell migration, invasion, proliferation, cell survival and induced the upregulation of mesenchymal markers and metalloproteinases. Moreover, PLC γ 1, another abundant PLC isoform in the brain, has been identified as a key element for the aggressiveness of glioblastoma. Data collected on patients' biopsies and engineered cell models, suggested a strong correlation between PLC γ 1 expression level and the acquisition of a more aggressive tumor phenotype. Finally, this trend was further probed using patient-derived glioblastoma stem cells (GSCs), which are a specific tumor population that drives aggressiveness, resistance, and recurrence in glioblastoma. GSCs analysis on the transcriptomic profiles confirmed that PLC γ 1 downregulation modulated positively the activation of pathways that negatively regulate cell motility and migration and led to a decreased expression of genes involved in cancer development and progression. Taken together, these data highlight the importance of further investigating phospholipases as potential prognostic biomarkers and targets in the development of new therapeutic strategies for glioblastoma.

Introduction

1. Brain tumors and gliomas

Definition

A brain tumor, or intracranial tumor, is an abnormal mass of tissue in which the cells grow without control, escaping the mechanisms that drive normal cells. More than 150 different brain tumors have been documented, but the two main groups of them are termed *primary* and *metastatic*¹.

Primary brain tumors include lesions that originate from brain tissues or from the brain's immediate surroundings. They are categorized as *glial tumors, or gliomas* (composed of glial cells, which surround, insulate, and supply nutrients to neurons¹) or *non-glial* tumors (which arise from different structures of the brain, including nerves, blood vessels and glands) and *benign* or *malignant*. Metastatic brain tumors include the ones that arise elsewhere in the body and migrate to the brain, usually through the bloodstream. Among the primary intracranial tumors, gliomas represent the most common ones in adults². Based on the specific subtype of the originating glial cells, we can define different types of gliomas as astrocytoma, oligodendroglioma and ependymoma. Each of them is further differentiated in other subtypes by grade, molecular pattern, and other clinically useful features as location or morphology³. Among astrocytomas, glioblastoma, historically known as Glioblastoma Multiforme (GBM), is a grade 4 brain tumor characterized by a heterogeneous population of cells that are widely genetically unstable, highly infiltrative, angiogenic, and resistant to the current therapeutic approaches⁴. The term “multiforme” is no longer used, according to the most recent classification⁵, for the integrated diagnosis of glioblastoma, as all gliomas are characterized by heterogeneous and unstable genetic profile, but it can still be used in common language for historical usage reasons. Traditionally, glioblastoma and grade 4 astrocytoma with mutation in Isocitrate Dehydrogenase (IDH), lesions which will be described in detail below, were considered the same kind of lesion, identified as glioblastoma. These two entities were divided in primary (or “de novo”) glioblastoma (IDH-wild type) and secondary glioblastoma (IDH-mutant) and mutations in Isocitrate Dehydrogenase (IDH) were considered relevant to clinically identify and distinguish these two categories. In particular, primary glioblastoma originated without the evidence of another pre-existing lower grade lesion, and it was characterized by poorer prognosis, while secondary glioblastoma gradually evolved from a less aggressive lesion to a highly infiltrative grade 4 tumor. This latter was characterized by better prognosis and by the possibility of early diagnosis. In the recent years, the molecular, clinical, and biological differences between these two entities have been investigated more in depth, as demonstrated by the 2021 WHO classification⁵, underlying important features that have diagnostic and prognostic impact.

World Health Organization (WHO) Classification^{5,6} of Adult Primary Central Nervous System (CNS) Tumors

The World Health Organization (WHO) approach incorporates and interrelates morphology, cytogenetics, molecular genetics, and immunologic characteristics to construct a tumor classification that is universally

applicable and prognostically valid. The classification of brain tumors is a continuously evolving process with newly recognized tumors added with each revision (the first edition dates to 1979). The most recent WHO classification (fifth edition) of Adult Primary Central Nervous System (CNS) tumors, published in 2021⁵ (WHO CNS5), lists more than 120 types of brain tumors, and builds on the updated fourth edition of 2016⁶ and on the recommendations of the Consortium to Inform Molecular and Practical Approaches to CNS Tumor Taxonomy (cIMPACT-NOW)³. In the past, the classification of CNS tumors was based on the recognition of morphological patterns and on the immunohistochemical identification of differentiation antigens, but with the development of molecular methodologies, particularly in genomics, transcriptomics and proteomics fields, a revolution has occurred in the classification of brain tumors. Indeed, traditionally, tumor's grade was exclusively related to its histological features, and it was classified as follows:

- *WHO grade I*: lesion with low proliferative potential, frequently discrete nature, and the possibility of cure following surgical resection.
- *WHO grade II*: infiltrating lesion with low mitotic activity but characterized by greater recurrence. This type of lesion could progress to higher grades of malignancy.
- *WHO grade III*: lesion with histologic evidence of malignancy, including nuclear atypia and increased mitotic activity. This lesion was characterized by anaplastic histology and infiltrative capacity and it was usually treated with aggressive adjuvant therapy.
- *WHO grade IV*: lesion that was mitotically active, prone to necrosis, and associated with a rapid progression and fatal outcome. This type of lesion was usually treated with aggressive adjuvant therapy.

Today, although morphology and histology still retain an important role for diagnostic and prognostic classifications, they are increasingly associated with the genetic characterization of neoplasms and with the research of molecular biomarkers.

Consequently, the main WHO CNS5 changes concerned taxonomy and nomenclature⁵, that are strictly related to the molecular patterns of the tumors. Therefore, it incorporated numerous molecular changes with clinicopathologic utility that are important for a more accurate classification of CNS neoplasms. As a matter of fact, the new classification emphasized the tumor's molecular characterization and made some changes:

- Tumor names have been simplified, and only location, age, or genetic characteristics with clinical utility have been used.
- The use of Arabic numbers was favored instead of the Roman ones in tumor's grading,
- CNS tumors are now graded within their types. Each independent neoplasm has a different range of grading (from 1 to 4) based on specific features, and not every tumor has all four grades.
- Some grades, particularly 1 and 4, must be used only for those lesions that are totally curable, with great life expectancy after surgery, or incurable, leading to death in a short period of time, respectively.
- The molecular phenotype and genetic mutations have acquired diagnostic and prognostic relevance. These modifications can, consequently, characterize a particular tumor subtype. The

best example is about the Isocitrate Dehydrogenase mutations. With the new classification, an astrocytoma grade 4 which is IDH-wildtype is automatically considered as glioblastoma, while an astrocytoma grade 4 IDH-mutant is no more considered as glioblastoma IDH-mutant, as this entity does not exist anymore.

Classification of gliomas

According to WHO CNS5 and to the Central Brain Tumor Registry of the United State (CBTRUS) Statistical Report⁷, gliomas represent the most common primary malignant brain neoplasms in the clinical practice of neuro-oncology and neurosurgery (*Fig. 1*).

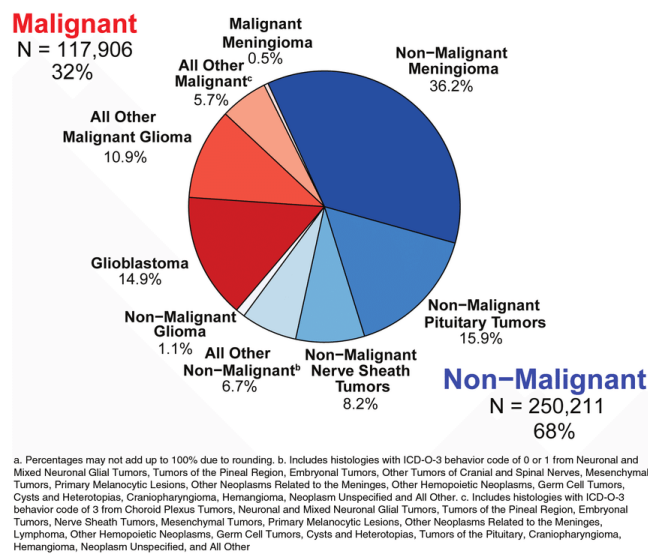


Figure 1: Distribution of Primary Brain and Other CNS Tumors by Behavior (N=368,117), CBTRUS Statistical Report: NPCR and SEER, 2009-2013⁷

Gliomas are primarily classified based on non-routine features, with a strong clinical relevance:

- **Cellular origin:** gliomas are firstly classified according to the type of glial cells which undergo neoplastic transformation. Therefore, gliomas are classified as astrocytoma (from astrocytes), oligodendroglioma (from oligodendrocytes), and ependymoma (from ependymocytes). Depending on the biological behavior and aggressiveness, some gliomas are histologically and cytologically completely undifferentiated. Moreover, they can also have a heterogeneous cellularity, and thus are classified as specific entities (i.e., oligoastrocytoma).
- **Localization and extension:** The macroscopic features of the tumor are usually defined by neuroradiologists and neurosurgeons through neuroimaging techniques as cranial Magnetic Resonance Imaging (MRI) and Positron Emission Tomography (PET). Concerning what was just mentioned, the most frequent type of glioma is the diffuse one. It is characterized by macroscopic growth and evidence of infiltration. Alternatively, a strictly localized lesion, without evident spreading or infiltration is considered as circumscribed glioma.

• **Grade:** gliomas can be divided in two categories⁸:

- high-grade gliomas (HGGs): generally characterized by poorer prognosis and high tendency to infiltrate and spread macroscopically. They are usually associated to grade 3 or 4.
- low-grade gliomas (LGGs): characterized by better prognosis and low rate of growth and extent. They are usually associated to grade 1 or 2⁸.

• **Patient's age at tumor onset:** WHO CNS5 divides diffuse gliomas in adult-type diffuse gliomas, pediatric-type diffuse low-grade gliomas and pediatric-type diffuse high-grade gliomas, according to several biological and prognostic differences which have recently been reported by several studies⁹.

This thesis will focus particularly on the description and analysis of adult-type diffuse gliomas.

Adult-type diffuse gliomas

Adult-type diffuse gliomas are the most represented primary malignant brain tumors and, according to the WHO CNS5, they can be divided into 3 tumor types⁵:

1. Astrocytoma, *IDH-mutant*;
2. Oligodendroglioma, *IDH-mutant* and *1p/19q-codeleted*
3. Glioblastoma, *IDH-wildtype*

According to the 2016 WHO classification⁶, IDH-mutant diffuse astrocytic tumors were assigned to three different tumor types (diffuse astrocytoma, anaplastic astrocytoma, and glioblastoma) depending on histological parameters. Following the last classification, all IDH-mutant diffuse astrocytic tumors are considered as astrocytoma, IDH-mutant with grade 2, 3, or 4. Instead, it is important to consider some genetic parameters to define a glioblastoma (IDH-wildtype, implicitly graded 4)^{10,11}. Consequentially, mutation of two different isoforms of isocitrate dehydrogenase (IDH1 and IDH2), a molecule involved in histone and DNA methylation, contribute to define two different types of glial lesions with relevant epidemiological, diagnostic, and prognostic differences: glioblastoma, implicitly IDH-wildtype and grade 4, and astrocytoma IDH-mutant, which can be graded 2, 3 or 4. IDH mutations, which occur at a single aminoacidic residue of the IDH active site, result in the loss of the enzyme's ability to catalyze conversion of isocitrate to α -ketoglutarate (α -KG). This affects DNA and histone methylation, and consequently, the chromosomal function¹². The most frequent mutation for IDH-1 is the R132H while for IDH-2 is R172H¹².

Consequentially, molecular profiles (*Fig. 2 and 3*) of adult-type diffuse gliomas have progressively acquired importance both from a pathophysiological point of view, and also in defining prognostic aspects, survival, and diagnosis. Indeed, the latest WHO CNS5⁵ defined the molecular characteristics of the tumors as the main drivers of their differentiation.

Astrocytoma IDH-mutant is an evolving tumor that is able to pass from a grade 2 lesion, mildly infiltrative and well differentiated, to a grade 3 or 4 lesion, characterized by higher aggressiveness and poor prognosis. Beyond IDH mutations, it is usually related to the suppression of ATRX gene, which regulates the expression of a chromatin remodeling protein whose main function is the deposition of the histone variant H3.3¹³. ATRX mutations correlate with alternative lengthening of telomeres (ALT) development¹³. Grade 4 astrocytoma is also related to Cyclin Dependent Kinase Inhibitor 2A (CDKN2A) and 2B (CDKN2B) mutations¹⁴. The homozygous deletions in CDKN2A and/or CDKN2B, are identified as a histology-independent adverse prognostic marker in gliomas and they are correlated to uncontrolled cell growth and tumor progression¹⁴.

Glioblastoma (IDH-wildtype) is a completely different lesion, as it cannot be diagnosed in a lower grade form, due to its rapid and infiltrative growth and to its excessive biological aggressiveness¹⁵. This behavior is reflected in glioblastoma's molecular phenotype, which is extremely complex. The most recurrent mutations, which became diagnostic parameters in WHO CNS5, are:

- Telomerase Reverse Transcriptase (TERT) promoter mutation¹⁶, which encodes for the catalytic subunit of telomerase;
- Epidermal Growth Factor Receptor (EGFR) amplification, a tyrosine kinase receptor involved in mitogen-activated protein kinase (MAPK) and Phosphoinositide 3-kinases (PI3K) survival pathways¹⁷;
- gain in chromosome 7p, which correlates with loss in chromosome 10q (+7/-10)¹⁸
- mutations of the tumor-suppressor gene p53 (TP53), which affects a wide variety of cellular responses, including cell apoptosis, maintenance of genomic stability, inhibition of angiogenesis, and regulation of cell metabolism and tumor microenvironment¹⁹.

Oligodendoglioma is a glial tumor originating from oligodendrocytes²⁰. It is specifically defined by 1p/19q codeletion, an unbalanced chromosomal translocation²¹. This lesion is usually characterized by less aggressivity and frequency compared to astrocytomas.

Tumor Type	Genes/Molecular Profiles Characteristically Altered ^a
Astrocytoma, IDH-mutant	IDH1, IDH2, ATRX, TP53, CDKN2A/B
Oligodendroglioma, IDH-mutant, and 1p/19q-codeleted	IDH1, IDH2, 1p/19q, TERT promoter, CIC, FUBP1, NOTCH1
Glioblastoma, IDH-wildtype	IDH-wildtype, TERT promoter, chromosomes 7/10, EGFR

Figure 2: Gene and molecular profiles altered in adult-type diffuse gliomas⁵

CNS WHO Grades of Selected Types	
Astrocytoma, IDH-mutant	2, 3, 4
Oligodendroglioma, IDH-mutant, and 1p/19q-codeleted	2, 3
Glioblastoma, IDH-wildtype	4

Figure 3: CNS WHO grades of adult-types diffuse gliomas⁵

Epidemiology

The average annual age-adjusted incidence rate of glioblastoma and grade 4 astrocytoma IDH-mutant is very mutable, ranging from 0.59 to 3.69 per 100,000 people and it is characterized by a median age of 64 years, being uncommon in children²². However, their incidence tends to be higher for glioblastoma (mean age of 55), than for grade 4 astrocytoma IDH-mutant (mean age of 40 years) and it is 1.6 times higher in males compared to females²³. Moreover, the incidence is 2.0 times higher in Caucasians compared to Africans and Afro-Americans, with lower incidence in Asians and American Indians²⁴. These tumors are most frequently located in the supratentorial region (frontal, temporal parietal, and occipital lobes), with the highest incidence in the frontal lobe or multiple lobes, followed by the temporal and parietal ones²⁵. On the other hand, oligodendrogliomas are less common, with an incidence of 0.2 per 100,000 people. These tumors comprise approximately 5% of all primary CNS tumors and they have a slight male predominance, reported as a possible variation of 25%-60% depending on the age¹.

Clinical manifestations

Although there are no standard clinical features to characterize gliomas, as all the signs and symptoms are nonspecifically related to different brain areas compression and intracranial hypertension, there are some common presenting symptoms which occur more frequently in glioma's patients²⁶:

- Focal neurological impairments that depend on the location and the growth rate of the tumor. Usually, the most represented ones are motor deficits, sensitive alterations, language impairments and cognitive disorders.
- Global neurological deterioration.
- Headaches, cervicalgia, or other types of localized head and neck pain, which are identified in 40–50% of patients.
- Visual impairments.
- Amnesia and concentration deficits, that are usually characterized by a slower gradual development.

- Focal seizures which are usually associated to low-grade tumors²⁷.

However, it should be remarked that patients affected by brain tumors may be asymptomatic, and that symptoms of high-grade gliomas typically progress over days to weeks, whereas symptoms of low-grade gliomas may progress over months to years. Absence of symptoms is more common with low-grade tumors and small lesions without surrounding edema.

Diagnosis

According to the 2021 WHO classification, cIMPACT-NOW 2019 recommendations and 2020 EANO (European Association of Neuro-Oncology) guidelines²⁸, adult-type diffuse gliomas need to be managed following a specific algorithm (*Fig. 6*). For this reason, recommendations for the diagnosis, treatment, and follow-up of adult patients with diffuse gliomas were recently provided.

The first choice of diagnostic imaging modality is the **Magnetic Resonance Imaging (MRI)** without/with the administration of a gadolinium-based contrast agent²⁸. MRI provides mostly morphological and functional information such as tumor localization, vascular permeability, cell density, and perfusion. It can also help to predict the tumor's nature, based on its radiological features²⁹. Glioblastoma and grade 4 astrocytoma IDH-mutant are mostly characterized by lesions with irregular contrasting, often with a ring-like aspect due to evident peripheral contrast enhancement (high vascular peripheral proliferation) and central necrosis (*Fig. 4*).

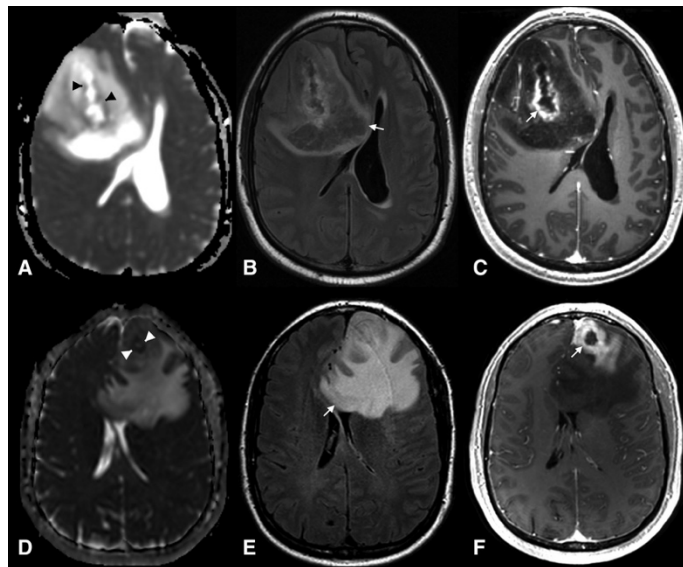


Figure 4: Comparison between astrocytoma IDH-mutant and glioblastoma IDH wild-type. Image extrapolated from the 2016 World Health Organization Classification of Tumors of the Central Nervous System³⁰. On the top row, brain MRI from a 37-year-old male with a right frontal astrocytoma IDH1-mutant, associated with ATRX and TP53 gene mutations, probably evolved from a lower grade astrocytoma. On the bottom row, brain MRI from a 48-year-old male patient diagnosed with a left frontal glioblastoma IDH wild-type accompanied with EGFR gene alteration. IDH mutant gliomas tend to have more defined borders compared with their wild-type counterpart.

On the other hand, oligodendrogliomas commonly appear as lesions involving the cortex or the subcortical white matter, with low attenuation on computed tomography (CT), hypointense compared to grey matter on T1 and hyperintense compared to grey matter on T2-weighted MRI images. Several imaging features have long been considered characteristic, although not specific, to oligodendrogliomas: relatively sharply delineated margins, calcification, and internal cysts³¹ (Fig.5).

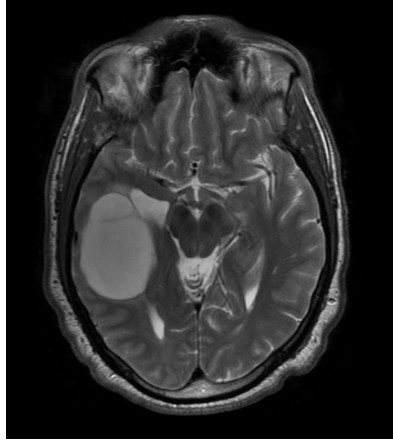


Figure 5: MRI/T2 image of a patient affected by oligodendroglioma. Image from <https://it.wikipedia.org/wiki/Oligodendroglioma>.

Other useful techniques for diagnosis, to be associated with MRI, are:

- **Diffusion-Tensor Imaging (DTI), functional MRI (fMRI) and Magnetic Resonance Spectroscopy (MRS)**^{32,33}. DTI and fMRI are mainly used to better localize the lesion and to minimize postsurgical neuro-deficits^{33,34}. MRS facilitates non-invasive determination of metabolic changes in brain tissue and may identify regions of tumor's infiltration and areas at high risk of recurrence³³.
- **PET (positron emission tomography) and Angiography (AGF)**: these are in-depth examinations useful to better define the characteristics of the lesion (metabolic changes, vascularization etc.), as well as to provide other clinical and prognostic features^{35,36}.
- **Tissue acquisition**: Treatment decisions in patients with gliomas are made based on tissue diagnosis, including the assessment of molecular markers relevant for diagnosis. Therefore, upfront surgery is commonly performed with both diagnostic and therapeutic intent²⁸. When microsurgical resection is not safely feasible (because of the tumor localization or the impaired clinical condition of the patient), a stereotactic biopsy is generally recommended. It is associated with low risk of morbidity and a high level of diagnostic accuracy³⁷. The tissue samples obtained with these techniques allow to highlight the molecular profile of the tumor. For example, it is possible to individuate IDH mutations, 1p/19q codeletion as well as O-6-methylguanine-DNA methyltransferase (MGMT) promoter methylation^{37,38}, which are homogeneously present within tumors and allow their classification. However, in some circumstances open biopsy approach is preferred to ensure that sufficient tissue is obtained for any molecular studies that might be required to guide clinical decision-making. The intraoperative assessment of cytological specimens or

frozen sections, ensures that sufficient tumor tissue is obtained to establish a diagnosis. Tumor tissue is formalin-fixed and embedded in paraffin for histological and immunohistochemical staining as well as for genetic and cytogenetic studies³⁷. Accordingly, glioma classification integrates histological characteristics and grading as well as the analyses of the main molecular markers, previously described, that characterize diffuse gliomas (Fig.6).

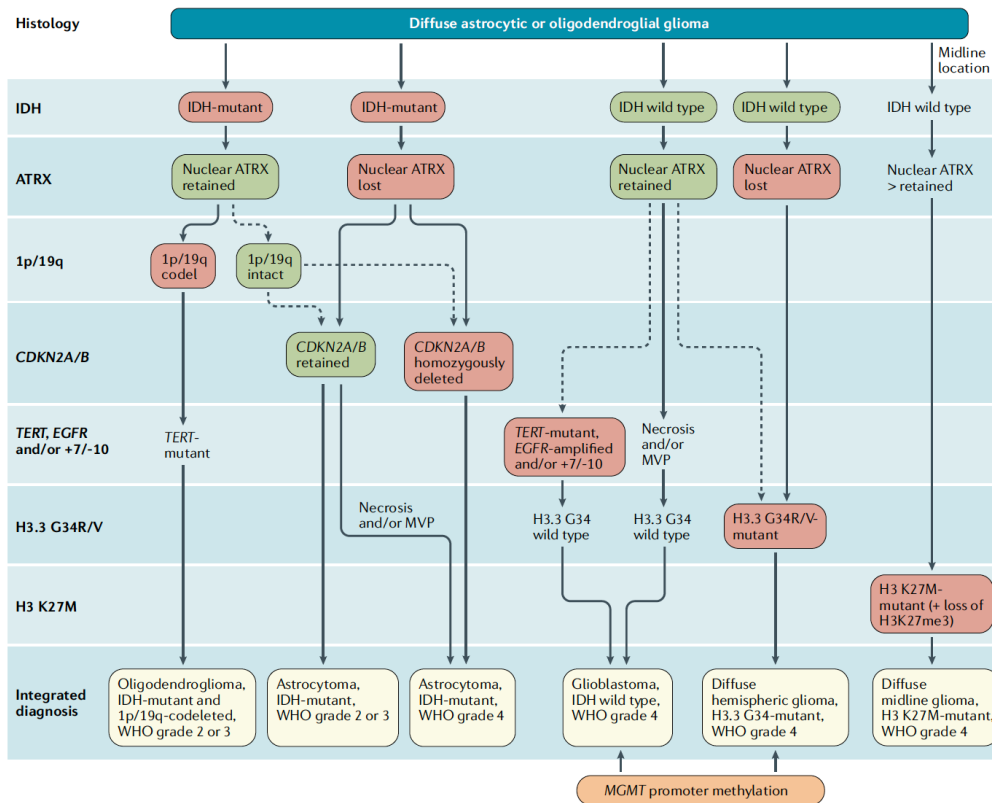


Figure 6: Diagnostic algorithm for the integrated classification of the major diffuse gliomas in adults²⁸.

Beyond the molecular profile, biopsy’s analysis, performed under a microscope, permits also to characterize the morphological tumor cells’ growth pattern.

Indeed, glioblastoma diagnostic histopathologic features are distinguished from the lower grade tumors’ ones because include phenomena of necrosis and microvascular hyperplasia³⁹. Necrotic foci are typically surrounded by “pseudo palisading” cells (pseudo palisading necrosis) and hyperplasia of adjacent blood vessels (vascular proliferation) in response to the hypoxic conditions³⁹ (Fig.7, left panel).

On the contrary, the hallmark morphologic features of oligodendroglioma, are the uniformly round nuclei with surrounding cytoplasmic clearing (“perinuclear halos”). This morphology often correlates with the combined deletion of chromosomal arms 1p/19q and predicts a favorable response to therapy⁴⁰ (Fig.7, right panel).

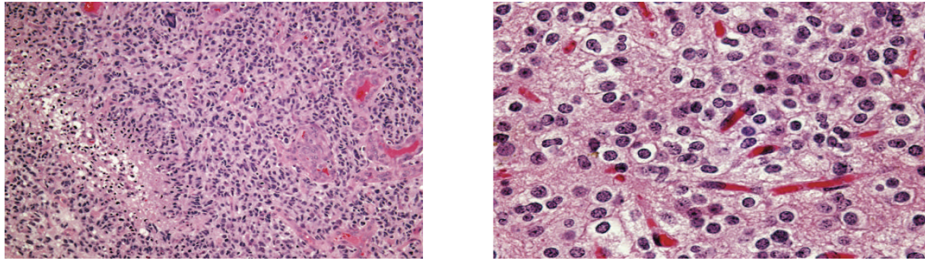


Figure 7: Left Panel: Histological features of Glioblastoma. Right Panel: Histological features of Oligodendroglioma. Images from Youmans and Winn Neurological Surgery 2017.

Prognosis, treatment and follow-up

Prognosis

Younger age and better performance status at the time of diagnosis are the major therapy-independent prognostic factors associated with favorable outcomes in adults affected by gliomas⁴¹. Moreover, molecular genetic factors, as 1p/19q codeletion and IDH mutation status, had a strong prognostic value in the classification of gliomas in the past but, since 2016, have become disease-defining features and are therefore no longer prognostic factors within a specific subtype. Therefore, MGMT promoter methylation status has become the most important prognostic factor in an era in which most adults with glioma are treated with alkylating agent-based chemotherapy⁴², especially *temozolomide* (TMZ). Indeed, MGMT gene is located at chromosome 10q26 and codes for a DNA repair enzyme that, if active, can counteract the effects of alkylating chemotherapy⁴³. Several studies demonstrated that patients with methylated MGMT promoter have a particularly high survival benefit from *temozolomide* therapy⁴⁴ and, as a result, patients with high MGMT expression are characterized by poorer prognosis compared to those with low expression⁴⁵. Therefore, MGMT promoter methylation status is an essential predictor of clinical responses to chemoradiation and overall survival, with patients methylated at the MGMT promoter exhibiting significantly better outcome.

Treatment

As for the therapeutic schedule, the approach for all the adult-type diffuse gliomas is similar and it is firstly based on surgical resection. The therapeutic goal of surgery is to remove as much tumor tissue as safely feasible using microsurgical techniques, without compromising neurological function²⁸. Then, the best choice is radiotherapy, that is fundamental to improve local control of the tumor without inducing neurotoxicity²⁸ and it usually starts within 3–5 weeks after surgery⁴⁶. Radiotherapy could be administered with or without concomitant chemotherapy, depending on the type of the tumor, followed by maintenance chemotherapy or polychemotherapy alone⁴⁷. Unfortunately, tumor recurrence is very common and almost all the patients relapse after a variable period⁴⁸. According to patient status and the secondary tumor's characteristics (90% relapse in the site of the primary tumor) specific therapies or palliative cares can be undertaken.

Accordingly, the pharmacological recommendations for standard first line concomitant and adjuvant therapy should be:

- Glioblastoma and grade 4 astrocytoma IDH-mutant, MGMT-methylated, age ≤ 70 years: it is recommended the use of concurrent TMZ in combination with radiotherapy followed by monthly adjuvant TMZ⁴⁹. A dual regimen of TMZ and *lomustine*, another chemotherapy drug with a non-alkylating mechanism of action^{44,50}, in combination with radiotherapy, is an alternative option in young MGMT-methylated patients. This combination therapy demonstrated an average increase of 10 months in patients' survival⁴⁴.
- Glioblastoma and grade 4 astrocytoma IDH-mutant MGMT-unmethylated or MGMT unknown, age ≤ 70 years: These patients are characterized by poorer prognosis, but the therapeutic recommendation is the same as for MGMT-methylated patients. Other molecules are being studied, as *Bevacizumab* and *Irinotecan*, which actually show increase in progression-free survival⁵¹, or PCV polychemotherapy (*Procarbazine*, *Lomustine*, *Vincristine*).
- Grade 3 oligodendroglioma: the combination radiotherapy-TMZ still remains the best options, but recently, two randomized trials showed that the addition of PCV, before/after radiotherapy, increased patients' overall survival, and thus should be considered as a first line treatment after surgery⁵².

TMZ (75 mg / m² / day) is usually administered for the duration of radiotherapy (60 Gy / 30 fractions) for a maximum of 7 weeks followed by six cycles of adjuvant TMZ (150- 200 mg / m² x 5 days, every 28 days). It has been shown that prolonged TMZ treatment (longer than six cycles) in stable patients does not increase survival but, on the contrary, exposes patients to different ongoing side effects⁵³. In addition, due to hematologic and nonhematologic TMZ toxicity, routine blood test should be taken weekly, and liver biochemical tests are recommended to be performed at baseline, midway through the first cycle, prior to each subsequent cycle, and approximately two to four weeks after the last dose of temozolomide⁵⁴.

Follow-up

Although there are no formal clinical trials that define the optimal frequency for follow-up after treatment, EANO guidelines recommend an initial interval between MRI scans of 2–6 months, after the completion of therapy. Longer intervals might be appropriate in cases of durable disease control and more benign tumors²⁸. It is also necessary to consider the complete disease trajectory, especially in patients with slow-growing untreated lesions⁵⁵. In the event of suspected disease progression, short-term control MRI within 4-8 weeks might be reasonable to confirm progression.

Unfortunately, as mentioned before, many patients often experience tumor recurrence, and based on the biological characteristics of the relapsed neoplasm and the clinical status of the patient, two possible options can be chosen:

- Second line salvage therapies: reoperation, re-irradiation, chemotherapy or, especially for glioblastoma patients, experimental treatments with *Bevacizumab*, *Regorafenib*, *Nivolumab*. This approach should be considered for those patients with good performance status and good first line response.
- Palliative care: suggested for those patients with poor clinical conditions, as usually the risks of pursuing subsequent treatment outweigh the benefits.

Survival rate

As a matter of fact, adult-type diffuse gliomas have a different survival rate:

- Treated patients with grade 3 oligodendroglioma, have around 30%-38% probability of survival at 5 years from diagnosis, with an average life expectancy of 3,5 years.
- Glioblastoma patients have an average survival of 12 to 15 months according to most recent studies. However some recent trials demonstrated a slight increase in life expectancy to 14-17 months following specific approaches, and an increase to 21 months according to a 2017 study which added tumor-treating electric fields to maintenance TMZ¹⁴.
- Grade 4 astrocytoma IDH-mutant patients, have a general better prognosis, with an overall survival of 24-31 months after the treatment.

However, it is important to underline that the expected survival of all glioma patients can vary depending on the therapeutic protocols, patient's age, MGMT methylation, IDH status, and all the other specific genetic alterations shown previously.

2. Phosphoinositides and Phospholipases

Phosphoinositides

All the membranes of eukaryotic cells contain specific molecules called Phosphoinositides (PIs), which are characterized by a hydrophilic inositol ring bound to a hydrophobic tail of glycerol and two fatty acid chains⁵⁶ (Fig.8).

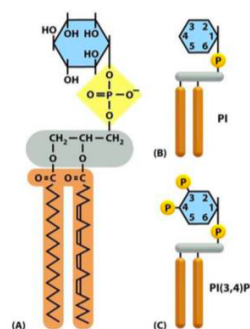


Figure 8: Phosphoinositides structure (Molecular Biology of the cell, Garland Science, 2008)

PIs are organic molecules with protein interaction and membrane integrity regulation functions and part of human tissue cells' biological functioning, including cell migration, regulation of gene expression, chromatin remodeling, membrane trafficking and differentiation, depends on these interactions and activities⁵⁷. As a result, it has been shown that phosphoinositide signaling is involved in different pathologies and disorders including cancer, epilepsy, neurodegenerative diseases, myelodysplastic syndromes, and others^{58,59}. Different enzymes are involved in the cleavage and processing of phosphoinositides, but the most studied ones are the phosphoinositide-specific phospholipases C (PI-PLCs or PLCs), present in mammals in 13 different isoforms split between six subfamilies, PLC β (1,4), PLC δ (1,2 and 4), PLC γ (1,2), PLC ϵ , PLC ζ and the recently discovered PLC η (1,2) isoform⁶⁰.

PLCs are responsible for interacting and hydrolyzing phosphatidylinositol 4,5-bisphosphate (PtdIns(4,5)P₂) to generate the two essential intracellular second messengers diacylglycerol (DAG) and inositol 1,4,5 trisphosphate (InsP₃)⁶⁰, which lead to the activation of protein kinase C (PKCs) and the release of calcium ions (Ca²⁺) from intracellular stores, respectively^{56,61} (Fig.9). This event represents a key point in the cellular signaling in various cancer types. For instance, PKCs are reported to be involved in cell proliferation, differentiation, migration and growth⁶² while Ca²⁺ release is critical in the regulation of cancer cell motility, division and death⁶³. In the same time, the decrease of PtdIns(4,5)P₂ concentration, via its hydrolysis by PLCs, has been reported to yield several essential signaling cascades involved in cancer, especially cell migration⁶⁴.

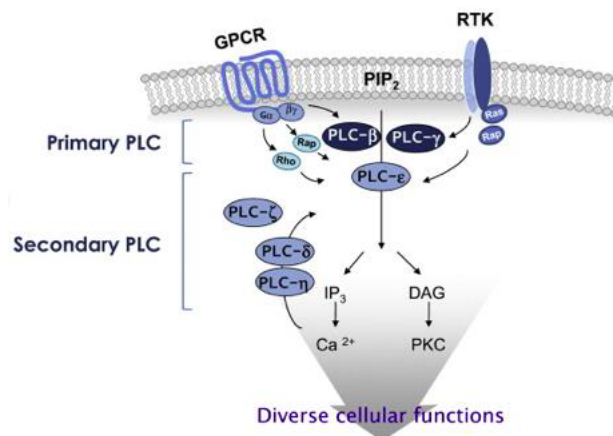


Figure 9: Signal transduction inositolide-dependent⁶⁵

Structure and Activation of Phospholipases Implicated in Cancer

So far, all reported PLC isoforms bear conserved domains such as the X and Y catalytic domains, the PH domain, the EF-hand (EF-H) domain and the PKC homology (C2) domain. Each of these regions have some functional roles⁶⁵ (Fig. 10):

- PH domain binds to PtdIns(4,5)P₂ and it is essential for the membrane linkage,

- EF-H play scaffolding roles to support guanosine triphosphate (GTP) hydrolysis upon G-protein coupled receptor (GPCR) binding,
- X and Y are catalytic domains in the form of a distorted Triose Phosphate Isomerase (TIM) barrel with a highly disordered, charged, and flexible intervening linker region,
- C2 participates in intra- and inter-molecular signaling processes.

As shown in *Fig. 10*, regulatory domains such as the C2 domain, the EF-H motif, RAS associating (RA) domain and the PH one, are uniquely distributed in PLC subtypes and this may explain their distinct functions and/or tissue distribution⁶⁵. PLCs are distributed across several cellular compartments depending on the localization of their substrate. For instance, PIs have been shown to localize within the nucleus together with their metabolic enzymes which help to generate a separate PI metabolism that is distinct from the cytoplasmic one^{56,66}.

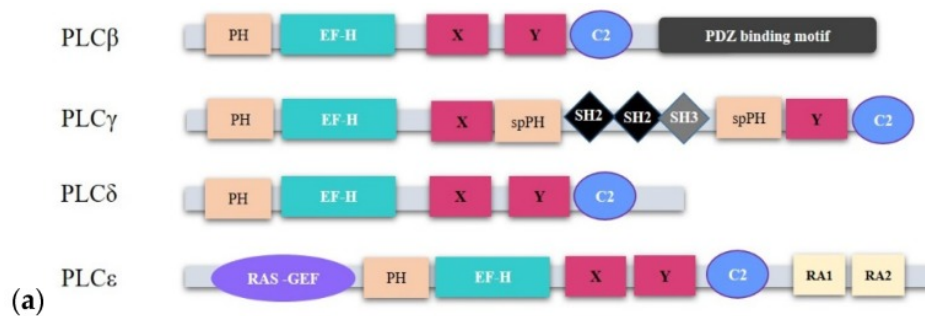


Figure 10: Structural organization of PLCs. PLC isoforms possess structurally conserved domains such as the EF, X and Y catalytic core, and the C2 domains⁶⁰.

PLCs can be activated by either tyrosine kinase receptors (TRK-R), B-cell receptors (BCR), Fc receptors, integrin adhesion proteins, or G protein-coupled receptors (GPCRs), through the binding of many ligands including neurotransmitters, histamine, hormones, and growth factors (GFs), to promote signaling and calcium mobilization⁶⁷. It has been shown that PLC β and PLC γ isoenzymes are primarily activated by extracellular stimuli⁶⁰. On the contrary, secondary PLCs (mainly PLC δ and PLC η) might be enhanced by intracellular calcium mobilization that amplifies the PLCs activity (*Fig. 11*).

In particular, it has been shown that PLC β isoforms are generally activated by the G α_q - and G $\beta\gamma$ - subunits of heterotrimeric G proteins, while PLC γ isoforms (PLC γ_1 and PLC γ_2) act through the phosphorylation mediated by the binding of their SH2 domain to phosphorylated tyrosine residues of activated and non-activated receptor tyrosine kinases (RTKs)⁶⁰. Most of the tyrosine kinases involved in the activation of

PLC γ are members of the growth factor receptor superfamily (PDGF, FGF, HGF, EGF, IGF, VEGF) and sometimes PLC γ activation depends on PI3K⁶⁰.

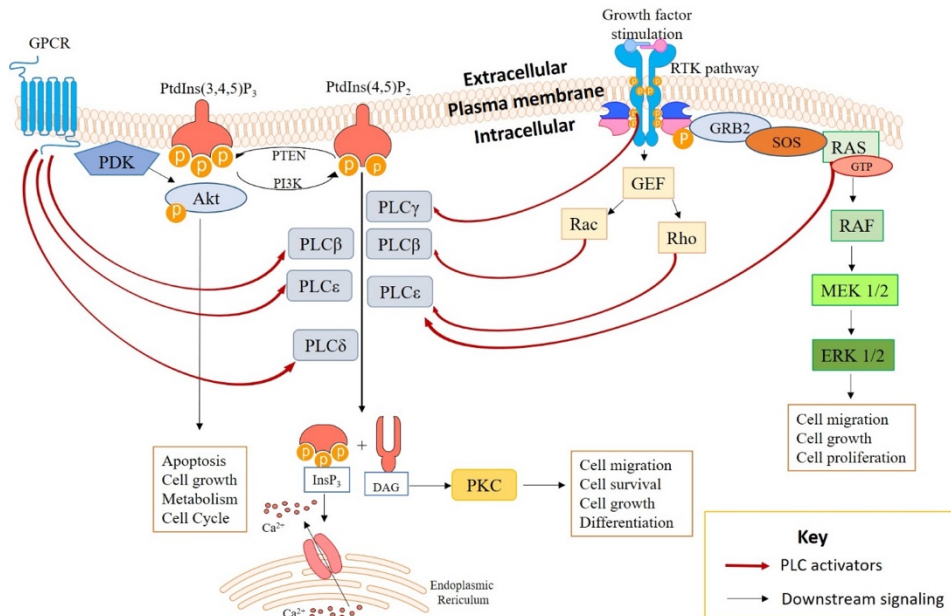


Figure 11: PLCs activation in cancer. PLCs are activated by different stimulations to promote the catalyzation of PtdIns(4,5)P₂ hydrolysis into InsP₃ and DAG, which subsequently induces the intracellular release of Ca²⁺ from the ER as well as PKC activation, respectively. Activation of PKC and Ca²⁺ release results in events that regulate cell migration, cell survival and differentiation in cancer. Activation of some PLCs are through by multiple mechanisms. These activation mechanisms may be cell type specific or stimuli dependent⁶⁰.

PLCs involvement in cancer

Since PLCs are significantly involved in mediating several critical cellular processes, deregulations in their functions and expression may be fatal to mammalian cells. Indeed, alterations in PLC activities have been shown in different human cancer types through *in vitro*, *in vivo* and clinical studies. For instance, PLC β 1 and PLC γ 1 have been reported to participate to the migratory or metastatic potential of different cancer types⁶⁰. It was demonstrated that PLC β 1, through the interaction with the Protein Tyrosine Phosphatase Receptor Type N2 (PTPRN2) protein, regulates cell migration in breast cancer cells by stimulating a decrease in plasma membrane levels of PtdIns(4,5)P₂, which is known to control actin dynamics and cell migration⁶⁸. Moreover, it was already evidenced PLC β 's involvement in hematopoietic malignancies⁶⁹ and the role of PLC β 1 as possible molecular marker able to define specific and personal therapeutic strategies in other tumor patients, as Myelodysplastic Syndromes (MDS) patients⁷⁰. On the other hand, alterations in PLC γ 's activities, and PLC γ 1's ones in particular, have been demonstrated in colon carcinoma, breast cancer, lymphocytic leukemia, angiosarcoma and Kaposi's sarcoma⁷¹⁻⁷³. As for the involvement of PLC γ 1

in breast cancer progression and metastasis⁷⁴, Sala et al. demonstrated that its knockdown resulted in a complete impairment of cell invasion, using U87-MG glioblastoma cells as control, due to their migration mechanism known to be PLC-dependent. Through this investigation it was shown a critical role of PLC γ 1 in the metastatic potential of cancer cells, indicating its inhibition as a potential therapeutic strategy for the treatment of metastasis dissemination⁷⁴. Moreover it was demonstrated the involvement of PLC δ in esophageal squamous cell carcinoma (ESCC)⁷⁵, and the involvement of PLC ϵ in gastric and colorectal cancers^{76,77}.

Role of PLCs in the nervous system

Up to now, PLCs aroused remarkable interest in neuroscientific fields and in the nervous system disorders. The most frequently characterized PLC isoforms in the brain are PLC β , with all its 4 isoforms, and PLC γ 1. Considering their distribution, the same isoforms can be found in several brain areas. On the other hand, two different isoforms can work in the same region, as it happens for PLC β 1 and PLC γ 1 in the hippocampus.

Several studies about gene expression showed that the highest expressed isoform of PLC in the brain is PLC β 1, at both cytoplasmic and nuclear level. It is significantly expressed in the hippocampus and cerebral cortex⁷⁸ and it is particularly predominant in cerebellar interneurons, telencephalic principal neurons and in somatodendritic neuronal elements⁷⁹. PLC β 4 is mostly expressed in cerebellum, retina⁸⁰ and cerebellar Purkinje cells starting at late embryonic stages⁸¹. PLC β 2 is used as a differentiation marker of taste buds and taste organs development, while PLC β 3 is detected in human cone photoreceptor neurons⁸². Instead, PLC γ 1 is highly expressed in hippocampus, amygdala, forebrain, and it is particularly abundant in the radial glia during fetal brain development⁸³. Furthermore, several studies focused on PLC γ 1 mRNA expression, showed its abundant presence in neurons, oligodendrocytes and astrocytes.

The scientific community has long accepted the existence of a nuclear PI metabolism independent from the cytoplasmic one^{61,84,85}, and this metabolism is important for different nuclear events such as mRNA export, DNA repair and gene transcription⁸⁶. PLC β 1 isoform has been found in different cell subtypes of the rat brain and in the neuronal nuclear compartment⁸⁷. In isolated nuclei from the adult rat brain cortex, double immunofluorescence against PLC β 1 and nuclear speckle markers SC-35 and NeuN/Fox3 showed a high overlap of them within the nuclear matrix. Moreover, western blot analyses showed that the expression of the two splice variants of PLC β 1 (PLC β 1 *Ia* and PLC β 1 *Ib*) were statistically higher in the cytoplasm than in the nuclear and plasma membrane fractions⁸⁷. Indeed, the gene encoding PLC β 1 is located on the short arm of chromosome 20 and from this gene two different messenger RNAs are generated by alternative splicing, due to differences in the C-terminal sequence that produce a shorter and a longer mRNA sequence. The shorter mRNA sequence gives rise to the *isoform a* of the protein (150 kDa), while the *isoform b* is produced by alternative splicing from the longer mRNA and leads to a protein of 140 kDa, that is truncated because of an additional stop codon within the C-terminal sequence⁸⁸. Considering that the variant PLC β 1 *Ia* has a nuclear localization sequence (NLS) followed by a nuclear export sequence (NES) at the 3'-sequence, it can be found

both at the cytoplasmic and nuclear level. Instead, the variant PLC β 1 *Ib*, which only has the NLS, is mainly restricted to the nucleus, localizing especially within the nuclear speckles⁸⁰. It has been demonstrated that nuclear PLC β 1 (*PLC β 1 Ib*) is involved in the endocannabinoid neuronal excitability through DAG synthesis and that it can be linked to the depolarization and receptor activation, maintaining the brain inhibitory pathways via 2-arachidonoyl-glycerol (2-AG), which is the most abundant endocannabinoid in the brain⁵⁹. Indeed, DAG can be hydrolyzed by DAG-lipase α (DAGL α) to produce an increase of 2-AG. After the releasing from the postsynaptic neuron, 2-AG can activate CB1 cannabinoid receptors on the presynaptic sites, thus preventing the release of other neurotransmitters⁸⁷.

Some PLC enzymes are also involved in the nervous system development, being able to regulate the PI metabolism balance at a spatio-temporal level through the cleavage of PI(4,5)P₂ into IP₃ and DAG, which both contribute to the regulation of Ca²⁺ levels in the nervous tissue⁸⁹. Indeed, Ca²⁺ triggers several mechanisms during neuronal development, like axon guidance, dendrite and neurite morphogenesis⁹⁰ and also the balance between self-renewal and differentiation of Neural Crest Cells (NCCs)⁹¹. Calcium regulation by PLCs is undoubtedly an essential point for the development and homeostasis of the brain, but PLCs can also act on other mechanisms. For example, several studies have shown that PLC β 1 signaling pathway is involved in the development of normal cortical circuit and in activity-dependent development of the cerebral cortex^{92,93}.

Therefore, neural development and maintenance of synaptic plasticity is regulated by PLC enzymes from embryonic development continuing into adulthood. Their connection with different molecules is fundamental for the activation of numerous pathways that regulate not only the development of the nervous system, but also the normal cerebral activity that, when altered, leads to pathological conditions⁸⁸. Among these pathways, it is important to mention the MAPK cascade, the dopamine signaling and the activation of transient receptor potential channels (TRPCs)⁸⁸.

PLCs involvement in brain disorders

Given the importance of primary PLCs in the nervous system, we can understand how a dysregulation of their signaling can lead to several brain disorders including epilepsy, movement and behavior disorders, neurodegenerative diseases and some neurooncological pathologies (*Fig. 12*). As mentioned above, among the most expressed PLC isoforms in the brain it is possible to highlight the presence of PLC β 1 and PLC γ 1. They are differentially distributed, suggesting a specific role for each subtype in different brain areas and, therefore, specific consequences following their alterations. For example, it was demonstrated that PLC β 1 signaling imbalance is linked to several brain disorders, including epilepsy, schizophrenia, bipolar disorders⁹⁴ and epileptic encephalopathies⁹⁵. On the other hand, different genetic studies suggested that alterations in the signaling mediated by PLC γ 1, can be associated with epilepsy, Huntington's disease, bipolar disorder, and depression⁹⁶⁻⁹⁸.

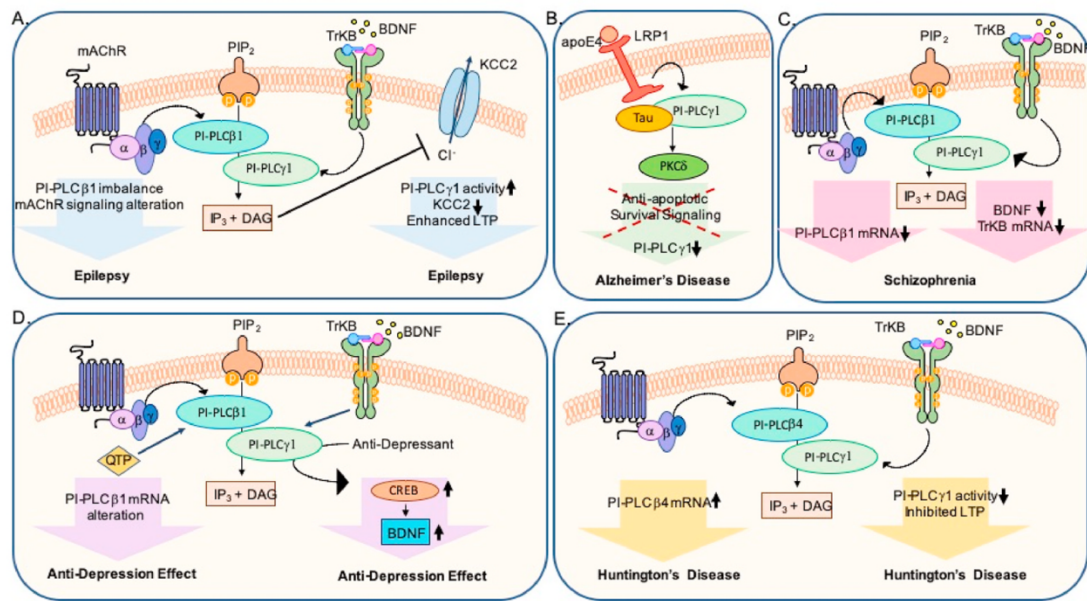


Figure 12: Implications of Phosphoinositide-specific phospholipases C (PLCs) in brain disorders⁸⁸.

Many pieces of evidence indicate that phospholipases are also implicated in glioblastoma carcinogenesis, due to the interactions of PKCs and other mediators^{99,100}. A study based on data analysis of the Cancer Genome Atlas (TCGA) and from Gene Expression Omnibus, revealed the potential role of PLCβ1 as biomarker in high-grade gliomas (HGGs)⁹⁹. In particular, an inverse correlation between PLCβ1 gene expression and glioma pathological grade has been highlighted (Fig. 13), suggesting PLCβ1 as a potential prognostic factor and a potential novel signature gene for the classification of HGGs. Moreover, the same study showed a correlation between PLCβ1 expression and patient's long-term survival, suggesting a correlation between PLCβ1 low expression and a worse prognosis⁹⁹.

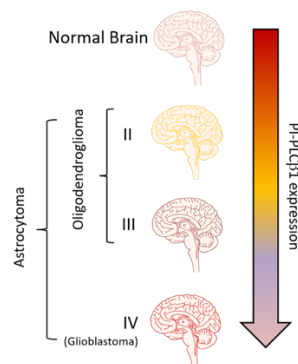


Figure 13: Image modified from the original article of Lu et al⁹⁹. that shows an inverse in silico correlation between PLCβ1 gene expression and the pathological grade of gliomas.; II, III, IV = glioma pathological grade.

Several other studies were conducted on the potential involvement of PLCs in glioblastoma pathogenesis. Among these studies, it was evidenced a potential link between PLC γ 1 inhibition and the arrest of glioma cell motility and invasion of fetal rat brain aggregates¹⁰¹. It is well known that in glioblastoma the upregulation of platelet-derived growth factor receptors (PDGFR), nerve growth factor (NGF), insulin-like growth factor (IGF-1) and, most importantly, EGFR, can mediate migration of glioblastoma cells into normal brain tissues. Interestingly, EGF and PDGF are upstream activators of PLC γ 1 and also major regulators of cell growth and proliferation¹⁰². Accordingly, PLC γ 1 inhibition leads to the arrest of glioblastoma cells invasion into normal brain tissues, careless of the combined signaling effects of PDGFR, NGF, IGF-1, and EGFR upregulation, suggesting possible anti-invasive therapeutic strategies for glioblastoma^{60,101,103} (Fig. 14).

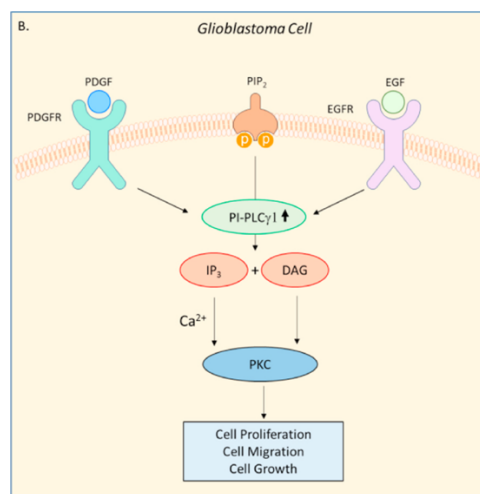


Figure 14: Platelet-derived growth factor (PDGF) and epidermal growth factor (EGF) as upstream activators of PLC γ 1. PDGF and EGF are the major regulators of cellular proliferation, migration, and growth in glioblastoma cells⁸⁸.

Therefore, PLCs' activation seems to regulate numerous signaling events in the brain and to represent a critical event in neuronal development, neurotransmission, and many other mechanisms, which are still mostly unknown and therefore require further investigations.

Aims

Given the importance of lipid signaling in the brain and the data already present in literature, the aim of this project is to define the pathological impact and the real function of phospholipases, in particular PLC β 1 and PLC γ 1, in glioblastoma pathogenesis and to determine if they and their mediators could be used as possible diagnostic and prognostic biomarkers in low- and high- grade gliomas, which are characterized by a great biological heterogeneity. Indeed, even though PLCs are clearly implicated in cancer development and progression, their specific regulatory functions in cancer are sometimes elusive and controversial and this underlines the necessity to better understand the molecular mechanisms underlying the pathogenesis of glioblastoma and to further investigate these PLCs isoforms, as a preliminary analysis, separately and in parallel. Indeed, these enzymes could trigger in a different way the same molecular mechanisms, representing promising prognostic or therapeutic targets in cancer therapies due to their influential roles in cell proliferation, migration, growth, and survival. The complete understanding of these events and the specific role of the investigated signaling pathways, could allow the correlation between tumor pathological mechanisms and the identification of future useful diagnostic and prognostic biomarkers in gliomas.

For this reason, we decided to start this project by confirming the data already present in literature through *in silico* analyses with online databases. Subsequently, we decided to start retrospective and prospective studies, involving a cohort of patients with different grades of glioma, thanks to the collaboration with IRCCS Bellaria Hospital of Bologna-ISNB (Institute of Neurological Sciences of Bologna). The molecular analysis conducted on these patients and the correlation of these data with the molecular ones collected on engineered cellular models (based on both immortalized and primary cell lines), whose PLC β 1 or PLC γ 1 has been modulated, could help to find successful targeted therapeutic strategies and to open new perspectives in HGGs research. In this way, it would be possible to stratify therapies, considering the molecular characteristics of patients, in order to achieve the best results with the minimum risks.

Notes

Most of the work was performed at the Cellular Signalling Laboratory (University of Bologna, Bologna, Italy) and most of the results from this study were published in “Cellular and Molecular Life Sciences” Journal¹⁰⁴ and “Advances in Biological Regulation” Journal¹⁰⁵ in 2022.

Materials and Methods

In silico data

The Chinese Glioma Genome Atlas (CGGA) RNA sequencing (RNA-seq) dataset (mRNAseq_325) with 325 glioma samples (103 WHO II, 79 WHO III, 139 WHO IV and 4 samples N/A of unknown nature) and the corresponding PLC β 1 or PLC γ 1 distribution and survival information, were downloaded from CGGA public database (<http://www.cgga.org.cn/>). The patients of validation set were divided into high- PLC β 1/PLC γ 1 and low-PLC β 1/PLC γ 1 expression group according to the cut-off value of PLC β 1/PLC γ 1 expression from CGGA dataset.

Collection of glioblastoma tumor samples for the retrospective study and collection of diffuse glioma tumor samples for the prospective study

Fifty (n=50) fresh-frozen glioblastoma tumor samples, from retrospective patients of the last ten (n=10) years, were obtained from the IRCCS Istituto delle Scienze Neurologiche di Bologna (Ospedale Bellaria), Italy. This study was approved by the AUSL Bologna Ethical Committee (Comitato Etico di Area Vasta Emilia Centro della Regione Emilia-Romagna (CE-AVEC) N° 183/2019/OSS/AUSLBO evaluated on 20/03/2019) and informed consents were obtained from all participants. Patients were diagnosed following the WHO 2016 and cIMPACT-NOW guidelines^{3,6}.

Twenty-three (n=23) tumor samples from different glioma prospective patients who undergone surgery over the last three years (2019-2022), were obtained from the IRCCS Istituto delle Scienze Neurologiche di Bologna. All the samples were characterized following the WHO 2021⁵, and cIMPACT-NOW guidelines³. The prospective study was approved by the AUSL Bologna Ethical Committee (N°=186/2019/OSS/AUSLBO) and informed consents were obtained from all participants.

Gliomas were classified according to different WHO (2016 or 2021) guidelines, considering the different moment of diagnosis and collection of such samples.

After surgical removal, the tumor biopsies were temporary kept (6 hours) in test tubes with physiological solution at 4°C and then brought to the Cellular Signalling Lab (DIBINEM) of the University of Bologna. There, the biopsies were washed, collected in nitrogen liquid and processed together, in a second moment, for RNA extraction. All the patients (prospective/retrospective) were described in a complete database containing all the personal and clinical information. The following information was collected for each patient: day of diagnosis and eventual death, topographic characteristics of the lesion, surgical treatment received, eventual adjuvant chemotherapy and radiotherapy and the consequent follow up. Integrated diagnostic data (morphology, type, histology, molecular profile and grade) were obtained from pathological and immunohistochemical diagnostic examinations.

DNA Mutation Analysis

DNA from fresh/frozen tissues was extracted using the MasterPure™ DNA purification kit. Mutational analysis was performed using a next generation sequencing protocol evaluating the following 4 genes: isocitrate dehydrogenase 1 (IDH1) (exon 4), isocitrate dehydrogenase 2 (IDH2) (exon 4), histone H3-3A (exon 1), Telomerase Reverse Transcriptase (TERT) (promoter). Locus-specific amplicon libraries with tagged primers were generated using overhang adapters at 5' based on Nextera™ sequence at the 5' for Illumina sequencing; these adapters were recognized by a second round of PCR (8 cycles) to add Illumina P5/P7 adapters and sample – specific indices¹⁰⁶. Amplicon products were purified with agencourt Ampure XP beads, quantified with the fluorometer Quantus™, pooled and loaded on MiSeq (Illumina). Each Next Generation Sequencings (NGS) experiment was designed to allocate $\geq 1k$ reads/region, to obtain a depth of coverage $\geq 1000x$. FASTQ files were processed in a Galaxy Project environment¹⁰⁷, using hg38 human reference genome with BWA (Burrows-Wheeler Aligner), and visualized on IGV (Integrative Genomics Viewer). Only mutations with a Variant Allele Frequency (VAF) threshold $> 5\%$ and a coverage depth of 10x in both strands were reported. All mutations were checked in COSMIC database.

DNA Methylation Analysis

Bisulfite treatment of genomic DNA (50-500 ng) was performed using the EZ DNA Methylation-Lightning Kit (Zymo Research Europe, Freiburg, Germany) according to the manufacturer's protocol. DNA methylation was evaluated using targeted bisulfite NGS for O-6-Methylguanine-DNA Methyltransferase (MGMT). In brief, genomic sequences stored in the Ensembl genome browser (<http://www.ensembl.org/index.html>) were employed as query sequences to identify putative CpG islands in the promoter and the enhancer regions. MethPrimer (<http://www.urogene.org/cgi-bin/methprimer/methprimer.cgi>) designing was applied to identify CpGs and the best primers of choice. Libraries were generated using the same approach for mutation analysis with two PCR steps. FASTQ files were processed in a Galaxy Project environment following a pipeline described previously¹⁰⁸, in brief after filtering for quality $>Q30$ and for read lengths (>80 bp), FASTQ files were then mapped by BWA-meth. BAM files were then in turn processed by MethylDackel using human GRCh38/hg38 as reference genome. The output files assigned the exact methylation level for each investigated CpG position¹⁰⁷. In parallel, the web tool EPIC-TABSAT was used to confirm DNA methylation level results¹⁰⁹.

Cell Cultures

Human glioblastoma astrocytic cell lines U87-MG (HTB-14 ATCC, Old Town Manassas, Virginia, US) and U-251 MG (09063001 Sigma-Aldrich, St Louis, MO, US) were cultured in Minimum Essential Medium Eagle (MEM) (Corning, New York, US) with 10% FBS and 1% Penicillin/Streptomycin (Sigma-Aldrich) and Dulbecco's Modification of Eagle's Medium (DMEM) (Corning) with 5% FBS and 1% Penicillin/Streptomycin, respectively. Human embryonic kidney HEK 293 T cells (Genecopoeia Inc, US) were cultured in DMEM (Corning) with 10% FBS and 1% Penicillin/Streptomycin. Human Astrocytes HA, isolated from cerebral cortex (Catalog #1800, ScienCell Research Laboratories, California, US), were cultured in Astrocyte Medium (AM, Cat. #1801, ScienCell). Patient-derived glioblastoma cells (hGSCs) were cultured as

neurospheres following a revised protocol of Gritti et al.¹¹⁰ and the subsequent analyses will be carried out after about 3/4 passages. The original fresh glioblastoma samples were collected from the Neurosurgery Unit of Rhode Island Hospital (Providence, RI, USA), and transported to the Laboratory of Cancer Epigenetics and Plasticity (Brown University, RI Hospital, Providence, USA) in a sterile tube containing DPBS on ice. Samples were transferred to a 60mm plate and cut into 1mm³ fragments. These latter were digested in 1mg/ml collagenase/dispase for 30 minutes at 37°C. Digested fragments were triturated to dissociate tissue and filtered, together with culture media, through a 70 µm cell strainer. Cell suspension was centrifuged at 110 rcf for 10 minutes. After counting, the cells were plated in non-TC treated dishes. All the cells were maintained in a humidified incubator at 37 °C with 5% CO₂.

Lentiviral Transduction for Immortalized cell lines and Human Astrocytes

HSH096803-LVRH1GP-b, HSH096803-LVRH1GP-c and CSHCTR001-LVRH1GP control vectors (Genecopoeia) were used to construct lentiviruses to silence PLCβ1 and express green fluorescent protein (GFP) as well as lentiviruses coding only for GFP, as control. The Lenti-Pac HIV expression packaging kit (Genecopoeia) was used as packaging system to transfect HEK293T cells according to manufacturer's protocol. The supernatants containing the viruses were harvested 24-48 hours after transfection and filtered through a 0.45 µm cellulose acetate filter. To perform viral transduction, U87-MG and U-251 MG were plated in a 6-well plate at a concentration of 5x10⁵ cells/well. Primary HA Astrocytes were seeded at a concentration of 5x10⁴/cm² in 6-well and 12-well plates. The next day virus supernatants together with polybrene 8 µg/ml for U87-MG and 6.4 µg/ml for U-251 MG and HA, were added to the target cells. U87-MG and U-251 MG cells were treated with 2 µg/ml and 1,5 µg/ml of puromycin (Sigma-Aldrich), respectively, 48 hours after transduction and were left in culture for one month in order to obtain a fully selected clone with stable PLCβ1 silencing. Instead, HA primary astrocytes were treated with 1 µg/ml of puromycin 24 hours after transduction and analysed after 96h.

HSH013238-LVRH1GH-a, HSH013238-LVRH1GH-c, HSH013238-LVRH1GH-d and CSHCTR001-LVRH1GH vectors (Genecopoeia) were used to construct lentiviruses to silence PLCγ1 and express green fluorescent protein (GFP) as well as lentiviruses coding only for GFP, as control, in U87-MG. EX-Z4417-Lv207 coding for Homo Sapiens PLCγ1 and EX-NEG-Lv207 vectors (Genecopoeia) were used to construct lentiviruses used to overexpress both PLCγ1 and GFP protein or only GFP, respectively. After the transduction, U87-MG were selected for 48 h in growth media supplemented with 750 µg/ml of Hygromycin B (CSNpharm, Inc. US). PLCγ1 expression analysis and migration or invasion tests were carried out 96 hours after the transduction.

TransIT Transfection for Glioma Stem cells

GSCs were grown as attached on cell-treated vessels coated with 10 µg/mL human plasma fibronectin (Millipore, FC010) and transfected with X2 (Mirus Bio) lipid and 25 nM of ON-TARGETplus Human PLCγ1 siRNA (Horizon Discovery, catalog number: J-003559-07-0002) to silence PLCγ1, or 25 nM of ON-

TARGETplus Non-targeting Control Pool for the control cells (Horizon Discovery, catalog number: D-001810-10-05), in complete media without heparin. Heparin-containing complete medium was replaced after 24 hours, and RNA and proteins were collected 72 hours post-transfection.

RNA extraction, reverse transcription, and real-time PCR for Immortalized Cell Lines and HA

RNeasy Lipid Tissue Mini Kit (Qiagen, Hilden, Germany) was used to extract total RNA from fresh-frozen tissues following manufacturer's protocol. Nanodrop spectrophotometer was used to quantify the extracted total RNA. Subsequently, Qubit fluorometer (Thermo Fisher Scientific, Waltham, MA, USA), and Qubit RNA IQ Assay, were used for quality analysis of the RNA extracted. Only samples with Qubit IQ number of 7 or greater, were selected for further experiments. Total RNA extracted from different brain lobes of healthy individuals (Biochain, Newark, CA: R1234062-P, R1234078-P, R1234051-P, R1234066-P) was used as control. A total of four (n=4) different pools were used, each containing total RNA from five (n=5) different healthy donors. RNeasy Mini Kit (Qiagen) was used to extract total RNA from immortalized cell lines and Human Astrocytes. Nanodrop spectrophotometer was used to quantify extracted RNA. Using the High-Capacity cDNA Reverse Transcription Kit (Thermo Fisher Scientific), 1 µg of total RNA was reverse transcribed into cDNA following the manufacturer's protocol. Real-time PCR was performed on 10 ng of cDNA per reaction, with QuantStudio1 Real-time PCR system (Thermo Fisher Scientific) using TaqMan Universal Master Mix II (Thermo Fisher Scientific) and TaqMan probes. GAPDH and 18S were used as housekeeping genes for cell lines and tissue samples, respectively. Data were presented as fold changes relative to the expression levels of control samples in accordance with the $2^{-\Delta\Delta C_t}$ formula. Validated gene probes used are described in *Table 1*.

18S	Hs99999901_s1 (Thermo Fisher Scientific)
GAPDH	Hs99999905_m1 (Thermo Fisher Scientific)
PLCβ1	Hs01001930_m1 (Thermo Fisher Scientific)
PLCγ1	Hs01008225_m1 (Thermo Fisher Scientific)

Table 1: Probes used in this study for gene expression analyses

RNA extraction, RNA sequencing and Differential Gene Analysis for GSCs

Total RNA from two different GSCs (silenced or not for PLCγ1), in duplicate, was isolated using TRIzol Reagent followed by DNA digestion with TURBO DNA-free™ Kit (Thermo Fisher Scientific). Next-generation RNA-sequencing was performed using an Illumina HiSeq2500 system. Sequence reads were aligned to the human genome (hg19) using *gsnap*. Subsequently, differential gene analysis was performed using DEBrowser, a R package, to detect significant changes in gene expression¹¹¹ following PLCγ1 downregulation. An adjusted p-value cut-off < 0.05 was used. Data visualization was performed using the

DEBrowser scatterplots built in options. Additionally, Enrichr was used for pathway enrichment within the respective sets of upregulated and downregulated genes¹¹².

Protein extraction and western blot

Immortalized cell lines and Human Astrocytes were lysed with T-PER lysis buffer supplemented with Halt protease and phosphatase inhibitor cocktails (Thermo Fisher Scientific). Lysed cells were sonicated for 15 seconds using 40–50% of power. Whole cell lysates were quantified with the Pierce™ Coomassie Plus (Bradford) Assay Reagent (Thermo Fisher Scientific). GSCs were lysed 72 hours post transfection with 1% SDS and quantified via Pierce Protein Assay (Thermofisher) and a spectrophotometer (Biotek) at 562 nm. For all the cell models, 30µg of total proteins were separated on bolt 4–12% polyacrylamide-0.1% commercial SDS gels (Thermo Fisher Scientific) and transferred onto nitrocellulose membrane. Membranes were washed with PBS-0.1% Tween-20 (PBST) and non-specific binding sites were blocked with blocking buffer (5% w/v non-fat dry milk in PBST) for 1 hour at room temperature. Lastly, membranes were incubated with primary antibodies overnight at 4 °C. The antibodies used were diluted in bovine serum albumin (BSA) (Sigma-Aldrich) or milk following manufacturer’s protocols. Membranes were washed again with PBST, then incubated with peroxidase conjugated secondary antibodies (Thermo Fisher Scientific) diluted 1:1500 (for anti-Mouse) and 1:10'000 (for anti-Rabbit) in PBST for 1 hour at room temperature. Westar Antares and Westar Supernova (Cyanagen, Bologna, Italy) were used as chemiluminescence reagents to detect immunoreactive bands. For the analyses conducted on immortalized cell lines and HA, images were captured with the iBright Imaging System (Thermo Fisher Scientific) and samples were analysed by total protein normalization through the iBright analysis software. For the analyses conducted on GSCs, images were taken with an Azure c300 chemiluminescent imaging system and band intensity was quantified using ImageJ. The antibodies used for western blot are summarized in the *Table 2*.

anti-PLCβ1	PA5-78430, Thermo Fisher Scientific
anti-Slug	sc-166476, SantaCruz Biotechnology
anti-N-Cadherin	33-3900, Thermo Fisher Scientific
anti-MMP-2	CST40994, Cell Signaling Technology
anti-MMP-9	MA5-32705, Thermo Fisher Scientific
anti- β-Catenin	CST9587, Cell Signaling Technology
anti-Non-phospho (Active) β-Catenin	CST8814, Cell Signaling Technology
anti-C-myc/N-myc	CST13987, Cell Signaling Technology
anti-PPARγ	CST2443, Cell Signaling Technology

anti-phospho-Stat3 Ser727	CST9134, Cell Signaling Technology
anti-phospho-Stat3 Tyr705	CST9131, Cell Signaling Technology),
anti-p44/42 MAPK (Erk1/2	CST4695, Cell Signaling Technology
anti-Phospho-p44/42 MAPK (Erk1/2)	CST4376, Cell Signaling Technology
anti-PLC γ 1	sc-7290, SantaCruz Biotechnology
Anti-GAPDH	CST5174, Cell Signaling Technology

Table 2: Antibodies used in this study for western blot

Immunocytochemistry

Cells were fixed in 2% paraformaldehyde at room temperature for 20 minutes. After blocking and permeabilizing with 1% BSA and 0,3% Tryton X-100 for 1 hour at room temperature, cells were incubated with primary antibody overnight at 4 °C. Dilutions of primary antibodies were in accordance with the manufacturer's instructions. Cells were then incubated in the dark at room temperature for 1 hour with corresponding secondary antibodies conjugated to Alexa Fluor plus 555 or Alexa Fluor 488 (Thermo Fisher Scientific). Lastly, nuclei were stained with Hoechst 33342 (Thermo Fisher Scientific) and the coverslips were mounted on the slides with Fluoromount-G (Thermo Fisher Scientific). Slides were then examined under a Zeiss AxioImager Z1 fluorescent microscope (Carl Zeiss International, Germany). Different fields were examined at 40x and 63x magnification. The antibodies used for immunocytochemistry are summarized in Table 3.

anti-PLC β 1	Thermo Fisher Scientific	1:100
anti-Ki67	Cell Signaling Technology	1:400
anti-Non-phospho (Active) β -Catenin	Cell Signaling Technology	1:600
Anti-PLC γ 1	SantaCruz Biotechnology	1:50

Table 3: Antibodies used in this study for Immunocytochemistry

Transwell migration and invasion assays

The cells were trypsinized and suspended in serum-free medium. 100 μ l of the cell suspensions containing 3×10^4 cells/ml (for migration assay) or 6×10^4 cells/ml (for invasion assay), were seeded into the upper chamber of a 24-well transwell (8 μ m pore size) (Sarstedt, Nümbrecht, Germany). For the invasion assay, a coating

with Geltrex (Thermo Fisher Scientific) was carried out 2 hours before the seeding and the plates with coated transwells were left 1 hour at 37°C and 1 hour at room temperature before the seeding. For both migration and invasion assays, after the seeding, transwells were inserted into a 24-well plate containing 600 µl of medium supplemented with 10% FBS and incubated at 37°C in a humidified atmosphere for 18 hours to allow the cells to migrate or invade. The next day, non-migrating and non-invading cells on the upper side of the filter were removed with cotton swabs. Migrating and invading cells on the lower side of the filter were fixed for 20 minutes using 70% EtOH and stained for 15 minutes with 0,2% Crystal Violet. The number of migrating and invading cells was manually counted in 4 random and non-repeated fields under an optical microscope (Magnification 20x). The average cell numbers of each group were then calculated. Each assay was performed in triplicate.

Wound Healing assay

Cells were plated in 6-well plates and the day after reaching 100% confluence a longitudinal scratch was made in the monolayer using a 100µl sterile micropipette tips. Two independent areas of each lesion were photographed at 0 h and 24 h (for U87-MG) or 48 h (for U-251 MG) using a phase contrast microscope (Motic AE21, Seneco Srl, Milano, Italy) with a digital camera (Visicam 3.0) at 10x magnification. The gap area was quantified with ImageJ software (National Institutes of Health, Bethesda, MD) and the wound healing effect was calculated as $(1-A_x/A_0)$ %, where A_0 and A_x represented the empty scratch area at 0 h and 24/48 hours, respectively.

Statistical analysis

Statistical analysis was carried out using Graph Pad Prism 5.0 software (San Diego, CA, US). Using the Shapiro-Wilk Test for patient's RNA expression analysis, data resulted not normally distributed. The difference between Healthy Controls and glioblastoma samples was evaluated using the Mann-Whitney test. One-way ANOVA test was used for the other analyses. The differences were considered statistically significant with * $p < 0.05$, ** $p < 0.01$ and *** $p < 0.001$.

Results

1. Histopathological and molecular characterization of glioma samples

Retrospective study and analysis of fifty glioblastoma patients' samples

Fifty (n=50) glioblastoma samples, from retrospective patients, were collected for this study and characterized following the WHO 2016 and cIMPACT-NOW guidelines³ (Table 4 for details). Among fifty glioblastoma samples, only six (n=6) were detected mutant for IDH1, p.R132H and none for IDH2 and histone H3-3A. These IDH1-mutated samples are classified as Adult-type diffuse astrocytoma, IDH mutant, grade 4 considering the recent tumor classification update⁵. TERT promoter was found to be mutated in thirty-two out of fifty cases (32/50) (twenty-nine for g.1,295,113 G>A and three for g.1,295,135 G>A). MGMT was detected hypermethylated in twenty-three out of fifty cases (23/50).

	MGMT	IDH1	IDH2	H3F3A	H3C2	H3C3	TERT	date of birth	age at diagnosis	Gender
Patient 1	UNMET	WT	WT	WT	WT	WT	g.1,295,113 G>A (VAF:39%)	01/02/25	68	M
Patient 2	UNMET	WT	WT	WT	WT	WT	g.1,295,113 G>A (VAF:26%)	08/09/35	57	M
Patient 3	MET	WT	WT	WT	WT	WT	g.1,295,113 G>A (VAF:42%)	23/01/29	69	M
Patient 4	MET	WT	WT	WT	WT	WT	g.1,295,113 G>A (VAF:42%)	29/05/23	69	F
Patient 5	MET	WT	WT	WT	WT	WT	WT	20/10/28	63	F
Patient 6	MET	WT	WT	WT	WT	WT	g.1,295,113 G>A (VAF:36%)	30/09/20	73	M
Patient 7	MET	WT	WT	WT	WT	WT	g.1,295,113 G>A (VAF:51%)	01/04/32	62	F
Patient 8	UNMET	WT	WT	WT	WT	WT	WT	27/10/45	54	M
Patient 9	MET	WT	WT	WT	WT	WT	g.1,295,113 G>A (VAF:44%)	22/03/34	66	M
Patient 10	UNMET	WT	WT	WT	WT	WT	WT	07/12/40	75	M
Patient 11	MET	p.R132H (VAF:44%)	WT	WT	WT	WT	WT	15/01/42	51	M
Patient 12	MET	p.R132H (VAF:30%)	WT	WT	WT	WT	WT	03/02/62	36	M
Patient 13	MET	p.R132H (VAF:34%)	WT	WT	WT	WT	WT	25/12/31	65	M
Patient 14	MET	WT	WT	WT	WT	WT	g.1,295,113 G>A (VAF:43%)	25/05/33	60	M
Patient 15	NA	WT	WT	WT	WT	WT	g.1,295,113 G>A (VAF:59%)	08/02/35	63	F
Patient 16	MET	p.R132H (VAF:43%)	WT	WT	WT	WT	WT	25/12/31	65	M
Patient 17	UNMET	WT	WT	WT	WT	WT	g.1,295,113 G>A (VAF:48%)	24/06/57	45	M
Patient 18	UNMET	WT	WT	WT	WT	p. T33T (VAF:50%)	g.1,295,113 G>A (VAF:42%)	27/06/31	72	F
Patient 19	MET	WT	WT	WT	WT	WT	g.1,295,113 G>A (VAF:55%)	28/05/29	68	F
Patient 20	NA	WT	WT	WT	WT	WT	g.1,295,113 G>A (VAF:47%)	02/03/47	56	M
Patient 21	MET	WT	WT	WT	WT	WT	g.1,295,135 G>A (VAF:41%)	02/06/37	66	M
Patient 22	UNMET	WT	WT	WT	WT	WT	g.1,295,113 G>A (VAF:38%)	23/06/32	70	M
Patient 23	UNMET	WT	WT	WT	WT	WT	g.1,295,135 G>A (VAF:64%)	07/02/61	41	M
Patient 24	UNMET	WT	WT	WT	WT	WT	g.1,295,113 G>A (VAF:37%)	08/09/32	70	M
Patient 25	UNMET	WT	WT	WT	WT	p. T33T (VAF:48%)	g.1,295,113 G>A (VAF:37%)	16/04/68	35	M
Patient 26	UNMET	p.R132H (VAF:11%)- p.W124* (VAF:5%)	WT	WT	WT	WT	g.1,295,113 G>A (VAF:55%)	12/08/44	58	M
Patient 27	UNMET	WT	WT	WT	WT	WT	g.1,295,113 G>A (VAF:47%)	05/10/33	69	M
Patient 28	UNMET	NA	WT	NA	WT	p. T33T (VAF 50%)	g.1,295,113 G>A (VAF:54%)	30/06/43	59	M
Patient 29	UNMET	WT	WT	WT	WT	WT	g.1,295,113 G>A (VAF:24%)	03/05/44	58	M
Patient 30	MET	WT	WT	WT	WT	WT	g.1,295,113 G>A (VAF:47%)	06/04/35	67	F
Patient 31	UNMET	WT	WT	WT	WT	WT	g.1,295,113 G>A (VAF:5%)	12/01/36	66	F
Patient 32	MET	WT	WT	NA	WT	WT	g.1,295,113 G>A (VAF:45%)	18/02/36	62	M
Patient 33	UNMET	WT	WT	WT	WT	WT	g.1,295,113 G>A (VAF:52%)	20/07/31	65	F
Patient 34	UNMET	WT	WT	WT	WT	WT	g.1,295,113 G>A (VAF:33%)	19/05/26	71	F
Patient 35	MET	WT	WT	WT	WT	WT	g.1,295,113 G>A (VAF:52%)	02/04/31	66	F
Patient 36	MET	p.R132H (VAF:36%)	WT	NA	WT	WT	WT	25/12/31	65	M
Patient 37	UNMET	WT	WT	WT	WT	p. T33T (55%)	g.1,295,113 G>A (VAF:31%)	25/05/45	52	M
Patient 38	UNMET	WT	WT	WT	WT	WT	g.1,295,135 G>A (VAF:18%)	19/12/29	66	M
Patient 39	MET	WT	WT	WT	WT	WT	g.1,295,113 G>A (VAF:41%)	18/02/36	60	M
Patient 40	MET	WT	WT	WT	WT	WT	g.1,295,113 G>A (VAF:44%)	12/04/25	68	M
Patient 41	MET	NA	NA	NA	NA	NA	NA	22/10/56	44	F
Patient 42	NA	NA	NA	NA	NA	NA	NA	15/02/53	46	F
Patient 43	UNMET	NA	NA	NA	NA	NA	NA	29/03/31	69	M
Patient 44	NA	NA	NA	NA	NA	NA	NA	30/08/34	67	M
Patient 45	MET	NA	NA	NA	NA	NA	NA	14/09/27	72	M
Patient 46	NA	NA	NA	NA	NA	NA	NA	25/02/33	70	M
Patient 47	MET	NA	NA	NA	NA	NA	NA	23/07/51	50	M
Patient 48	MET	NA	NA	NA	NA	NA	NA	27/06/43	57	F
Patient 49	UNMET	NA	NA	NA	NA	NA	NA	13/10/46	54	F
Patient 50	NA	NA	NA	NA	NA	NA	NA	28/02/32	67	F

Table 4: Data and Molecular characterization of samples from 50 glioblastoma patients.

Prospective study and analysis of twenty-three glioma patients' samples

Among the twenty-three (n=23) glioma samples, obtained from prospective patients, seventeen (n=17=74%) were diagnosed as glioblastoma, grade 4, IDH wildtype (both IDH1 and IDH2), according to the new classification⁵. Five (n=5=22%) samples were classified as grade 3 oligodendroglioma, intrinsically characterized by 1p/19q codeletion and IDH-mutation. Among these samples, four out of five (4/5) were mutant for IDH1 p.R132H, c.395G>A, exon 4, while one out of five (1/5) was mutant for IDH2 p.R172S, c.516G>T, exon 4. Only one sample (n=1=4%) was diagnosed as a low-grade undefined glioma (LGG) IDH1/2 wildtype, histologically classified between grade 1 and 2. None of them turned out as a grade 4 astrocytoma IDH-mutant, a rarer glioma with better prognosis compared to glioblastoma (*Fig. 15 and Table 5 for details*).

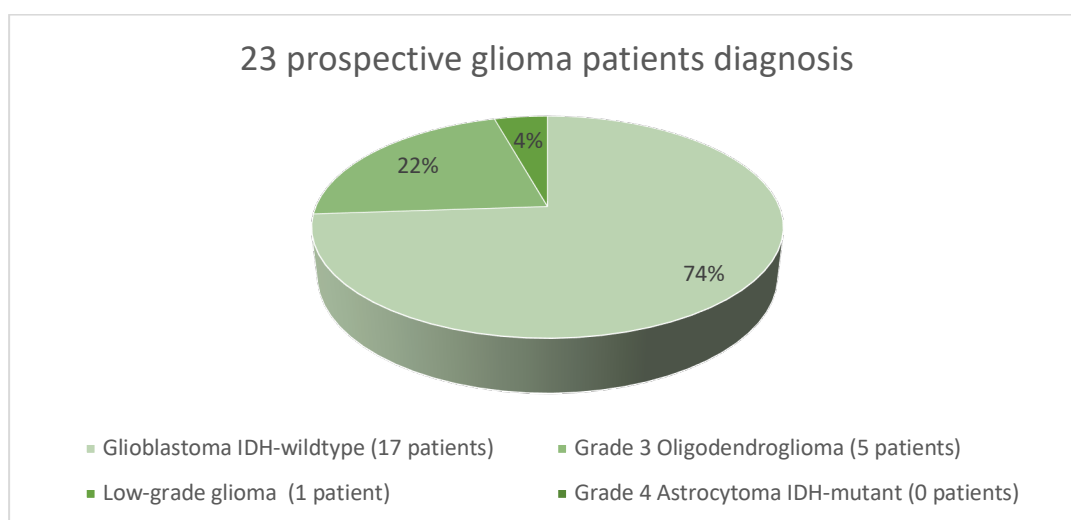


Figure 15: Integrated diagnosis of the 23 prospective glioma patients.

TERT promoter was found to be mutated in 21 out of 23 (21/23) cases: sixteen (n=16) characterized by 124 C>T (C228T) mutation, while five (n=5) by 146C>T (C250T) mutation. MGMT was detected hypermethylated, thus defining a favorable prognosis feature, in 14 out of 23 cases (14/23), all of them with > 20% of MGMT genes methylated except for one (n=1) sample (GBM 21), characterized by < 20% MGMT methylation. All the five (n=5) oligodendrogliomas were represented among these fourteen (n=14) MGMT methylated samples, with a > 20% MGMT methylation level. Moreover, one (n=1) sample (GBM 24) was found to be mutated for p.Ala148Thr, which is, according to *Varosome Database*, a likely pathogenic variant of Phosphatase and Tensin homolog (PTEN), a tumor suppressor whose mutation is associated with cancer development and progression¹¹³. Eventually, p53 protein, a tumor suppressor associated with glioma's development¹⁹, has been found mutated and hyper expressed in 6 cases out of 23 (6/23).

SAMPLE	DIAGNOSIS	GRADE
GBM 7	Glioblastoma	4
GBM 8	Glioblastoma	4

GBM 9	Glioblastoma	4
GBM 10	Glioblastoma	4
GBM 11	Glioblastoma	4
OLIGO 1	OLIGODENDROGLIOMA	3
OLIGO 2	OLIGODENDROGLIOMA	3
OLIGO 3	OLIGODENDROGLIOMA	3
GBM 14	Glioblastoma	4
GBM 16	Glioblastoma	4
GBM 17	Glioblastoma	4
GBM 18	Glioblastoma	4
GBM 19	Glioblastoma	4
OLIGO 4	OLIGODENDROGLIOMA	3
GBM 21	Glioblastoma	4
GBM 22	Glioblastoma	4
GBM 23	Glioblastoma	4
GBM 24	Glioblastoma	4
GBM 25	Glioblastoma	4
OLIGO 5	OLIGODENDROGLIOMA	3
GBM 27	Glioblastoma	4
GBM 28	Glioblastoma	4
GLIOMA 29	LOW-GRADE GLIOMA	1 or 2

Table 5: List of the 23 glioma samples derived from prospective patients' biopsies, organized and named after encoded nomenclature, together with their diagnosis and grade.

2. Study of the impact of PLC β 1 in Glioblastoma

Glioblastoma is characterized by reduced PLC β 1 gene expression compared to both low-grade gliomas and healthy patients

In order to perform PLC β 1 gene expression study, we firstly examined the CGGA online public database containing PLC β 1 RNA-seq and survival data of patients with different glioma grades (from II to IV). From an initial analysis, it emerged an inverse correlation between the expression of PLC β 1 and the pathological grade of gliomas (*Fig. 16a*). Indeed, WHO IV gliomas showed a lower expression of PLC β 1 gene compared to WHO II and III gliomas, confirming data that were already present in literature. In addition, the results of the survival analysis carried out with the CGGA database showed that patients with low- or high- grade gliomas, characterized by low expression of PLC β 1 have a shorter survival time in both primary and recurrent gliomas compared to patients with high-PLC β 1 expression (*Fig. 16b*).

Subsequently, we started a retrospective study, through the analysis of PLC β 1 gene expression in fifty (n=50) tissues coming from fresh-frozen glioblastoma patients of the last ten (n=10) years, compared to four (n=4) healthy samples pools, each one containing total RNA derived from five (n=5) different healthy donors, used as controls (twenty (n=20) patients in total). As shown in the graph (*Fig. 16c*), it was highlighted an overall lower expression of PLC β 1 in glioblastoma samples compared to the healthy ones. To further investigate this result, we stratified patients based on their PLC β 1 expression, obtaining thirty-eight patients out of fifty (38/50) with lower PLC β 1 expression compared to the PLC β 1 mean expression of the healthy pools (PLC β 1<1) and twelve patients out of fifty (12/50) with higher PLC β 1 expression (PLC β 1>1) compared to controls' mean expression. After patients' stratification, the reduction in PLC β 1 expression resulted to be statistically significant in thirty-eight (n=38) glioblastoma patients compared to the healthy controls. On the other hand, the higher PLC β 1 expression that characterized the other twelve (n=12) glioblastoma patients was not statistically relevant. Considering these results, we concluded that glioblastoma patients were characterized by an overall reduced PLC β 1 expression compared to both healthy samples and low-grade gliomas.

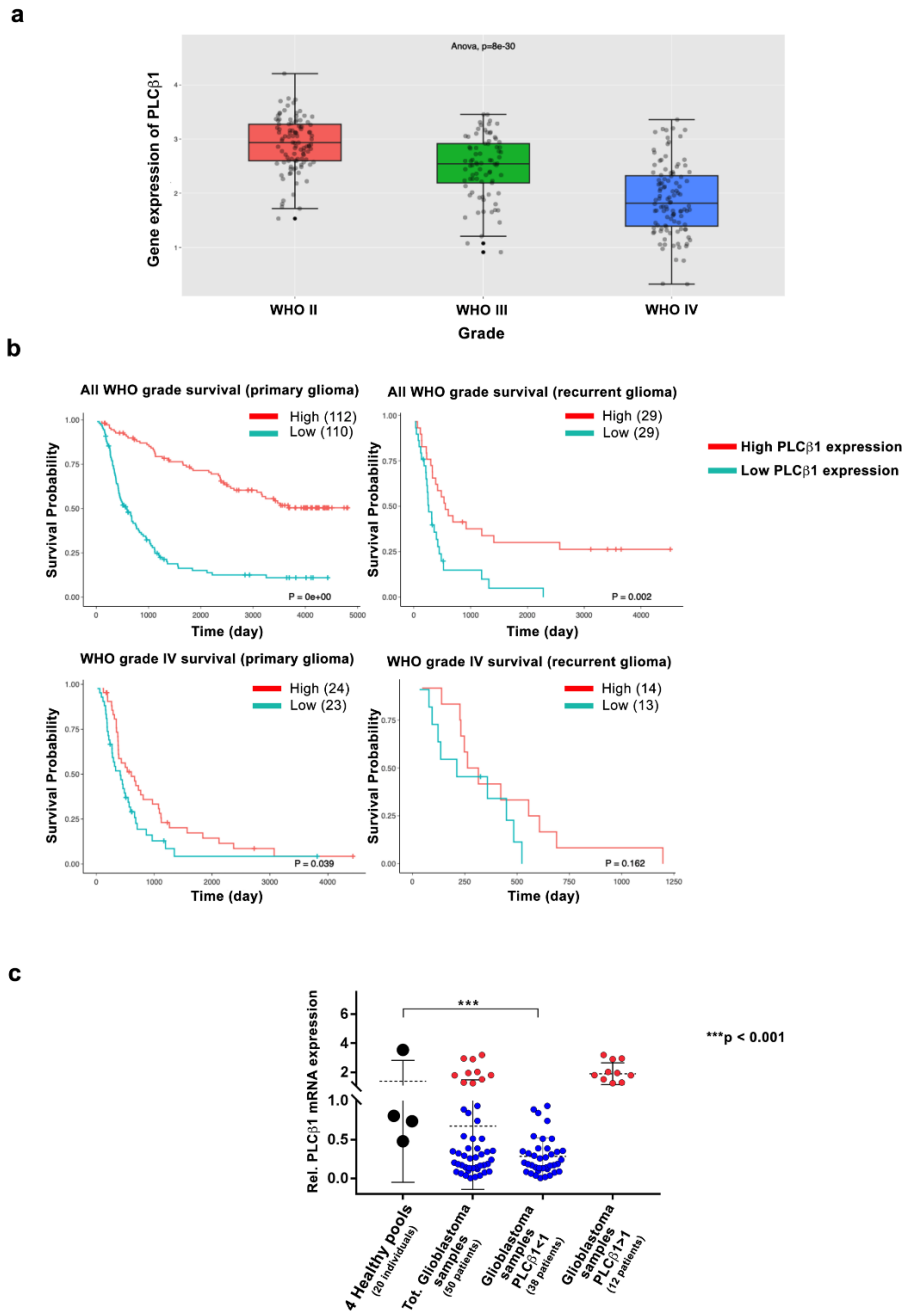


Figure 16: PLC β 1 expression inversely correlates with the pathological grade of gliomas. Panel a: Distribution of PLC β 1 expression in gliomas according to WHO grade status in the CGGA database. WHO II, n=103; WHO III, n=79; WHO IV, n=139. The WHO grading of gliomas inversely correlated with mRNA levels of PLC β 1. Panel b: Kaplan-Meier survival curves of PLC β 1 high or low expression groups in different glioma patients from the CGGA dataset. Patients were divided according to the median level of PLC β 1 mRNA expression. Panel c: PLC β 1 mRNA expression in 50 glioblastoma samples and 4 healthy pools of 5 donors each (20 healthy samples in total). Scatter plots display the distribution of PLC β 1 gene expression in glioblastoma samples compared to healthy samples. Glioblastoma patients were stratified based on their PLC β 1 gene expression: patients with higher PLC β 1 expression compared to controls' mean PLC β 1 expression, are represented in red (12 patients), while patients with lower PLC β 1 expression are shown in blue (38 patients). 18S was used as housekeeping gene and the values are presented as mean \pm SD. Asterisks indicate statistically significant differences between the groups, with ***p < 0.001.

In a second phase of the study, we analyzed PLC β 1 mRNA expression in twenty-three (n=23) fresh-frozen tissues from prospective patients who underwent surgery for glioma resection over the last three years. PLC β 1 gene expression in gliomas' samples was compared to the one in four (n=4) healthy sample pools used as control. It was highlighted an overall lower expression of PLC β 1 in all twenty-three (n=23) glioma samples (22 HGGs and 1 LGG) compared to the healthy ones (*Fig. 17a*). Later, the patients were stratified based on their PLC β 1 expression, obtaining 20 patients out of 23 (20/23) with lower PLC β 1 expression compared to the PLC β 1 mean expression of the healthy pools (PLC β 1<1) and 3 patients out of 23 (3/23) with higher PLC β 1 expression (PLC β 1>1) compared to controls' mean expression. Interestingly, among the patients with PLC β 1>1, two (n=2) were diagnosed as glioblastoma, while one (n=1) was diagnosed as low-grade glioma. Moreover, among the twenty (n=20) patients characterized by PLC β 1<1, 15 out of 20 (15/20) samples were classified as glioblastomas, while 5 out of 20 (5/20) samples were classified as grade 3 oligodendrogliomas. Through the analysis of these samples, it was observed less PLC β 1 expression level in glioblastoma patients compared to the oligodendroglioma ones (*Fig. 17b*). The studied population did not show a normal distribution according to Shapiro-Wilk test, thus allowing to refer to these findings only as a descriptive trend. However, the obtained results were consistent with our previous analyses confirming that PLC β 1 expression inversely correlated with glioma's grade, and it was lower in the most aggressive phenotypes.

PLC β 1 low expression is associated to a greater tendency to relapse

Among the twenty-three (n=23) patients that underwent surgery and first line adjuvant therapies after diagnosed with glioma, 4 out of 23 (4/23), all diagnosed as glioblastomas (GBM 11, GBM 14, GBM 17, GBM 23), relapsed after variable amount of time since the surgical removal of the lesion, and started different second line therapies. As these patients were characterized by a faster development of the neoplasm, we decided to analyse PLC β 1 gene expression in their primary lesion and to compare it with the one that characterized the nineteen (n=19) non-relapsed patients. Interestingly, there was a lower mean PLC β 1 expression in those four (n=4) patients who received recurrence diagnosis compared to the non-relapsed ones (*Fig. 17c*). This result identifies PLC β 1 as a gene capable of stratifying not only the various glioma's grades, but among the high ones, even those with the highest probability of recurrence.

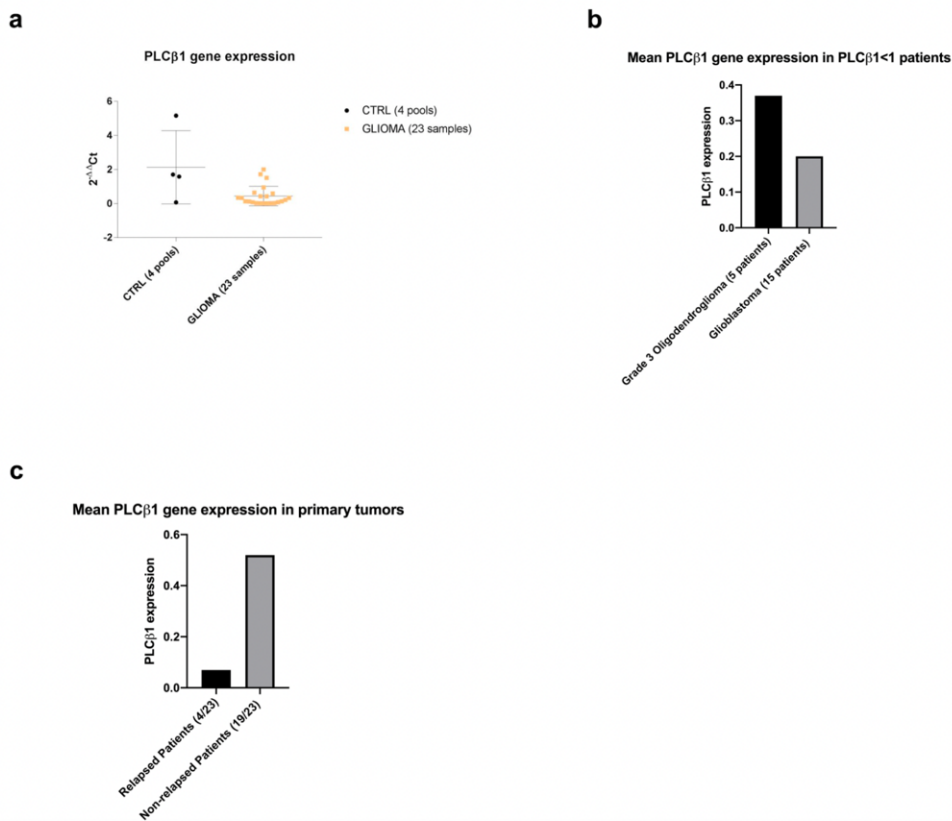


Figure 17: PLCβ1 gene expression analysis in 23 different prospective glioma samples. Panel a: PLCβ1 mRNA expression in 23 different glioma samples and 4 healthy pools of 5 donors each (20 healthy samples in total). Scatter plot displays the distribution of PLCβ1 gene expression in glioblastoma samples compared to healthy samples. 18S was used as housekeeping gene. Panel b: Comparison between the mean PLCβ1 expression in grade 3 oligodendrogliomas and glioblastomas stratified for PLCβ1<1. Panel c: Comparison between the mean PLCβ1 expression in the primary tumor of relapsed patients (4/23) and non-relapsed patients (19/23).

PLCβ1 silencing leads to an increase in the expression of mesenchymal markers and matrix metalloproteinases

In order to investigate the possible role of PLCβ1 in glioblastoma pathogenesis, we silenced PLCβ1 in two different glioblastoma cell line models. Firstly, we transduced U87-MG and U-251 MG cell lines and we created stable clones after a month of selection with puromycin. Silenced cells (shPLCβ1 cells) were tested for PLCβ1 protein (Fig. 18a,d) and gene expression (Fig. 18b,e) and compared to wild type cells (WT) and to cells transduced with empty vectors coding only for GFP (shCTRL). Moreover, PLCβ1 expression and localization were evaluated by immunofluorescence (Fig. 18c,f). In addition, in order to better deepen our study, we introduced a new cell model, based on Human Primary Astrocytes (HA). HA were analysed for PLCβ1 protein (Fig. 18g), gene expression (Fig. 18h), and localization (Fig. 18i), 24 hours after puromycin treatment and 96 hours after the transduction, revealing a slightly lower efficiency than the immortalized cell lines.

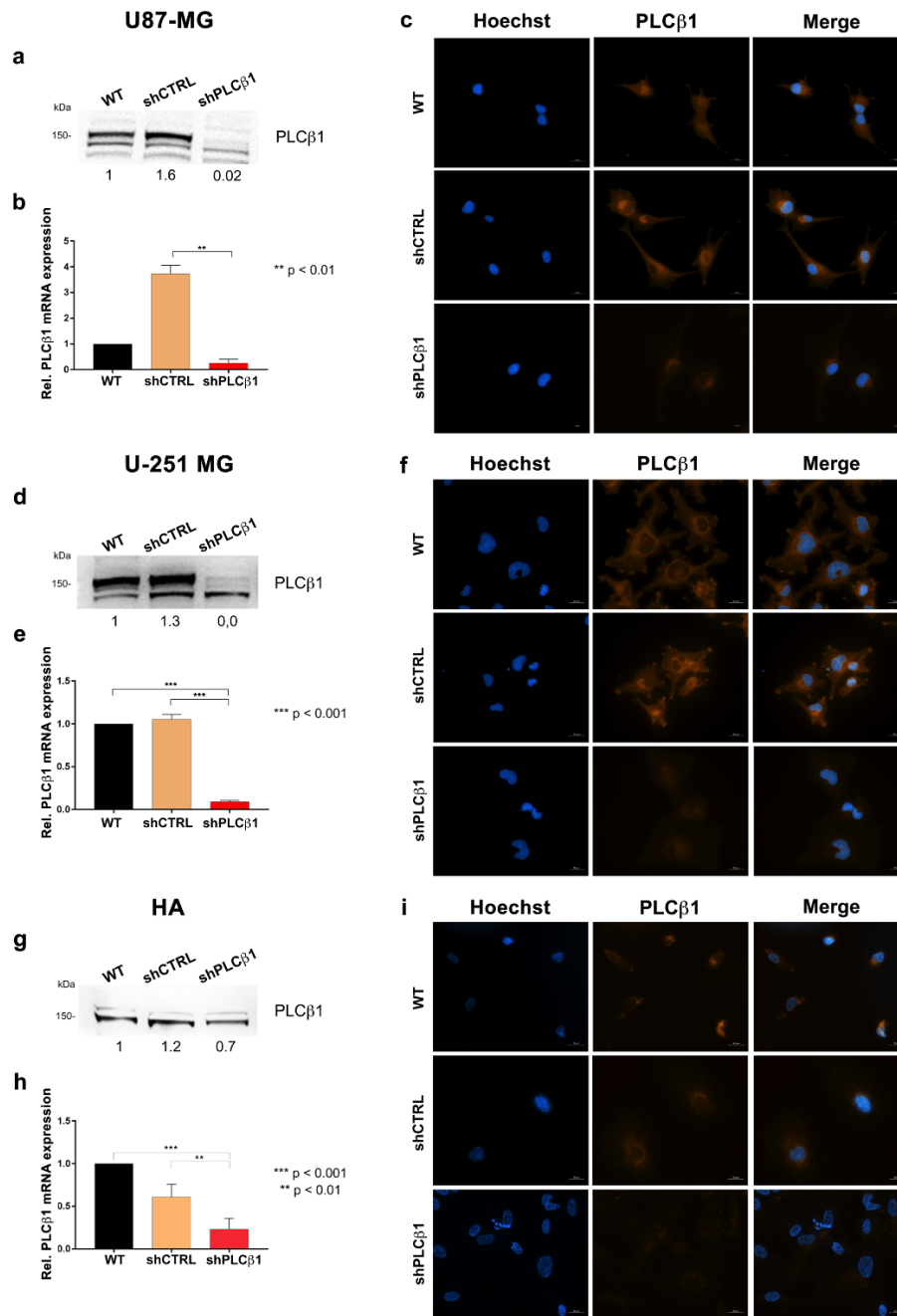


Figure 18: PLCβ1 silencing on U87-MG, U-251 MG cell lines and HA primary astrocytes. Following transduction and antibiotic selection, PLCβ1 mRNA expression, protein levels and localization were evaluated in U87-MG, U-251 MG cells and HA primary astrocytes. PLCβ1-silenced cells (shPLCβ1) were compared to wild type (WT) and mock-transduced cells (shCTRL). U87-MG and U-251 MG cells were tested after one month of antibiotic selection, while HA primary astrocytes were analysed after 48 h of puromycin selection, i.e. 96 h after transduction overall. Panels a, d and g: western blot analysis of PLCβ1 expression in U87-MG (a), U-251 MG (d) and HA primary astrocytes (g). Densitometric analysis was performed with total protein normalization through the iBright analysis software. Western blot results are representative of three independent experiments. Panels b, e and h: PLCβ1 mRNA expression in U87-MG (b), U-251 MG (e) and HA primary astrocytes (h). GAPDH was used as housekeeping gene and all the analysis derived from three independent experiments, with **p < 0.01, ***p < 0.001. Panels c, f and i: immunofluorescence staining of PLCβ1 (red) in U87-MG (c), U-251 MG (f) and HA primary astrocytes (i) (Magnification 40x, bar: 20μm). Nuclei were stained with Hoechst 33342 (blue). Results are representative of at least five different fields.

Since the highly infiltrative and migratory abilities of glioblastoma cells into the healthy brain are responsible for glioblastoma malignancy and its worse prognosis, it was necessary to examine the signaling pathways and the molecular mechanisms that drive glioma cell motility and proliferation¹¹⁴. These complex mechanisms are regulated by different elements, that include the transition to a mesenchymal phenotype¹¹⁵, and changes in the extracellular matrix (ECM)¹¹⁶ through matrix metalloproteinases (MMPs).

In order to investigate the effects of PLC β 1 downregulation on these molecular mechanisms that regulate cancer aggressiveness, we started evaluating the expression of the mesenchymal phenotype-associated molecule N-Cadherin and of one of the main epithelial-mesenchymal transition (EMT) regulatory transcription factors Slug. Following stable or transient PLC β 1 downregulation, western blot analysis revealed that both cell lines and HA showed an increase in the expression of the two markers, revealing that PLC β 1 downregulation determined a more undifferentiated state compared to controls. Indeed, the mesenchymal markers were upregulated in all PLC β 1-silenced models (*Fig. 19a,b,c*).

Next, following PLC β 1 downregulation, we also observed a significant higher protein expression of metalloproteinase 2 (MMP-2) and 9 (MMP-9), which are involved in ECM degradation and in the epithelial-mesenchymal transition, in U87-MG and HA. (*Fig. 19d,e*). Usually, MMPs expression in an unaffected brain is low, but it increases in gliomas and the most involved metalloproteinases in gliomas' invasive processes are exactly MMP-2 and MMP-9, which correlate their expression with tumor grade and progression^{117,118}. Data were not shown on U-251 MG cell line due to the lack of expression of MMPs, which were not detectable in this model. All in all, these data suggested that PLC β 1 silencing led to a more aggressive phenotype.

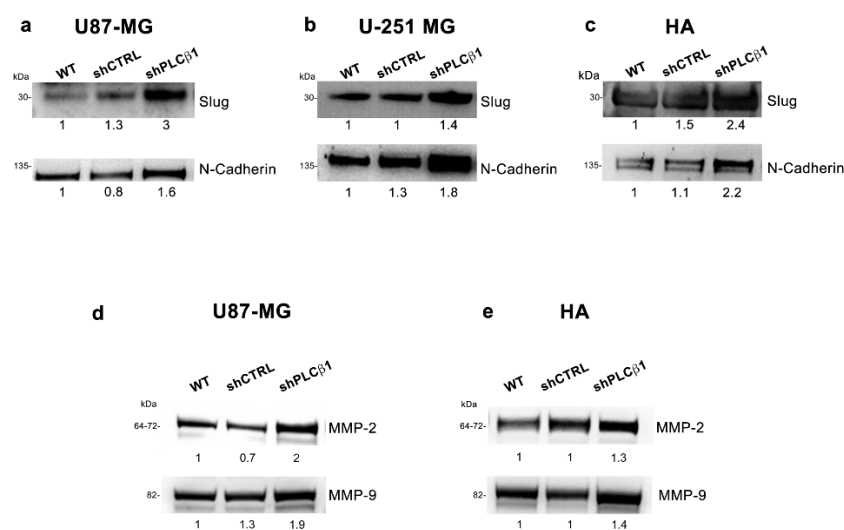


Figure 19: PLC β 1 silencing led to increased mesenchymal markers and matrix metalloproteinases expression. Panels a, b, and c: western blot analysis of the expression of mesenchymal markers Slug and N-Cadherin after PLC β 1 downregulation on U87-MG (a), U-251 MG (b) and HA primary astrocytes (c). Panels d and e: western blot analysis of matrix metalloproteinases MMP-2 and MMP-9 expression on U87-MG (d) and HA primary astrocytes (e). PLC β 1-silenced cells (shPLC β 1) were compared to wild type (WT) and mock-transduced (shCTRL) samples. Densitometric analysis was performed with total protein normalization through the iBright analysis software. Western blot results are representative of three independent experiments.

Migration, Invasion and Proliferation abilities are increased in PLCβ1-silenced cells

Based on the previous data, we next examined the migration and invasion ability of PLCβ1-silenced cells. Following PLCβ1 downregulation, both U87-MG and U-251 MG cells exhibited significantly higher migration potential compared to their respective controls (shCTRL) and wild type cells (WT). This result was confirmed by both transwell migration assay (Fig. 20a,b,c,d), and wound healing assay (Fig. 20e,f,g,h). Going into detail, PLCβ1-silenced U87-MG and U-251 MG cells were able to almost completely repair the wound after 24 and 48 hours, respectively, while their controls, failed to totally repair the wound in the same time frame.

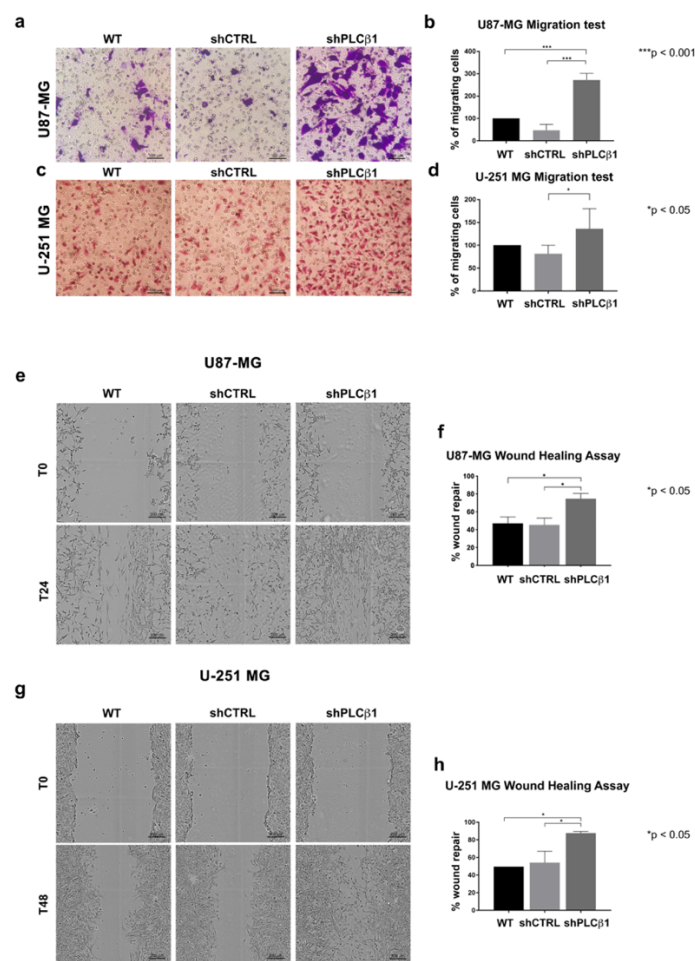
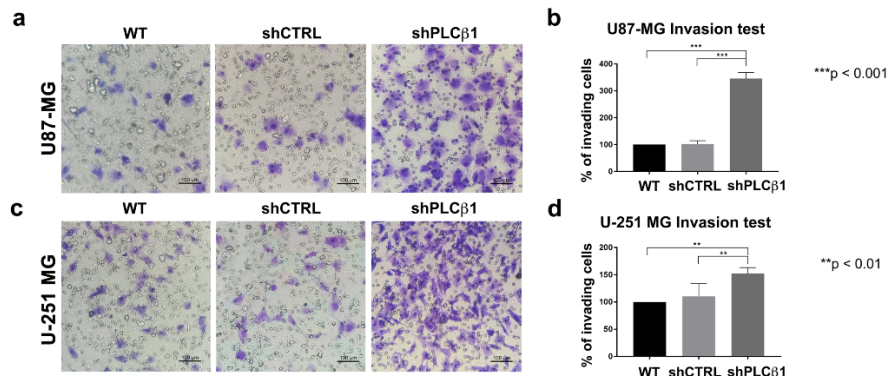


Figure 20: PLCβ1 silencing caused increased cell migration in U87-MG and U-251 MG cell lines. Panels a and c: Representative images of transwell migration assays in U87-MG (a) and U-251 MG (c) cell lines. PLCβ1-silenced cells (shPLCβ1) were compared to wild type (WT) and mock-transduced (shCTRL) cells. Magnification 20x (bar: 100 μm) Panels b and d: Graphical representations of transwell migration assays of PLCβ1-silenced cells (shPLCβ1) compared to wild type (WT) and mock-transduced (shCTRL) cells in U87-MG (b) and U-251 MG (d) cell lines. Columns show the mean ± SD of three independent experiments with *p < 0.05, ***p < 0.001. Panels e and g: Wound healing assays of U87-MG (e) and U-251 MG (g) cell lines. PLCβ1-silenced cells (shPLCβ1) were compared to wild type (WT) and mock-transduced (shCTRL) cells. Representative pictures were taken at 0 h, 24 h (for U87-MG) and 0 h, 48 h (for U-251 MG) after scratching. Magnification 10x (bar: 200 μm). Panels f and h: Graphical representations of wound healing assays of PLCβ1-silenced cells (shPLCβ1) compared to wild type (WT) and mock-transduced (shCTRL) cells in U87-MG (f) and U-251 MG (h) cell lines. Columns show the mean ± SD of three independent experiments with *p < 0.05.

Next, to evaluate the invasion potential of U87-MG and U-251 MG, we performed the transwell assay with a Geltrex coating. This revealed that both PLC β 1-silenced cell lines had significantly higher invasion potential than the respective controls (*Fig. 21a,b,c,d*).



*Figure 21: PLC β 1 silencing determined increased cell invasion in U87-MG and U-251 MG cell lines. Panels a and c: Representative images of transwell invasion assays with Geltrex coating in U87-MG (a) and U-251 MG (c) cell lines. PLC β 1-silenced cells (shPLC β 1) were compared to wild type (WT) and mock-transduced (shCTRL) cells. Magnification 20x (bar: 100 μ m). Panels b and d: Graphical representations of transwell invasion assays of PLC β 1-silenced cells (shPLC β 1) compared to wild type (WT) and mock-transduced (shCTRL) cells in U87-MG (b) and U-251 MG (d) cell lines. Columns show the mean \pm SD of three independent experiments with **p < 0.01 ***p < 0.001.*

The same assays were further carried out on HA model. PLC β 1-silenced astrocytes were able to migrate faster (*Fig. 22a,b*), invade faster (*Fig. 22c,d*) and almost completely repair the wound (*Fig. 22e,f*) compared to control and wild type cells. Therefore, an inverse correlation between PLC β 1 expression and the cellular migration and invasion abilities was confirmed in all the engineered models.

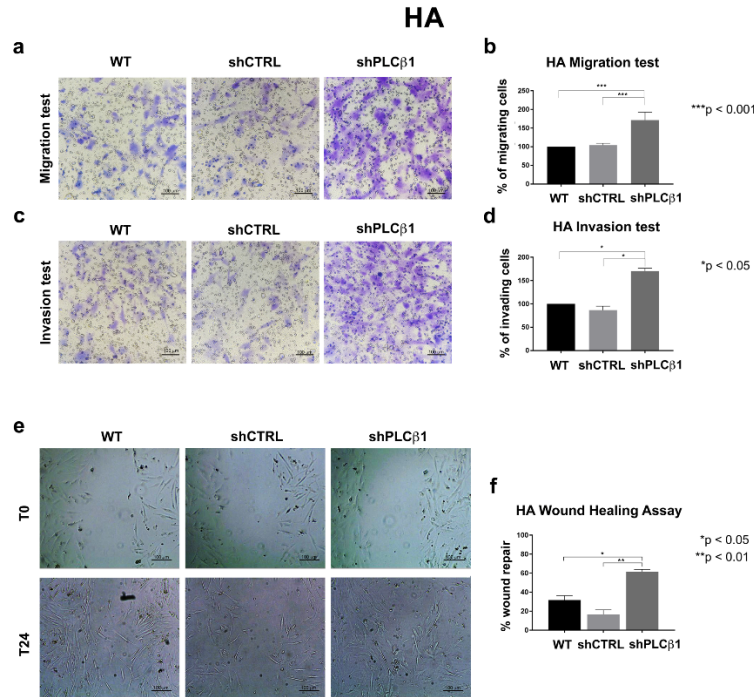


Figure 22: PLCβ1 silencing caused increased cell migration and invasion in HA primary astrocytes. Panel a: Representative images of transwell migration assay in HA primary astrocytes. PLCβ1-silenced cells (shPLCβ1) were compared to wild type (WT) and mock-transduced (shCTRL) cells. Magnification 20x (bar: 100 μm). Panels b: Graphical representation of transwell migration assay of PLCβ1-silenced cells (shPLCβ1) compared to wild type (WT) and mock-transduced (shCTRL) cells. Columns show the mean ± SD of three independent experiments with ***p < 0.001. Panel c: Representative images of transwell invasion assay with Geltrex coating in HA primary astrocytes. PLCβ1-silenced cells (shPLCβ1) were compared to wild type (WT) and mock-transduced (shCTRL) cells. Magnification 20x (bar: 100 μm). Panel d: Graphical representation of transwell invasion assay of PLCβ1-silenced cells (shPLCβ1) compared to wild type (WT) and mock-transduced (shCTRL) cells. Columns show the mean ± SD of three independent experiments with *p < 0.05. Panel e: Wound healing assay of HA primary astrocytes. PLCβ1-silenced cells (shPLCβ1) were compared to wild type (WT) and mock-transduced (shCTRL) cells. Representative pictures were taken at 0 h and 24 h after scratching. Magnification 10x (bar: 100 μm). Panels f: Graphical representation of wound healing assays of PLCβ1-silenced cells (shPLCβ1) compared to wild type (WT) and mock-transduced (shCTRL) cells. Columns show the mean ± SD of three independent experiments with *p < 0.05 and **p < 0.01.

In order to verify if PLCβ1 downregulation was also related to increased proliferation, we evaluated the expression of the proliferation marker Ki-67 by immunocytochemistry (ICC). Fig. 23 shows the expression of Ki-67 in wild-type (WT), mock-transduced (shCTRL), and PLCβ1-silenced cells (shPLCβ1). Both U87-MG and U-251 MG showed a higher expression of Ki-67 (in red) in PLCβ1-silenced cells compared to their controls and wild type cells (Fig. 23a,b). Next, we evaluated Ki-67 expression in HA primary astrocytes. Since this model evidenced a lower transduction efficiency compared to the immortalized cell lines, we decided to acquire also the GFP signal (in green) to identify the cells correctly transduced. Comparing Ki-67 expression in GFP positive cells, it was confirmed that PLCβ1-silenced HA had higher Ki-67 expression compared to shCTRL and wild type cells (Fig. 23c). Accordingly, cell proliferation was markedly affected by PLCβ1 reduced expression in both cell lines and primary astrocytes.

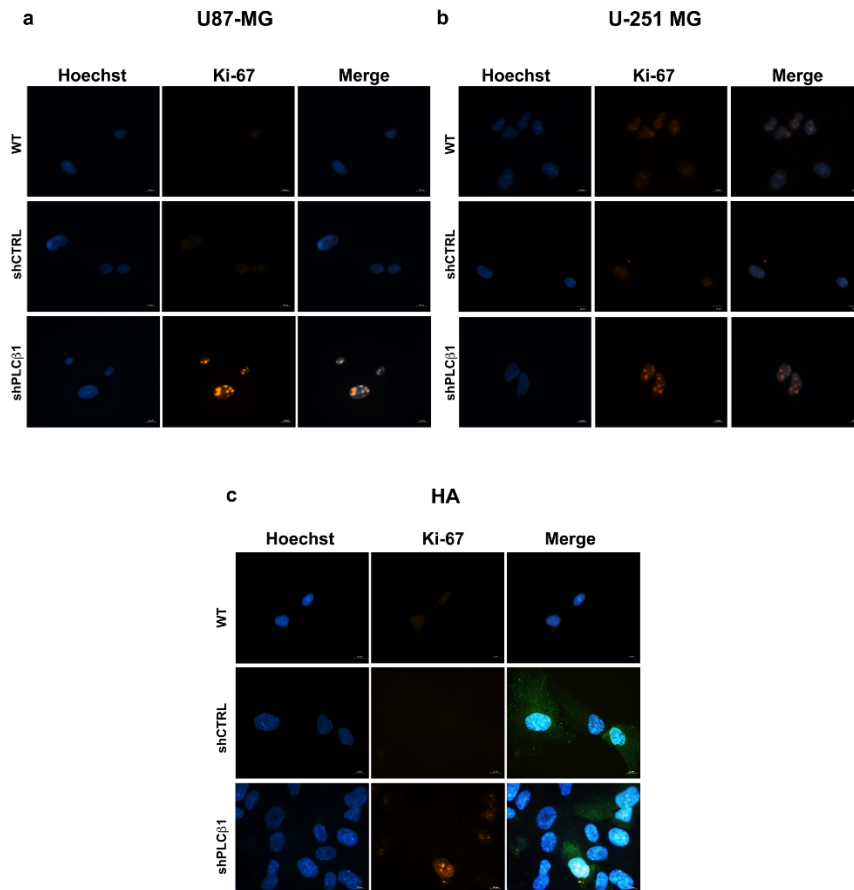


Figure 23: *PLCβ1* silencing led to increased cell proliferation. Panels a and b: Immunofluorescence staining of Ki-67 (red) at 63x magnification (bar: 10 μm) in U87-MG (a) and U-251 MG (b). Panel c: Immunofluorescence staining of Ki-67 (red) and GFP (green) at 63x magnification (bar: 10 μm) in HA primary astrocytes. *PLCβ1*-silenced cells (sh*PLCβ1*) were compared to wild type (WT) and mock-transduced (shCTRL) cells. Nuclei were stained using Hoechst 33342 (blue). Results are representative of at least five different fields.

PLCβ1 silencing enhances the activation of survival pathways

As a result of the data shown above, we decided to investigate the signaling molecules involved in different survival pathways, such as β-catenin, Stat3 and ERK1/2 pathways, to determine if these signaling cascades were influenced by *PLCβ1* expression's modulation. β-catenin pathway, which belongs to the canonical Wnt-pathway, is particularly involved in migration, invasion and proliferation and it was demonstrated to be overexpressed in glioblastoma^{119,120}. Together with this signaling pathway, also the MAPK cascade, which includes extracellular signal-regulated protein kinases 1 and 2 (ERK1/2), is often modulated in this tumor and implicated in the most aggressive tumor phenotypes¹²¹. Glioma cell growth, differentiation and motility are modulated also by signal transducer and activator of transcription-3 (Stat3) pathway, which has been shown to be associated with glioblastoma oncogenesis and epithelial-mesenchymal transition¹²². Fig. 24a,b shows that in both U87-MG and U-251 MG cells, *PLCβ1* downregulation led to an increase in the activation of the main survival pathways mentioned above. In both cell lines it was possible to observe

an increment in the expression of the active form of β -Catenin (non-phosphorylated form on residues Serine 33, Serine 37 and Threonine 41) and, in U87-MG, an increase of the total one, following PLC β 1 downregulation. We also evaluated the protein expression of the proto-oncogene c-Myc, as a well-known β -catenin target, in order to determine if the amount of active β -catenin affected the expression of its targets. Interestingly, PLC β 1-silenced cells showed a marked increase of c-Myc expression in both cell lines compared to the controls (WT and shCTRL). Moreover, the immunofluorescence of the active form of β -catenin in the cell lines revealed a nuclear presence of active β -catenin in PLC β 1-silenced cells (*Fig. 24d,e*), particularly evident in U87-MG. Indeed, while wild-type and control cells showed a comparable diffuse cytoplasmic localization of active β -catenin, shPLC β 1 cells revealed a concomitant nuclear presence of it. This evidence confirmed that the active form of β -catenin translocated into the nucleus to act as a transcriptional activator in both the cell lines, following PLC β 1 downregulation. Next, we investigated the effect of PLC β 1 modulation on the expression of the nuclear receptor Peroxisome Proliferator-Activated Receptor γ (PPAR γ), which is known to act in opposition to β -catenin in several cellular models. *Fig. 24* shows that PLC β 1-silenced cells display a decrease of PPAR γ . This downregulation is more marked in U-251 MG compared to U87-MG. In addition, it was observed that the activation of Stat3 pathway was increased in PLC β 1-silenced cells compared to the controls. Both U87-MG and U-251 MG cells displayed high levels of phosphorylated Stat3 (both on Serine 727 and Tyrosine 705) compared to the respective controls. Finally, it was also demonstrated that the phosphorylation levels of p44/42 MAPK (ERK1/2) was affected by PLC β 1 modulation. Indeed, shPLC β 1-cells showed increased phosphorylation's level of ERK1/2.

All these results were later strengthened and confirmed also in HA primary astrocytes (*Fig. 24c*). Indeed, as well as in U87-MG and U-251 MG, also in primary HA model, a marked increase of the active form of β -catenin was observed, together with the increase of its target c-Myc, as a consequence of PLC β 1 downregulation. Furthermore, a decrease in the expression of PPAR γ , was observed in PLC β 1-silenced cells. In support of these data, it was also found an increased expression of the phosphorylated forms of Stat3 and ERK1/2.

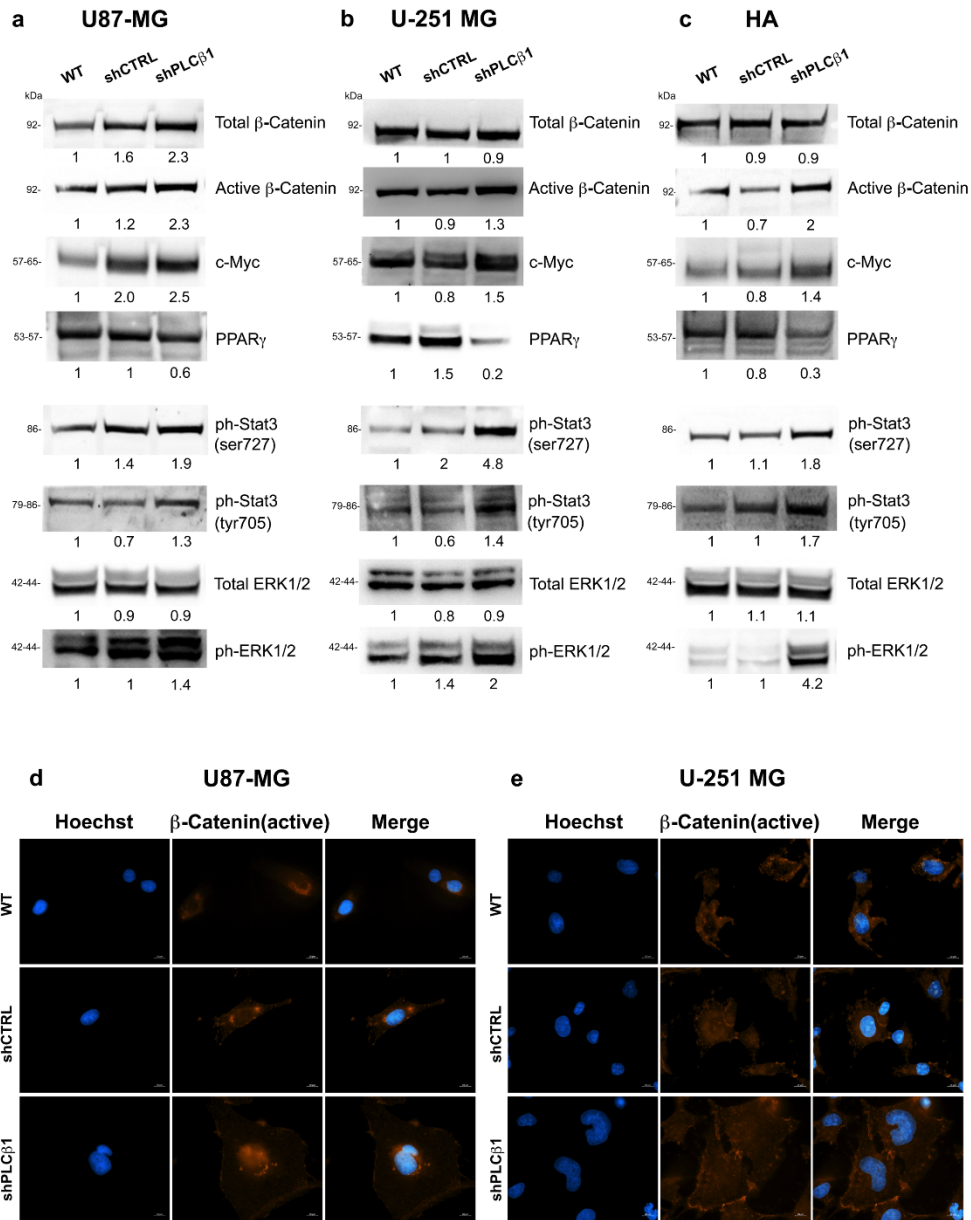


Figure 24: Effects of PLCβ1 silencing on the activation of survival pathways. Panels a, b and c: The expression and the phosphorylation of molecules belonging to different survival pathways were evaluated in U87-MG (a), U-251 MG (b) and HA primary astrocytes (c). PLCβ1-silenced cells (shPLCβ1) were compared to wild type (WT) and mock-transduced (shCTRL) cells. Densitometric analysis was performed with total protein normalization through the iBright analysis software. Western blot results are representative of three independent experiments. Panels d and e: Immunofluorescence staining of active β-catenin (red) at 63x magnification (bar: 10 μm) in U87-MG (d) and U-251 MG (e). PLCβ1-silenced cells (shPLCβ1) were compared to wild type (WT) and mock-transduced (shCTRL) cells. Nuclei were stained using Hoechst 33342 (blue). Results are representative of at least five different fields.

3. Study of the impact of PLC γ 1 in glioblastoma

PLC γ 1 gene expression correlates with the pathological grade of gliomas

In order to evaluate the potential role of PLC γ 1 in the pathogenesis of HGGs, we started from the analysis of three hundred twenty-five (n=325) samples collected in the same online public database used for PLC β 1 (CGGA). From this analysis it was evidenced that PLC γ 1 gene expression positively correlates with the gliomas' pathological grade. WHO IV gliomas showed a higher PLC γ 1 gene expression compared to WHO II and WHO III (Fig. 25a). Furthermore, Kaplan-Meier curves, processed with the same public database, support the hypothesis that patients characterized by an overall higher PLC γ 1 gene expression have a lower survival probability, regardless of the grade of gliomas in both primary and recurrent ones (Fig. 25b).

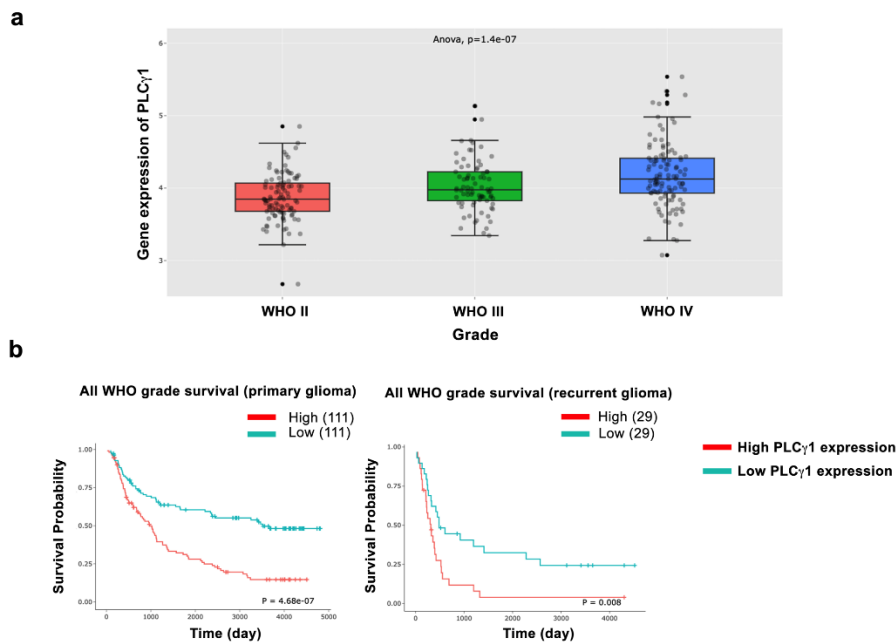


Figure 25: PLC γ 1 gene expression correlates with gliomas' pathological grade. Panel a: Distribution of PLC γ 1 expression in gliomas according to WHO classification of patients collected in the CGGA database. WHO II, n=103; WHO III, n=79; WHO IV, n=139. PLC γ 1 mRNA expression positively correlates with gliomas' pathological grade ($p=1.4e-07$). Panel b: Kaplan-Meier survival curves, extracted from the CGGA dataset, of PLC γ 1 high or low expression patient groups. Patients were divided according to the median level of PLC γ 1 mRNA expression ($p < 4.68e-07$ and $p = 0.008$).

Glioblastoma patients are characterized by higher PLC γ 1 gene expression compared to healthy individuals

In order to deepen the retrospective study focused on the role of phospholipases in glioblastoma, we analysed the same fifty (n=50) tissue samples used for PLC β 1 analysis, for their PLC γ 1 gene expression, comparing them with the four (n=4) healthy samples pools. The expression analysis showed that glioblastoma patients

were characterized by an overall higher PLC γ 1 gene expression compared to healthy controls (*Fig. 26a*). This result led to the idea that this phospholipase could play a fundamental role in the pathogenesis of glioblastoma and that it could be valued as a signature gene for the molecular classification of high-grade tumors.

Patients with mutated IDH1 have lower PLC γ 1 expression than patients with IDH1 wild type

The retrospective patients' samples database showed only six out of a total of fifty samples (6/50) as IDH1-mutated. Considering that these point mutations appear to define molecularly tumors that are associated with younger age and more favorable outcome¹²³, we decided to deepen our analysis evaluating the PLC γ 1 gene expression in these two populations differing in IDH1 mutation presence.

It is important to specify that before the new 2021 WHO classification of gliomas⁵, glioblastoma and grade 4 astrocytoma with mutation in IDH, were considered the same kind of lesion, identified as glioblastoma. Only in the recent years, the molecular, clinical, and biological differences between these two entities have been investigated more in depth. Consequentially, considering that these patients' samples were collected and diagnosed before 2021, we considered them as glioblastomas.

Data were calculated stratifying the entire glioblastoma population, where PLC γ 1 expression was calculated as fold changes relative to the expression levels of the four (n=4) control pools. From this evaluation it emerged a lower PLC γ 1 gene expression in the six (n=6) IDH-mutated samples (IDH1-mut) compared to the IDH1 wild-type (IDH1-wt) population (forty-four samples) (*Fig. 26b*). This difference, however, does not reach statistical significance, possibly due to the difference in the numerosity of IDH1 mutated cases compared to the rest of glioma population, which reflects our database samples situation. However, these data support the correlation between PLC γ 1 gene expression and tumor aggressiveness, since IDH1-wt gliomas are commonly associated with an overall poorer prognosis for patients¹²⁴.

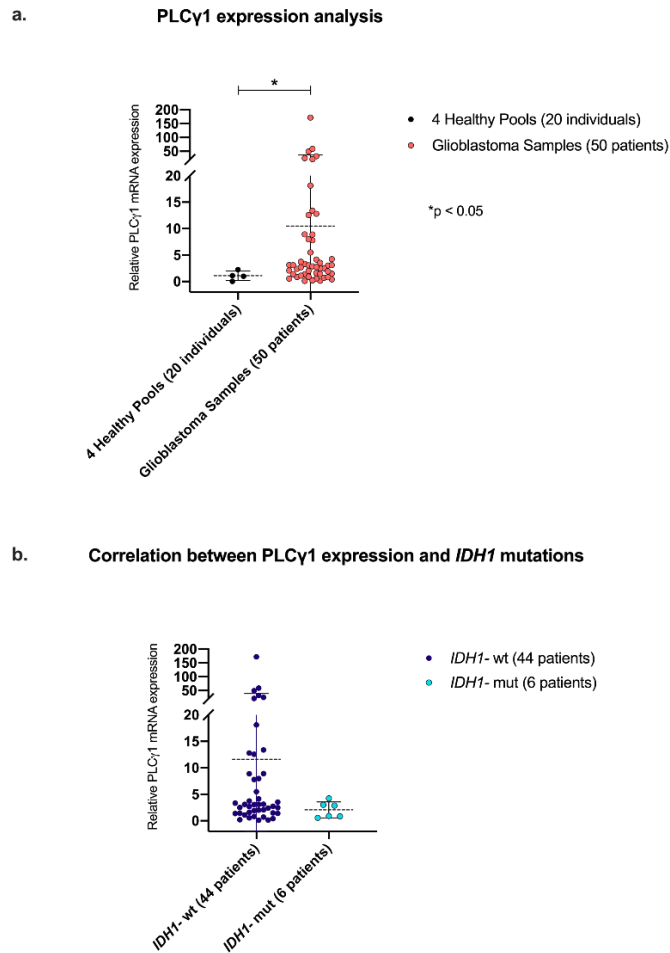


Figure 26: Panel a: Glioblastoma patients are characterized by higher PLCγ1 gene expression compared to healthy individuals. PLCγ1 gene expression in 50 glioblastoma patients' samples and 4 healthy pools of 5 donors each, used as controls (20 individuals in total). The distribution of PLCγ1 gene expression in glioblastoma tissue samples compared to controls was displayed through scatter plots. 18S was used as housekeeping gene and data were presented as fold changes relative to the expression levels of control samples in accordance with the $2^{-\Delta\Delta C_t}$ formula. Asterisks indicate statistically significant differences between the groups, with $*p < 0.05$. Panel b: Correlation between PLCγ1 expression and IDH1 mutations. Evaluation of PLCγ1 gene expression in 50 glioblastoma patients' samples which were divided according to the presence or absence of IDH1 mutations. Six IDH1 mutated patients' samples (IDH1-mut) were compared to forty-four IDH1-wild-type (IDH1-wt) patients' samples. Scatter Plots displayed data as fold changes relative to the expression levels of control samples in accordance with the $2^{-\Delta\Delta C_t}$ formula.

PLCγ1 silencing leads to decreased cell migration and invasion in U87-MG

To better understand the role of PLCγ1 in glioblastoma, we decided to create an *in vitro* model based on U87-MG glioblastoma cell line. We transiently silenced PLCγ1 in this cell model to analyse the effect on the main aggressiveness mechanisms related to tumor transformation, such as migration and invasion. Firstly, U87-MG silenced cells (shPLCγ1) were tested for PLCγ1 gene expression and compared to wild type (WT) cells and to cells transduced with empty vectors coding only for GFP (shCTRL) (Fig. 27a). Later, we examined the migration potential of PLCγ1-silenced cells through a transwell method. It was showed that, following PLCγ1 downregulation, U87-MG cells exhibited significantly reduced potential of migration compared to control cells (Fig. 27b,c). Next, the same transwell assay was performed with the addition of a Geltrex coating in order to

evaluate the consequences of PLC γ 1 silencing on the invasion ability of the cells. This test displayed that PLC γ 1-silenced U87-MG had significantly lower invasion ability than the respective controls (Fig. 27d,e).

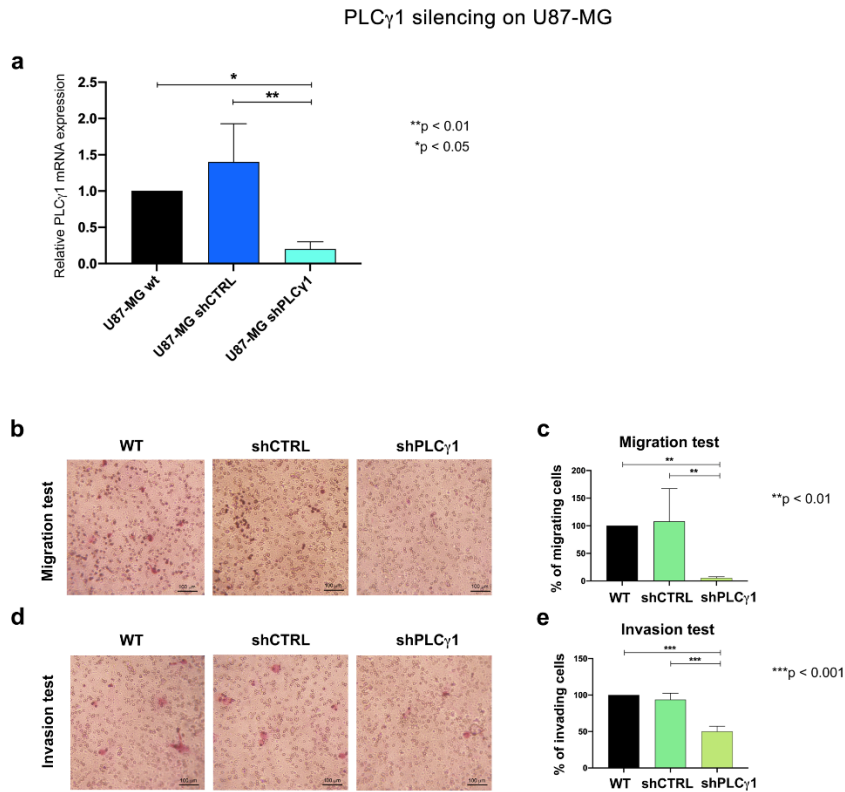


Figure 27: PLC γ 1 silencing on U87-MG cell line and relative consequences analyses on migration and invasion abilities. Panel a: PLC γ 1 mRNA expression on U87-MG cell line after PLC γ 1 silencing. PLC γ 1-silenced cells (shPLC γ 1) were compared to wild type (WT) and mock-transduced cells (shCTRL). U87-MG were analyzed after 48 h of hygromycin selection, i.e. 96 h after transduction overall. GAPDH was used as housekeeping gene and three independent experiments were carried out for the analysis, with $**p < 0.01$, $*p < 0.05$. Panels b and c: Representative images of transwell migration assay in U87-MG cell line (b), with the relative graphical representation (c). PLC γ 1-silenced cells (shPLC γ 1) were compared to wild type (WT) and mock-transduced (shCTRL) cells. Magnification 20x (bar: 100 μ m). Columns show the mean \pm SD of three independent experiments with $**p < 0.01$. Panels d and e: Representative images of transwell invasion assay, with a Geltrex coating, in U87-MG (d), with the relative graphical representation (e). PLC γ 1-silenced cells (shPLC γ 1) were compared to wild type (WT) and mock-transduced (shCTRL) cells. Magnification 20x (bar: 100 μ m). Columns show the mean \pm SD of three independent experiments with $***p < 0.001$.

PLC γ 1 overexpression leads to increased cell migration and invasion in U87-MG

To reinforce all these evidences, we decided to carry out a transient PLC γ 1 overexpression on the same cell model. Even under these circumstances, PLC γ 1 gene expression and the relative overexpression were first confirmed through a Real-Time PCR analysis (Fig. 28a), comparing U87-MG cells overexpressing PLC γ 1 (ovPLC γ 1) to the respective controls (WT and negCTRL). Therefore, transwell migration assay evidenced that cells overexpressing PLC γ 1 had a higher ability to migrate than controls (Fig. 28b,c). The transwell invasion assay with the Geltrex coating was further carried out, confirming an opposite attitude to the one emerged

following PLC γ 1 downregulation. Indeed, after the overexpression of PLC γ 1, there was an increase in the ability of U87-MG cells to invade (Fig. 28d,e). Therefore, a positive correlation between PLC γ 1 expression level and the cellular migration and invasion potential was confirmed in U87-MG, strengthening what was already present in literature.

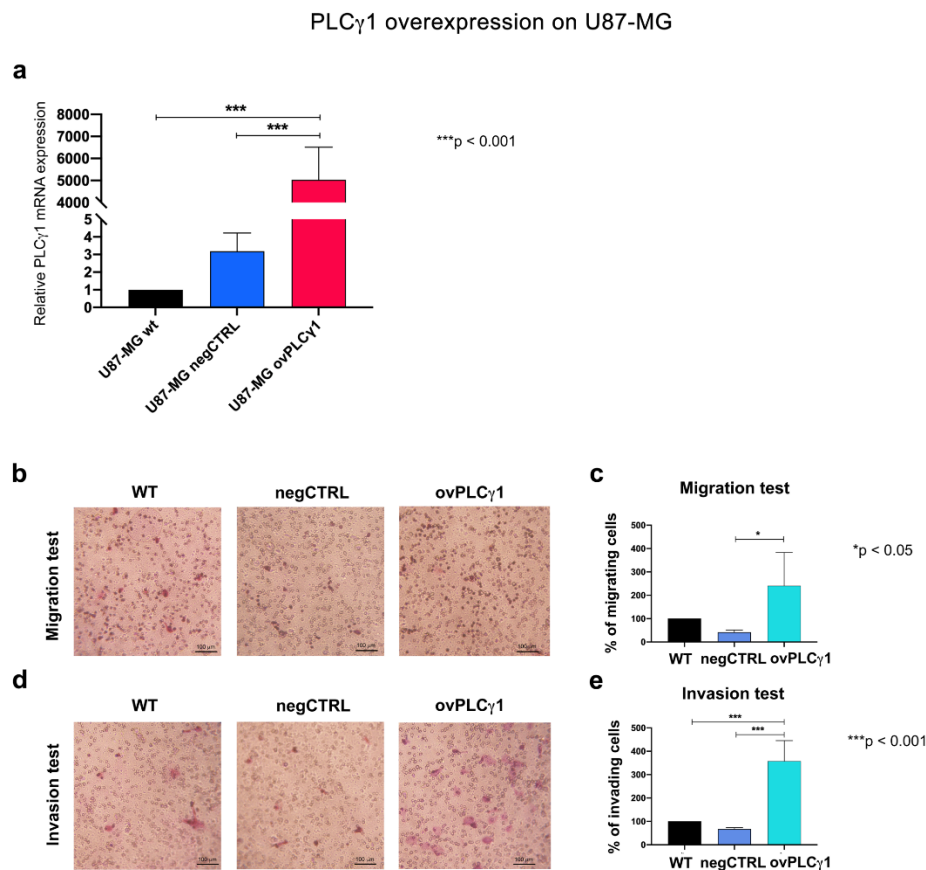


Figure 28: PLC γ 1 overexpression on U87-MG cell line and relative consequences analyses on migration and invasion cell abilities. Panel a: PLC γ 1 mRNA expression on U87-MG cell line after PLC γ 1 overexpression. Cells overexpressing PLC γ 1 (ovPLC γ 1) were compared to wild type (WT) and mock-transduced cells (negCTRL). U87-MG were analyzed after 48 h of hygromycin selection, i.e. 96 h after transduction overall. GAPDH was used as housekeeping gene and three independent experiments were carried out for the analysis, with *** $p < 0.001$. Panels b and c: Representative images of transwell migration assay in U87-MG cell line (b), with the relative graphical representation (c). Cells overexpressing PLC γ 1 (ovPLC γ 1) were compared to wild type (WT) and mock-transduced (negCTRL) cells. Magnification 20x (bar: 100 μ m). Columns show the mean \pm SD of three independent experiments with * $p < 0.05$. Panels d and e: Representative images of transwell invasion assay, with a Geltrex coating, in U87-MG (d), with the relative graphical representation (e). Cells overexpressing PLC γ 1 (ovPLC γ 1) were compared to wild type (WT) and mock-transduced (negCTRL) cells. Magnification 20x (bar: 100 μ m). Columns show the mean \pm SD of three independent experiments with *** $p < 0.001$.

PLC γ 1 downregulation in GSCs affects the expression of some transcripts implicated in the mechanisms of tumor aggressiveness

Given the preliminary data collected on immortalized cell lines at the University of Bologna on the possible role of PLC γ 1 in the pathogenesis of glioblastoma, we decided to continue this study at Brown University (Laboratory of Cancer Epigenetics and Plasticity) by using patient-derived glioblastoma stem cells (GSCs).

These cells are part of a specific tumor population that drives aggressiveness, resistance, and recurrence in glioblastoma. Initially, seven (n=7) different GSCs were screened, at protein level, to identify the ones with higher PLC γ 1 expression (Fig. 29a). Due to their high levels of PLC γ 1, GB2 and GB9 cells were selected and used as main cell models. Next, PLC γ 1 was transiently silenced in these GSCs and RNA and proteins were collected 72 hours post-transfection. After this time, silenced cells (siPLC γ 1 cells) were tested for PLC γ 1 protein expression and compared to cells transduced with only the empty vectors (siCTRLs) (Fig. 29b).



Figure 29: PLC γ 1 protein expression in wild type cells and PLC γ 1-downregulated cells. Panel a: PLC γ 1 protein expression in 7 different GSCs. Panel b: western blot analysis of PLC γ 1 expression in GB2 and GB9 following PLC γ 1 downregulation. Western blot results are representative of three independent experiments. GAPDH was used as housekeeping gene.

Analyses of the effect of the PLC γ 1 level variation on the GSCs' transcriptomic profile via RNA-seq were performed after confirming an optimal PLC γ 1 downregulation. Principal Component Analysis (PCA) plots (Fig. 30a,b) showed that the PLC γ 1 downregulation effect is reproducible since GSCs segregated by condition. Going into more detail:

- 1) Differential analysis in GB2, revealed sixty-three (n=63) number of differentially expressed genes. Among these genes, nineteen (n=19) were upregulated and forty-two (n=42) were downregulated (Fig. 30c).
- 2) Differential analysis in GB9, revealed two hundred and five (n=205) number of differentially expressed genes. Among these genes one hundred and twelve (n=112) were upregulated and ninety-three (n=93) were downregulated (Fig. 30d).

By grouping the common genes between the two GSCs, the analysis revealed the presence of twenty-five (n=25) shared dysregulated genes (4 upregulated, 21 downregulated) following PLC γ 1 downregulation (genes are listed in Table 6 and Table 7). GO enrichment analysis of the shared upregulated genes (Fig. 30e) exhibited a significant (p<0.05) enrichment for pathways that negatively regulate cell motility and migration. Among these genes it was possible to evidence Neuron navigator 3 (NAV3), which reduction is associated to cancer development¹²⁵ and Dual Specificity Phosphatases 10 (DUSP10), which belongs to a family of stress-induced enzymes that provide feedback inhibition on mitogen-activated protein kinases (MAPKs), critical in key aspects of oncogenic signalling¹²⁶. GO enrichment analysis of the shared downregulated genes (Fig. 30f)

exhibited a significant ($p < 0.05$) enrichment for pathways involved in cancer development and progression (EGFR pathway and ERBB signaling pathway). These results on GSCs, although preliminary, confirmed a correlation between PLC γ 1 expression level and the presence of a more aggressive cellular phenotype in glioma.

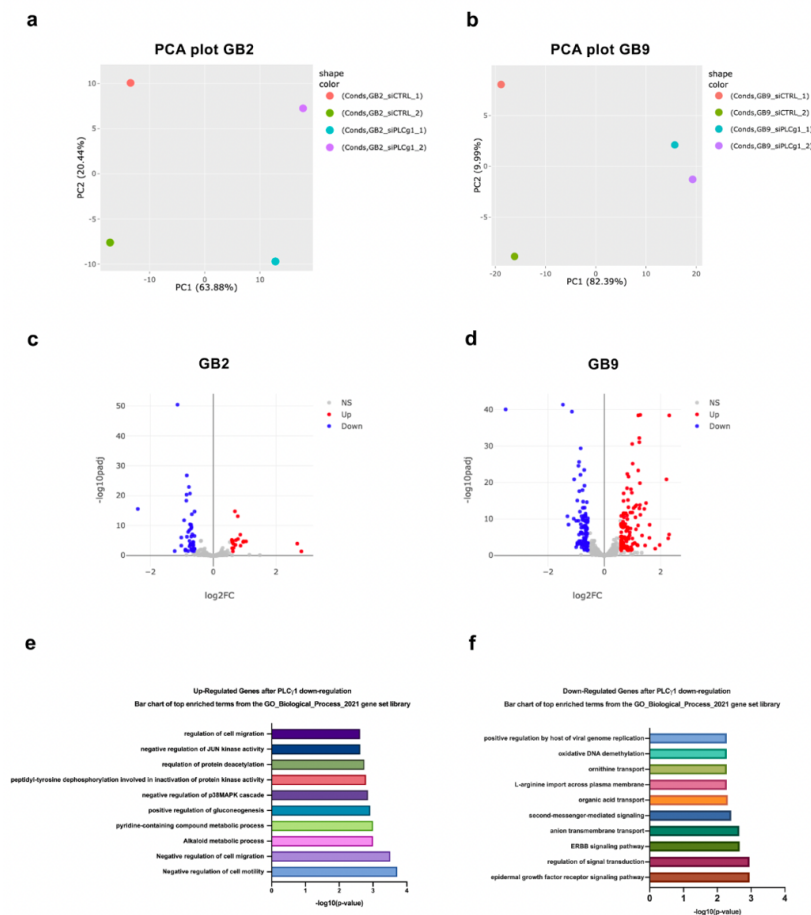


Figure 30: Analysis of the effect of PLC γ 1 downregulation on GSCs' (GB2 and GB9) transcriptomic profile via RNA-seq. Panels a and b: PCA plots for transcriptomic data of R in GB2 and GB9, respectively. For each GSC two samples were analysed, for ensure the biological duplicate. Panels c and d: RNA-seq volcano plots of differentially expressed genes which emphasizes upregulated (red) and downregulated subset of genes (blue) following PLC γ 1 downregulation ($P < 0.05$, $FC = 1.5$) in GB2 and GB9, respectively. Panels e and f: The top 10 enrichment scores in the GO pathway enrichment analysis of the (e) 4 shared upregulated and (f) downregulated genes.

Shared Upregulated Genes
NAV3
TFPI2
DUSP10
NNMT

Table 6: List of the 4 shared upregulated genes in GB2 and GB9 following PLC γ 1 downregulation. Analysis was conducted with DEBrowser. $P < 0.05$, $FC = 1.5$

Shared Downregulated Genes
SLC7A2
MAP4K5
SZRD1
NUTF2
TOR1AIP1
TRIB2
NUCKS1
TLE2
TDG
SOBP
XPR1
SLC23A2
SESN3
IGFBP4
PLCG1
SIMC1
DYNLT1
DGKD
LMO4
CNNM3
DNP1

Table 7: List of the 21 shared downregulated genes in GB2 and GB9 following PLC γ 1 downregulation. Analysis was conducted with DEBrowser. $P < 0.05$, $FC = 1.5$

Discussion

Glioblastoma is the most aggressive and lethal brain tumor in adults. The standard care of treatment is tumor resection, radiotherapy, and chemotherapy but despite these invasive therapeutic approaches, glioblastoma prognosis remains unchanged. Indeed, this kind of tumor develops resistance to treatments and recur quickly, due to its great complexity and heterogeneity¹²⁷. For this reason, the management of glioblastoma represents a great challenge and the understanding of the molecular mechanisms related to tumor transformation could help to find a successful targeted therapeutic strategy. Several studies have shown the significance of lipid signaling and phospholipases (PLCs) in the regulation of different cellular mechanisms such as cell proliferation, differentiation, migration and cell cycle⁶⁰ and in many physio-pathological brain processes^{59,88}. It has been also documented that some PLCs are involved in several brain disorders including epilepsy, movement and behavior disorders, neurodegenerative diseases, and also high-grade gliomas⁸⁸. A 2016 *in silico* study reported that PLC β 1, one of the most expressed PLC isoforms in the brain, was a potential prognostic factor and accordingly, a candidate signature gene for specific subtypes of glioblastoma and that PLC β 1 gene expression was inversely correlated with the pathological grade of gliomas⁹⁹. It was also demonstrated that glioma patients with intermediate PLC β 1 expression survived significantly longer than PLC β 1 downregulated group⁹⁹. Moreover, it has been already evidenced in literature the possible involvement of PLC γ 1, another PLC isoform highly represented in the brain, in glioblastoma progression and aggressiveness, also considering its upstream activators: PDGF and EGF, which are dominant mediators of cell growth and proliferation¹⁰². Furthermore, PLC γ 1 mutation and involvement in the processes of tumorigenesis, including migration, invasion, and proliferation, in different tumors were already frequently evidenced¹²⁸. For example, PLC γ 1 activation is related to angiosarcoma progression, and its upregulation and mutation have been consistently associated with poor patient survival¹²⁹. PLC γ 1 role is also linked to squamous cell carcinoma¹³⁰, colorectal and gastric cancers¹³¹. PLC γ 1 key role in the progression of different tumors is probably related to PLC γ 1 strategic position at a convergence point of various signaling pathways, including growth factor receptor signaling and adhesion receptor signaling for cell spreading, invasion, and migration.

Our study was focused on searching key molecules in the mechanisms of tumor pathological progression that can possibly be used as diagnostic or prognostic factors in HGGs, which are characterized by a great biological heterogeneity. Therefore, in order to highlight the importance that phospholipases could have in the pathogenesis of these complex tumors, we started two studies in parallel, focused on the possible pathological impact in glioblastoma of PLC β 1 and PLC γ 1, respectively. *In silico* studies were firstly carried out by using an online analysis platform: the Chinese Glioma Genome Atlas (CGGA) RNA sequencing (RNA-seq) dataset (mRNAseq_325) with 325 glioma samples. Through this database it was evaluated the gene expression of PLC β 1 and PLC γ 1 in different types of gliomas. Interestingly, this study confirmed data already present in literature, showing that PLC β 1 gene expression was significantly reduced in all WHO IV gliomas (glioblastomas), compared to WHO II and WHO III ones, suggesting a strongly pathological role of PLC β 1

low expression. Furthermore, Kaplan-Meier survival curves from CGGA dataset, demonstrated that patients with indistinct grade of gliomas, characterized by low expression of PLC β 1, had a shorter survival time in both primary and recurrent gliomas compared to patients with high-PLC β 1 expression. These data confirmed that PLC β 1 expression level is inversely correlated with the pathological grade of gliomas and that PLC β 1 low expression may be related to patients' worse prognosis. On the contrary, it was demonstrated that PLC γ 1 expression increased in high-grade gliomas compared to low-grade ones. The previous *in silico* data were strengthened by the retrospective analysis of PLC β 1 and PLC γ 1 mRNA expression in fifty (n=50) fresh-frozen glioblastoma tissue samples in comparison with twenty (n=20) healthy individuals divided into four (n=4) different pools. This analysis confirmed that PLC β 1 gene expression was lower in glioblastoma samples not only compared to low-grade tumors, but also compared to healthy individuals. The opposite trend was instead confirmed for PLC γ 1, suggesting this phospholipase as an ideal future biomarker with the potential to assess cancer risk and to promote early diagnosis. Moreover, the retrospective analysis showed a difference in PLC γ 1 expression level also between populations characterized by the presence or absence of isocitrate dehydrogenase 1 (IDH1) mutation, highlighting an overall lower PLC γ 1 gene expression in six (n=6) IDH1-mutated patients' samples compared to forty-four (n=44) IDH1-wt ones. IDH1-mutated samples are classified as Adult-type Diffuse Astrocytoma, IDH mutant, grade 4, following the recent tumor classification update⁵. Considering that gliomas expressing the mutated isoforms of IDH1/2 have better prognosis than wild-type ones¹²⁴, our analysis strengthened a positive correlation between PLC γ 1 expression and glioma aggressiveness.

As for PLC β 1, the previous results were further strengthened through a prospective study. Twenty-three (n=23) patients characterized by different grade of gliomas were enrolled and analyzed for their PLC β 1 expression comparing them with twenty (n=20) healthy individuals' samples divided in four (n=4) different pools used as control. Interestingly, this study highlighted an overall lower PLC β 1 gene expression in all the twenty-three (n=23) glioma samples compared to the healthy controls. Although this result evidenced only a descriptive trend and the necessity for further analyses with a larger number of participants, it confirmed that PLC β 1 could be a pivotal gene involved in glioma's carcinogenesis and progression, probably acting as an onco-suppressor. Through the analysis of these samples, it was also observed less PLC β 1 expression level in glioblastoma patients compared to the oligodendroglioma ones confirming our previous analyses that showed a PLC β 1 lower expression in the most aggressive gliomas' phenotypes. Through the same study it was also evidenced that the mean PLC β 1 expression was consistently lower in the only four (n=4) patients who received recurrence diagnosis compared to the non-relapsed ones, suggesting PLC β 1 as a gene capable of stratifying not only the various glioma's grades, but among the high ones, even those with the highest probability of recurrence.

Subsequently, in order to verify the pathological effects of PLC β 1 downregulation, two different *in vitro* models were generated by PLC β 1 stable downregulation on U87-MG and U-251 MG (glioblastoma immortalized cell lines). Moreover, a transient silencing was also performed on Human Primary Astrocytes (HA), in order to mimic and best represent the tumor heterogeneity, working on both engineered tumor cell lines and normal astrocytes. Since tumor proliferation, invasion and migration are the main causes of resistance

to current therapies, we focused the analyses on these mechanisms of aggression. It is known that during metastasis formation, glioblastoma cells are characterized by morphological and molecular changes shifting the lesion towards a more undifferentiated state, acquiring mesenchymal features, including ECM remodeling and degradation¹³². Accordingly, we focused our study on the expression analysis of some of the main mesenchymal characters of ECM degradation. In all the models silenced for PLC β 1, it was observed an increased expression of Slug, an essential transcriptional factor that is involved in the regulation of mesenchymal phenotype, and N-Cadherin, one of the main mesenchymal markers. In addition, since the main driver of ECM degradation is proteolytic digestion by matrix metalloproteinases (MMPs), which expression is strongly linked to the acquisition of a mesenchymal phenotype¹³², we evaluated MMP-2 and MMP-9, which expression increased following PLC β 1 downregulation. These data were further enhanced by the increment of migration and invasion abilities of the PLC β 1-downregulated cells, suggesting that the downregulation of PLC β 1 in glioblastoma promoted a shift towards a more aggressive cellular phenotype. Moreover, PLC β 1 downregulation also affected cell proliferation, as demonstrated by the increased expression of the nuclear marker Ki-67¹³³ in all the silenced models compared to the controls. It is well known the role of β -Catenin, a component of the cell-cell adhesion complex, in the regulation of proliferation and migration in different cell models and tumors¹¹⁹, and interestingly, the active form of this protein was overexpressed in all the models silenced for PLC β 1. Following PLC β 1 downregulation in our models, the translocation of active β -catenin into the nucleus of the cells appeared to be favored, as shown by the immunocytochemical analysis. As a result, this event led β -catenin to recruit, in the nucleus, transcriptional factors and to regulate the activation of different target genes related to proliferation and invasion, such as c-Myc and MMPs, both of which increased in our PLC β 1-silenced models. It was also evidenced an increment in ERK1/2 pathway activation following PLC β 1 downregulation. This latter is a fundamental pro-surviving factor involved in tumor progression and resistance to current therapies¹³⁴. In glioma cells, the epidermal growth factor (EGF)/EGFR signaling through ERK1/2 leads to the phosphorylation of α -catenin, which, together with cadherin, forms a complex linked to the cytoskeleton, promoting β -catenin transactivation and glioma cell invasion¹³⁵. Furthermore, considering the key role of PPAR γ in the CNS¹³⁶ and the well-known crosstalk between this latter and β -catenin pathway¹³⁷, we considered the consequences of PLC β 1 downregulation on its protein expression. All the PLC β 1-silenced cells showed a decline in PPAR γ protein expression compared to control samples, confirming its opposite behavior compared to β -catenin pathway. Substantially, our engineered models showed how PLC β 1 downregulation led to an increased cell survival. Indeed, following PLC β 1 silencing, it was also shown an increased activation of Stat3 pathway, which is a well-defined oncogenic transcription factor that plays a role in tumor resistance and cancer development in glioblastoma¹³⁸. The increased activation of the pathways mentioned above, reinforced the hypothesis that PLC β 1 downregulation in glioblastoma promotes a more aggressive phenotype. All in all, *in silico* data from database, data collected on glioblastoma samples through both the retrospective and the prospective study, together with cellular and molecular data on engineered immortalized and primary cell lines, suggest a potential role of PLC β 1 in maintaining a normal or less

aggressive phenotype of glioma (Fig. 31). However, the mechanisms by which PLC β 1 is downregulated in high-grade tumors are not clear yet. Further studies to detect epigenetic anomalies associated with glioblastoma are necessary. This step could result fundamental in the detection of responsible genes that could respond to hypomethylating therapies. This work suggests that PLC β 1 silencing and the consequent involvement of its downstream pathways, can determine different relevant physio-pathological alterations, leading the cells to acquire a greater ability to migrate, invade, proliferate and survive, fundamental mechanisms for the acquisition of resistance to common therapies.

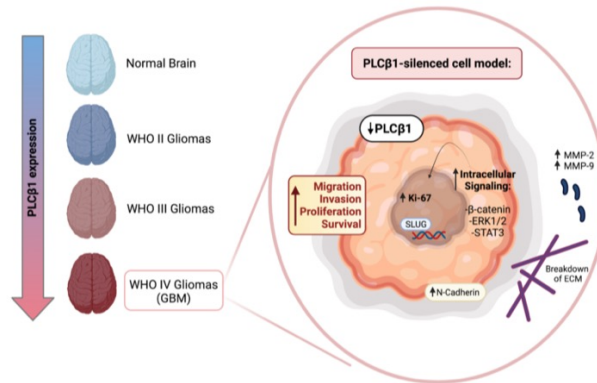


Figure 31: Image that summarizes the possible involvement of PLC β 1 in glioblastoma¹⁰⁴.

As for the study focused on the effective pathological role of PLC γ 1 in glioblastoma, it was carried out an *in vitro* study based on engineered U87-MG cell line, already cited in literature as a cell model whose migration is PLC-dependent⁷⁴. These cells were in parallel subjected to PLC γ 1 transient downregulation and overexpression, in order to evaluate the effects of these modulations on cell migration and invasion, which, as already mentioned, represent the main mechanisms that drive tumor aggressiveness¹²⁷. As expected, PLC γ 1-silenced cells showed less ability to migrate and invade compared to the respective controls. On the contrary, cells overexpressing PLC γ 1 acquired greater aggressiveness linked to an increased ability of migration and invasion (Fig.32).

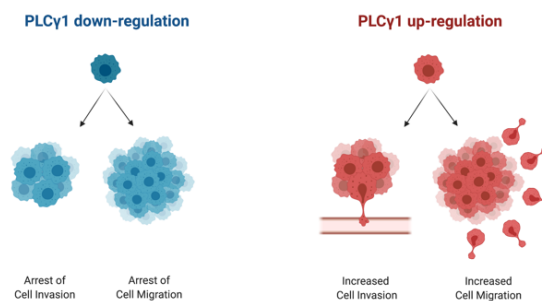


Figure 32: Image that summarizes the consequences of PLC γ 1 modulation¹⁰⁵.

All in all, data collected on patients' biopsies and engineered cell models, suggested a strong correlation between PLC γ 1 expression and the acquisition of a more aggressive tumor phenotype. Finally, this trend was further investigated at Brown University, using patient-derived glioblastoma stem cells (GSCs) as cell models. Effectively, these cells are usually responsible for aggressiveness, resistance, and recurrence in glioblastoma¹³⁹. GSCs analysis on the transcriptomic profiles, confirmed that PLC γ 1 downregulation modulated positively the expression of genes involved in pathways that negatively regulate cell motility and migration. Moreover, it was evidenced that PLC γ 1 downregulation led also to a decreased expression of genes involved in cancer development and progression, confirming a correlation between PLC γ 1 expression and the presence of a more aggressive cellular and glioma's phenotype. This result highlights the importance of further investigating PLC γ 1 as potential biomarker for glioblastoma stratification and target for personalized medicine in the development of new therapeutic strategies for glioblastoma. Indeed, in a second phase of the study, based on PLC γ 1 putative protein structure, it will be possible to carry out a virtual screen with the use of digital libraries of small molecules, to predict new potential drugs directed against this target. Moreover, although PLC β 1 and PLC γ 1 appear to have an opposite trend in glioblastoma, these two enzyme isoforms do not seem to have a compensatory trend between each other (*Fig. 33*), highlighting the importance of investigating deeply the pathological or protective role of phospholipases and their intermediaries in glioblastoma, making them potential targets in the search for new therapeutic approaches. All in all, the complete understanding of the events linked to phospholipases, and the specific role of the investigated signaling pathways related to them, could allow the correlation between tumor pathological mechanisms and the identification of future useful prognostic biomarkers and targets in the development of new therapeutic strategies for glioblastoma.

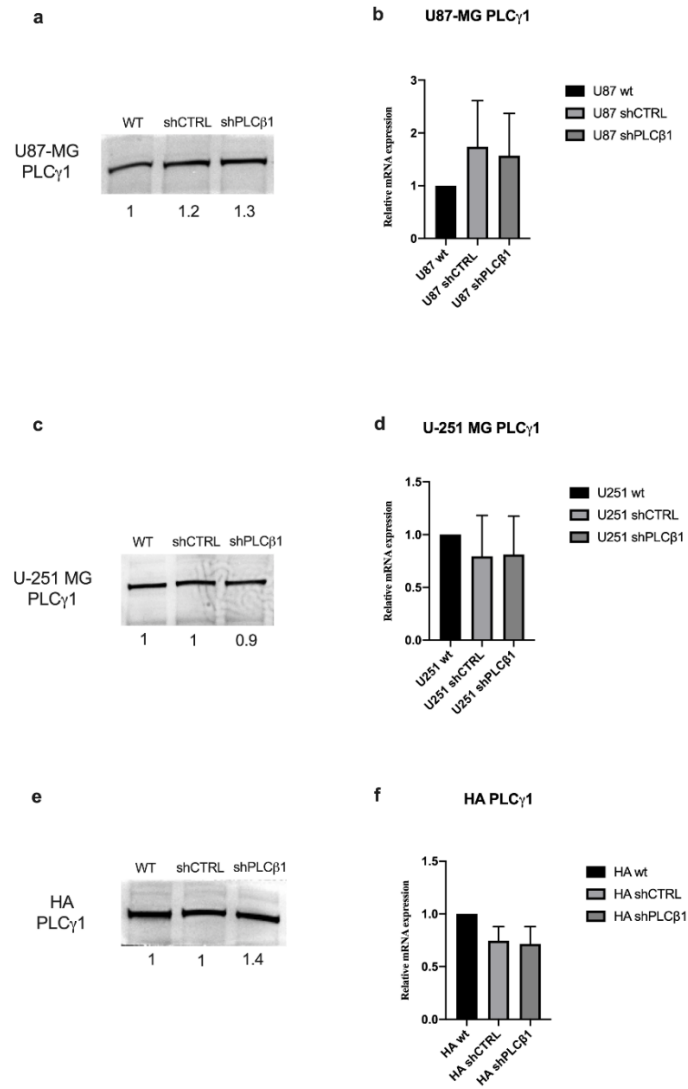


Figure 33: Consequences of PLC β 1 modulation on PLC γ 1 expression: Panels a, c and e: Western blot analysis of PLC γ 1 expression after PLC β 1 silencing on U87-MG (a), U-251 MG (c) and HA primary astrocytes (e). This analysis showed that although PLC β 1 and PLC γ 1 appear to have an opposite trend in glioblastoma, these two enzyme isoforms do not have a compensatory trend between each other.

Conclusions

So far, these studies confirmed the role of PLC β 1 and PLC γ 1 as novel potential modulators of aggressiveness in glioblastoma. Indeed, PLC β 1 and PLC γ 1 appear to be pathophysiologically involved in tumor's origin, development and progression. In particular, it has been reported the potential involvement of PLC γ 1 in the aggressiveness of glioblastoma. A positive correlation has been highlighted between its gene expression and tumor aggressiveness both in retrospective patients and in cellular models. On the contrary, it was shown that PLC β 1 gene expression level inversely correlates with the pathological grade of gliomas, suggesting PLC β 1 as a potential prognostic factor and accordingly, a novel signature gene for the molecular classification of high-grade gliomas. However, the mechanisms by which phospholipases are modulated in high-grade tumors are not clear yet and further studies to detect genetic and epigenetic anomalies associated with glioblastoma are needed. All in all, the use of a translational approach, with both molecular and clinical evaluations, and the combination between prospective and retrospective studies could allow to find specific biomarkers capable of stratifying low- and high- grade tumors, characterized by important biological heterogeneity. This could result in the possibility of stratifying therapies, considering the molecular pedigree of patients. The use of more specific therapies could thus lead to best treatment results and to a risk reduction for the patients, with a very strong social impact. Considering that therapies remained almost unchanged for more than 20 years, this project could have also a strong economic impact, proposing new potential therapeutic targets, as PLC γ 1, or new diagnostic and / or prognostic markers, as PLC β 1, able to stratify the various types of gliomas, their grade and also their phenotypic characteristics, including the probability of recurrence. This could lead to pharmaceutical industries or biomedical companies' involvement in the potential results of this study.

References

- 1 Davis, M. E. Epidemiology and Overview of Gliomas. *Semin Oncol Nurs* **34**, 420-429 (2018). <https://doi.org:10.1016/j.soncn.2018.10.001>
- 2 Ostrom, Q. T., Gittleman, H., Stetson, L., Virk, S. M. & Barnholtz-Sloan, J. S. Epidemiology of gliomas. *Cancer Treat Res* **163**, 1-14 (2015). https://doi.org:10.1007/978-3-319-12048-5_1
- 3 Louis, D. N. *et al.* cIMPACT-NOW update 6: new entity and diagnostic principle recommendations of the cIMPACT-Utrecht meeting on future CNS tumor classification and grading. *Brain Pathol* **30**, 844-856 (2020). <https://doi.org:10.1111/bpa.12832>
- 4 Gimple, R. C., Bhargava, S., Dixit, D. & Rich, J. N. Glioblastoma stem cells: lessons from the tumor hierarchy in a lethal cancer. *Genes Dev* **33**, 591-609 (2019). <https://doi.org:10.1101/gad.324301.119>
- 5 Louis, D. N. *et al.* The 2021 WHO Classification of Tumors of the Central Nervous System: a summary. *Neuro Oncol* **23**, 1231-1251 (2021). <https://doi.org:10.1093/neuonc/noab106>
- 6 Wesseling, P. & Capper, D. WHO 2016 Classification of gliomas. *Neuropathol Appl Neurobiol* **44**, 139-150 (2018). <https://doi.org:10.1111/nan.12432>
- 7 Ostrom, Q. T. *et al.* CBTRUS Statistical Report: Primary Brain and Other Central Nervous System Tumors Diagnosed in the United States in 2009-2013. *Neuro Oncol* **18**, v1-v75 (2016). <https://doi.org:10.1093/neuonc/now207>
- 8 Hwan-Ho Cho & Hyunjin Park. Classification of low-grade and high-grade glioma using multi-modal image radiomics features. *Annu Int Conf IEEE Eng Med Biol Soc* **2017**, 3081-3084 (2017). <https://doi.org:10.1109/EMBC.2017.8037508>
- 9 Jones, C., Perryman, L. & Hargrave, D. Paediatric and adult malignant glioma: close relatives or distant cousins? *Nat Rev Clin Oncol* **9**, 400-413 (2012). <https://doi.org:10.1038/nrclinonc.2012.87>
- 10 Brat, D. J. *et al.* cIMPACT-NOW update 3: recommended diagnostic criteria for "Diffuse astrocytic glioma, IDH-wildtype, with molecular features of glioblastoma, WHO grade IV". *Acta Neuropathol* **136**, 805-810 (2018). <https://doi.org:10.1007/s00401-018-1913-0>
- 11 Tesileanu, C. M. S. *et al.* Survival of diffuse astrocytic glioma, IDH1/2 wildtype, with molecular features of glioblastoma, WHO grade IV: a confirmation of the cIMPACT-NOW criteria. *Neuro Oncol* **22**, 515-523 (2020). <https://doi.org:10.1093/neuonc/noz200>
- 12 Losman, J. A. & Kaelin, W. G. What a difference a hydroxyl makes: mutant IDH, (R)-2-hydroxyglutarate, and cancer. *Genes Dev* **27**, 836-852 (2013). <https://doi.org:10.1101/gad.217406.113>
- 13 Haase, S. *et al.* Mutant ATRX: uncovering a new therapeutic target for glioma. *Expert Opin Ther Targets* **22**, 599-613 (2018). <https://doi.org:10.1080/14728222.2018.1487953>
- 14 Molinaro, A. M., Taylor, J. W., Wiencke, J. K. & Wrensch, M. R. Genetic and molecular epidemiology of adult diffuse glioma. *Nat Rev Neurol* **15**, 405-417 (2019). <https://doi.org:10.1038/s41582-019-0220-2>

- 15 Oronsky, B., Reid, T. R., Oronsky, A., Sandhu, N. & Knox, S. J. A Review of Newly Diagnosed Glioblastoma. *Front Oncol* **10**, 574012 (2020). <https://doi.org:10.3389/fonc.2020.574012>
- 16 Olympios, N. *et al.* Promoter Alterations in Glioblastoma: A Systematic Review. *Cancers (Basel)* **13** (2021). <https://doi.org:10.3390/cancers13051147>
- 17 Furnari, F. B. *et al.* Malignant astrocytic glioma: genetics, biology, and paths to treatment. *Genes Dev* **21**, 2683-2710 (2007). <https://doi.org:10.1101/gad.1596707>
- 18 Inda, M. M. *et al.* Chromosomal abnormalities in human glioblastomas: gain in chromosome 7p correlating with loss in chromosome 10q. *Mol Carcinog* **36**, 6-14 (2003). <https://doi.org:10.1002/mc.10085>
- 19 Zhang, Y. *et al.* The p53 Pathway in Glioblastoma. *Cancers (Basel)* **10** (2018). <https://doi.org:10.3390/cancers10090297>
- 20 van den Bent, M. J. & Chang, S. M. Grade II and III Oligodendroglioma and Astrocytoma. *Neurol Clin* **36**, 467-484 (2018). <https://doi.org:10.1016/j.ncl.2018.04.005>
- 21 Lv, L., Zhang, Y., Zhao, Y., Wei, Q. & Yi, Q. Effects of 1p/19q Codeletion on Immune Phenotype in Low Grade Glioma. *Front Cell Neurosci* **15**, 704344 (2021). <https://doi.org:10.3389/fncel.2021.704344>
- 22 De Vleeschouwer, S. (2017).
- 23 Ostrom, Q. T. *et al.* CBTRUS statistical report: Primary brain and central nervous system tumors diagnosed in the United States in 2006-2010. *Neuro Oncol* **15 Suppl 2**, ii1-56 (2013). <https://doi.org:10.1093/neuonc/not151>
- 24 Song, W. *et al.* Genetic epidemiology of glioblastoma multiforme: confirmatory and new findings from analyses of human leukocyte antigen alleles and motifs. *PLoS One* **4**, e7157 (2009). <https://doi.org:10.1371/journal.pone.0007157>
- 25 Chakrabarti, I., Cockburn, M., Cozen, W., Wang, Y. P. & Preston-Martin, S. A population-based description of glioblastoma multiforme in Los Angeles County, 1974-1999. *Cancer* **104**, 2798-2806 (2005). <https://doi.org:10.1002/cncr.21539>
- 26 Posti, J. P. *et al.* Presenting symptoms of glioma in adults. *Acta Neurol Scand* **131**, 88-93 (2015). <https://doi.org:10.1111/ane.12285>
- 27 Sharma, A. & Graber, J. J. Overview of prognostic factors in adult gliomas. *Ann Palliat Med* **10**, 863-874 (2021). <https://doi.org:10.21037/apm-20-640>
- 28 Weller, M. *et al.* EANO guidelines on the diagnosis and treatment of diffuse gliomas of adulthood. *Nat Rev Clin Oncol* **18**, 170-186 (2021). <https://doi.org:10.1038/s41571-020-00447-z>
- 29 Ellingson, B. M., Wen, P. Y. & Cloughesy, T. F. Modified Criteria for Radiographic Response Assessment in Glioblastoma Clinical Trials. *Neurotherapeutics* **14**, 307-320 (2017). <https://doi.org:10.1007/s13311-016-0507-6>

- 30 Louis, D. N. *et al.* The 2016 World Health Organization Classification of Tumors of the Central Nervous System: a summary. *Acta Neuropathol* **131**, 803-820 (2016). <https://doi.org:10.1007/s00401-016-1545-1>
- 31 Johnson, D. R. *et al.* Genetically Defined Oligodendroglioma Is Characterized by Indistinct Tumor Borders at MRI. *AJNR Am J Neuroradiol* **38**, 678-684 (2017). <https://doi.org:10.3174/ajnr.A5070>
- 32 Ullrich, R. T., Kracht, L. W. & Jacobs, A. H. Neuroimaging in patients with gliomas. *Semin Neurol* **28**, 484-494 (2008). <https://doi.org:10.1055/s-0028-1083696>
- 33 Shukla, G. *et al.* Advanced magnetic resonance imaging in glioblastoma: a review. *Chin Clin Oncol* **6**, 40 (2017). <https://doi.org:10.21037/cco.2017.06.28>
- 34 Bogomolny, D. L. *et al.* Functional MRI in the brain tumor patient. *Top Magn Reson Imaging* **15**, 325-335 (2004). <https://doi.org:10.1097/00002142-200410000-00005>
- 35 Suchorska, B., Tonn, J. C. & Jansen, N. L. PET imaging for brain tumor diagnostics. *Curr Opin Neurol* **27**, 683-688 (2014). <https://doi.org:10.1097/WCO.000000000000143>
- 36 Strumia, M. *et al.* Glioma vessel abnormality quantification using time-of-flight MR angiography. *MAGMA* **29**, 765-775 (2016). <https://doi.org:10.1007/s10334-016-0558-z>
- 37 Eigenbrod, S. *et al.* Molecular stereotactic biopsy technique improves diagnostic accuracy and enables personalized treatment strategies in glioma patients. *Acta Neurochir (Wien)* **156**, 1427-1440 (2014). <https://doi.org:10.1007/s00701-014-2073-1>
- 38 Grasbon-Frodl, E. M. *et al.* Intratumoral homogeneity of MGMT promoter hypermethylation as demonstrated in serial stereotactic specimens from anaplastic astrocytomas and glioblastomas. *Int J Cancer* **121**, 2458-2464 (2007). <https://doi.org:10.1002/ijc.23020>
- 39 Rong, Y., Durden, D. L., Van Meir, E. G. & Brat, D. J. 'Pseudopalisading' necrosis in glioblastoma: a familiar morphologic feature that links vascular pathology, hypoxia, and angiogenesis. *J Neuropathol Exp Neurol* **65**, 529-539 (2006). <https://doi.org:10.1097/00005072-200606000-00001>
- 40 Wesseling, P., van den Bent, M. & Perry, A. Oligodendroglioma: pathology, molecular mechanisms and markers. *Acta Neuropathol* **129**, 809-827 (2015). <https://doi.org:10.1007/s00401-015-1424-1>
- 41 Ostrom, Q. T. *et al.* CBTRUS Statistical Report: Primary Brain and Other Central Nervous System Tumors Diagnosed in the United States in 2012-2016. *Neuro Oncol* **21**, v1-v100 (2019). <https://doi.org:10.1093/neuonc/noz150>
- 42 Rao, A. M., Quddusi, A. & Shamim, M. S. The significance of MGMT methylation in Glioblastoma Multiforme prognosis. *J Pak Med Assoc* **68**, 1137-1139 (2018).
- 43 Riemenschneider, M. J., Hegi, M. E. & Reifenberger, G. MGMT promoter methylation in malignant gliomas. *Target Oncol* **5**, 161-165 (2010). <https://doi.org:10.1007/s11523-010-0153-6>
- 44 Herrlinger, U. *et al.* Lomustine-temozolomide combination therapy versus standard temozolomide therapy in patients with newly diagnosed glioblastoma with methylated MGMT promoter (CeTeG/NOA-09): a randomised, open-label, phase 3 trial. *Lancet* **393**, 678-688 (2019). [https://doi.org:10.1016/S0140-6736\(18\)31791-4](https://doi.org:10.1016/S0140-6736(18)31791-4)

- 45 He, Z. C. *et al.* Lower MGMT expression predicts better prognosis in proneural-like glioblastoma. *Int J Clin Exp Med* **8**, 20287-20294 (2015).
- 46 Buszek, S. M. *et al.* Optimal Timing of Radiotherapy Following Gross Total or Subtotal Resection of Glioblastoma: A Real-World Assessment using the National Cancer Database. *Sci Rep* **10**, 4926 (2020). <https://doi.org:10.1038/s41598-020-61701-z>
- 47 Wang, Z., Yang, G., Zhang, Y. Y., Yao, Y. & Dong, L. H. A comparison between oral chemotherapy combined with radiotherapy and radiotherapy for newly diagnosed glioblastoma: A systematic review and meta-analysis. *Medicine (Baltimore)* **96**, e8444 (2017). <https://doi.org:10.1097/MD.0000000000008444>
- 48 Campos, B., Olsen, L. R., Urup, T. & Poulsen, H. S. A comprehensive profile of recurrent glioblastoma. *Oncogene* **35**, 5819-5825 (2016). <https://doi.org:10.1038/onc.2016.85>
- 49 Stupp, R. *et al.* Radiotherapy plus concomitant and adjuvant temozolomide for glioblastoma. *N Engl J Med* **352**, 987-996 (2005). <https://doi.org:10.1056/NEJMoa043330>
- 50 Weller, M. & Le Rhun, E. How did lomustine become standard of care in recurrent glioblastoma? *Cancer Treat Rev* **87**, 102029 (2020). <https://doi.org:10.1016/j.ctrv.2020.102029>
- 51 Herrlinger, U. *et al.* Bevacizumab Plus Irinotecan Versus Temozolomide in Newly Diagnosed O6-Methylguanine-DNA Methyltransferase Nonmethylated Glioblastoma: The Randomized GLARIUS Trial. *J Clin Oncol* **34**, 1611-1619 (2016). <https://doi.org:10.1200/JCO.2015.63.4691>
- 52 Cairncross, G. *et al.* Phase III trial of chemoradiotherapy for anaplastic oligodendroglioma: long-term results of RTOG 9402. *J Clin Oncol* **31**, 337-343 (2013). <https://doi.org:10.1200/JCO.2012.43.2674>
- 53 Balana, C. *et al.* A phase II randomized, multicenter, open-label trial of continuing adjuvant temozolomide beyond 6 cycles in patients with glioblastoma (GEINO 14-01). *Neuro Oncol* **22**, 1851-1861 (2020). <https://doi.org:10.1093/neuonc/noaa107>
- 54 Gerber, D. E., Grossman, S. A., Zeltzman, M., Parisi, M. A. & Kleinberg, L. The impact of thrombocytopenia from temozolomide and radiation in newly diagnosed adults with high-grade gliomas. *Neuro Oncol* **9**, 47-52 (2007). <https://doi.org:10.1215/15228517-2006-024>
- 55 Gui, C., Lau, J. C., Kosteniuk, S. E., Lee, D. H. & Megyesi, J. F. Radiology reporting of low-grade glioma growth underestimates tumor expansion. *Acta Neurochir (Wien)* **161**, 569-576 (2019). <https://doi.org:10.1007/s00701-018-03783-3>
- 56 Ratti, S. *et al.* Nuclear Inositide Signaling Via Phospholipase C. *J Cell Biochem* **118**, 1969-1978 (2017). <https://doi.org:10.1002/jcb.25894>
- 57 Balla, T. Phosphoinositides: tiny lipids with giant impact on cell regulation. *Physiol Rev* **93**, 1019-1137 (2013). <https://doi.org:10.1152/physrev.00028.2012>
- 58 Xian, J. *et al.* Nuclear Inositides and Inositide-Dependent Signaling Pathways in Myelodysplastic Syndromes. *Cells* **9** (2020). <https://doi.org:10.3390/cells9030697>

- 59 Ratti, S. *et al.* Nuclear phospholipase C isoenzyme imbalance leads to pathologies in brain, hematologic, neuromuscular, and fertility disorders. *J Lipid Res* **60**, 312-317 (2019). <https://doi.org:10.1194/jlr.R089763>
- 60 Owusu Obeng, E. *et al.* Phosphoinositide-Dependent Signaling in Cancer: A Focus on Phospholipase C Isozymes. *Int J Mol Sci* **21** (2020). <https://doi.org:10.3390/ijms21072581>
- 61 Poli, A. *et al.* Nuclear Localization of Diacylglycerol Kinase Alpha in K562 Cells Is Involved in Cell Cycle Progression. *J Cell Physiol* **232**, 2550-2557 (2017). <https://doi.org:10.1002/jcp.25642>
- 62 Martelli, A. M. *et al.* Intranuclear 3'-phosphoinositide metabolism and Akt signaling: new mechanisms for tumorigenesis and protection against apoptosis? *Cell Signal* **18**, 1101-1107 (2006). <https://doi.org:10.1016/j.cellsig.2006.01.011>
- 63 Monteith, G. R., Prevarskaya, N. & Roberts-Thomson, S. J. The calcium-cancer signalling nexus. *Nat Rev Cancer* **17**, 367-380 (2017). <https://doi.org:10.1038/nrc.2017.18>
- 64 Rhee, S. G. Regulation of phosphoinositide-specific phospholipase C. *Annu Rev Biochem* **70**, 281-312 (2001). <https://doi.org:10.1146/annurev.biochem.70.1.281>
- 65 Cocco, L., Follo, M. Y., Manzoli, L. & Suh, P. G. Phosphoinositide-specific phospholipase C in health and disease. *J Lipid Res* **56**, 1853-1860 (2015). <https://doi.org:10.1194/jlr.R057984>
- 66 Manzoli, L. *et al.* Phosphoinositide signaling in nuclei of Friend cells: tiazofurin down-regulates phospholipase C beta 1. *Cancer Res* **55**, 2978-2980 (1995).
- 67 Gresset, A., Sondek, J. & Harden, T. K. The phospholipase C isozymes and their regulation. *Subcell Biochem* **58**, 61-94 (2012). https://doi.org:10.1007/978-94-007-3012-0_3
- 68 Audhya, A. & Emr, S. D. Regulation of PI4,5P2 synthesis by nuclear-cytoplasmic shuttling of the Mss4 lipid kinase. *EMBO J* **22**, 4223-4236 (2003). <https://doi.org:10.1093/emboj/cdg397>
- 69 Follo, M. Y. *et al.* Phosphoinositide-phospholipase C beta1 mono-allelic deletion is associated with myelodysplastic syndromes evolution into acute myeloid leukemia. *J Clin Oncol* **27**, 782-790 (2009). <https://doi.org:10.1200/JCO.2008.19.3748>
- 70 Manzoli, L. *et al.* Strategic Role of Nuclear Inositide Signalling in Myelodysplastic Syndromes Therapy. *Mini Rev Med Chem* (2014).
- 71 Arteaga, C. L. *et al.* Elevated content of the tyrosine kinase substrate phospholipase C-gamma 1 in primary human breast carcinomas. *Proc Natl Acad Sci U S A* **88**, 10435-10439 (1991). <https://doi.org:10.1073/pnas.88.23.10435>
- 72 Koss, H., Bunney, T. D., Behjati, S. & Katan, M. Dysfunction of phospholipase Cγ in immune disorders and cancer. *Trends Biochem Sci* **39**, 603-611 (2014). <https://doi.org:10.1016/j.tibs.2014.09.004>
- 73 Nomoto, K. *et al.* Expression of phospholipases gamma 1, beta 1, and delta 1 in primary human colon carcinomas and colon carcinoma cell lines. *Mol Carcinog* **12**, 146-152 (1995). <https://doi.org:10.1002/mc.2940120306>

- 74 Sala, G. *et al.* Phospholipase C γ 1 is required for metastasis development and progression. *Cancer Res* **68**, 10187-10196 (2008). <https://doi.org/10.1158/0008-5472.CAN-08-1181>
- 75 Fu, L. *et al.* Characterization of a novel tumor-suppressor gene PLC delta 1 at 3p22 in esophageal squamous cell carcinoma. *Cancer Res* **67**, 10720-10726 (2007). <https://doi.org/10.1158/0008-5472.CAN-07-2411>
- 76 Chen, J. *et al.* Differential expression of phospholipase C epsilon 1 is associated with chronic atrophic gastritis and gastric cancer. *PLoS One* **7**, e47563 (2012). <https://doi.org/10.1371/journal.pone.0047563>
- 77 Danielsen, S. A. *et al.* Phospholipase C isozymes are deregulated in colorectal cancer--insights gained from gene set enrichment analysis of the transcriptome. *PLoS One* **6**, e24419 (2011). <https://doi.org/10.1371/journal.pone.0024419>
- 78 Raghu, P., Joseph, A., Krishnan, H., Singh, P. & Saha, S. Phosphoinositides: Regulators of Nervous System Function in Health and Disease. *Front Mol Neurosci* **12**, 208 (2019). <https://doi.org/10.3389/fnmol.2019.00208>
- 79 Fukaya, M. *et al.* Predominant expression of phospholipase C β 1 in telencephalic principal neurons and cerebellar interneurons, and its close association with related signaling molecules in somatodendritic neuronal elements. *Eur J Neurosci* **28**, 1744-1759 (2008). <https://doi.org/10.1111/j.1460-9568.2008.06495.x>
- 80 Suh, P. G. *et al.* Multiple roles of phosphoinositide-specific phospholipase C isozymes. *BMB Rep* **41**, 415-434 (2008). <https://doi.org/10.5483/bmbrep.2008.41.6.415>
- 81 Kano, M. *et al.* Phospholipase c β 4 is specifically involved in climbing fiber synapse elimination in the developing cerebellum. *Proc Natl Acad Sci U S A* **95**, 15724-15729 (1998). <https://doi.org/10.1073/pnas.95.26.15724>
- 82 Miyoshi, M. A., Abe, K. & Emori, Y. IP(3) receptor type 3 and PLC β 2 are co-expressed with taste receptors T1R and T2R in rat taste bud cells. *Chem Senses* **26**, 259-265 (2001). <https://doi.org/10.1093/chemse/26.3.259>
- 83 Markó, K. *et al.* Isolation of radial glia-like neural stem cells from fetal and adult mouse forebrain via selective adhesion to a novel adhesive peptide-conjugate. *PLoS One* **6**, e28538 (2011). <https://doi.org/10.1371/journal.pone.0028538>
- 84 Follo, M. Y. *et al.* Inositide-Dependent Nuclear Signalling in Health and Disease. *Handb Exp Pharmacol* **259**, 291-308 (2020). https://doi.org/10.1007/164_2019_321
- 85 García del Caño, G. *et al.* Nuclear diacylglycerol lipase- α in rat brain cortical neurons: evidence of 2-arachidonoylglycerol production in concert with phospholipase C- β activity. *J Neurochem* **132**, 489-503 (2015). <https://doi.org/10.1111/jnc.12963>
- 86 Irvine, R. F. Nuclear lipid signalling. *Nat Rev Mol Cell Biol* **4**, 349-360 (2003). <https://doi.org/10.1038/nrm1100>

- 87 Montaña, M. *et al.* Cellular neurochemical characterization and subcellular localization of phospholipase C β 1 in rat brain. *Neuroscience* **222**, 239-268 (2012). <https://doi.org:10.1016/j.neuroscience.2012.06.039>
- 88 Rusciano, I. *et al.* Location-dependent role of phospholipase C signaling in the brain: Physiology and pathology. *Adv Biol Regul* **79**, 100771 (2021). <https://doi.org:10.1016/j.jbior.2020.100771>
- 89 Lo Vasco, V. R. Phosphoinositide pathway and the signal transduction network in neural development. *Neurosci Bull* **28**, 789-800 (2012). <https://doi.org:10.1007/s12264-012-1283-x>
- 90 Frebel, K. & Wiese, S. Signalling molecules essential for neuronal survival and differentiation. *Biochem Soc Trans* **34**, 1287-1290 (2006). <https://doi.org:10.1042/BST0341287>
- 91 Carey, M. B. & Matsumoto, S. G. Spontaneous calcium transients are required for neuronal differentiation of murine neural crest. *Dev Biol* **215**, 298-313 (1999). <https://doi.org:10.1006/dbio.1999.9433>
- 92 Hannan, A. J. *et al.* PLC-beta1, activated via mGluRs, mediates activity-dependent differentiation in cerebral cortex. *Nat Neurosci* **4**, 282-288 (2001). <https://doi.org:10.1038/85132>
- 93 Spires, T. L. *et al.* Activity-dependent regulation of synapse and dendritic spine morphology in developing barrel cortex requires phospholipase C-beta1 signalling. *Cereb Cortex* **15**, 385-393 (2005). <https://doi.org:10.1093/cercor/bhh141>
- 94 Yang, Y. R. *et al.* Primary phospholipase C and brain disorders. *Adv Biol Regul* **61**, 80-85 (2016). <https://doi.org:10.1016/j.jbior.2015.11.003>
- 95 Kurian, M. A. *et al.* Phospholipase C beta 1 deficiency is associated with early-onset epileptic encephalopathy. *Brain* **133**, 2964-2970 (2010). <https://doi.org:10.1093/brain/awq238>
- 96 Giralt, A. *et al.* Brain-derived neurotrophic factor modulates the severity of cognitive alterations induced by mutant huntingtin: involvement of phospholipaseCgamma activity and glutamate receptor expression. *Neuroscience* **158**, 1234-1250 (2009). <https://doi.org:10.1016/j.neuroscience.2008.11.024>
- 97 He, X. P., Pan, E., Sciarretta, C., Minichiello, L. & McNamara, J. O. Disruption of TrkB-mediated phospholipase Cgamma signaling inhibits limbic epileptogenesis. *J Neurosci* **30**, 6188-6196 (2010). <https://doi.org:10.1523/JNEUROSCI.5821-09.2010>
- 98 Rantamäki, T. *et al.* Pharmacologically diverse antidepressants rapidly activate brain-derived neurotrophic factor receptor TrkB and induce phospholipase-Cgamma signaling pathways in mouse brain. *Neuropsychopharmacology* **32**, 2152-2162 (2007). <https://doi.org:10.1038/sj.npp.1301345>
- 99 Lu, G. *et al.* Phospholipase C Beta 1: a Candidate Signature Gene for Proneural Subtype High-Grade Glioma. *Mol Neurobiol* **53**, 6511-6525 (2016). <https://doi.org:10.1007/s12035-015-9518-2>
- 100 Ramos, A. R., Elong Edimo, W. & Erneux, C. Phosphoinositide 5-phosphatase activities control cell motility in glioblastoma: Two phosphoinositides PI(4,5)P2 and PI(3,4)P2 are involved. *Adv Biol Regul* **67**, 40-48 (2018). <https://doi.org:10.1016/j.jbior.2017.09.001>

- 101 Khoshyomn, S. *et al.* Inhibition of phospholipase C-gamma1 activation blocks glioma cell motility and invasion of fetal rat brain aggregates. *Neurosurgery* **44**, 568-577; discussion 577-568 (1999). <https://doi.org:10.1097/00006123-199903000-00073>
- 102 Engebraaten, O., Bjerkvig, R., Pedersen, P. H. & Laerum, O. D. Effects of EGF, bFGF, NGF and PDGF(bb) on cell proliferative, migratory and invasive capacities of human brain-tumour biopsies in vitro. *Int J Cancer* **53**, 209-214 (1993). <https://doi.org:10.1002/ijc.2910530206>
- 103 Penar, P. L., Khoshyomn, S., Bhushan, A. & Tritton, T. R. Inhibition of glioma invasion of fetal brain aggregates. *In Vivo* **12**, 75-84 (1998).
- 104 Ratti, S. *et al.* Impact of phospholipase C β 1 in glioblastoma: a study on the main mechanisms of tumor aggressiveness. *Cell Mol Life Sci* **79**, 195 (2022). <https://doi.org:10.1007/s00018-022-04198-1>
- 105 Marvi, M. V. *et al.* Role of PLC γ 1 in the modulation of cell migration and cell invasion in glioblastoma. *Adv Biol Regul*, 100838 (2021). <https://doi.org:10.1016/j.jbior.2021.100838>
- 106 Gabusi, A. *et al.* Prognostic impact of intra-field heterogeneity in oral squamous cell carcinoma. *Virchows Arch* **476**, 585-595 (2020). <https://doi.org:10.1007/s00428-019-02656-z>
- 107 Afgan, E. *et al.* The Galaxy platform for accessible, reproducible and collaborative biomedical analyses: 2018 update. *Nucleic Acids Res* **46**, W537-W544 (2018). <https://doi.org:10.1093/nar/gky379>
- 108 Tresch, N. S. *et al.* Temozolomide is additive with cytotoxic effect of irradiation in canine glioma cell lines. *Vet Med Sci* (2021). <https://doi.org:10.1002/vms3.620>
- 109 Krainer, J. *et al.* EPIC-TABSAT: analysis tool for targeted bisulfite sequencing experiments and array-based methylation studies. *Nucleic Acids Res* **47**, W166-W170 (2019). <https://doi.org:10.1093/nar/gkz398>
- 110 Gritti, A. *et al.* Multipotential stem cells from the adult mouse brain proliferate and self-renew in response to basic fibroblast growth factor. *J Neurosci* **16**, 1091-1100 (1996).
- 111 Kucukural, A., Yukselen, O., Ozata, D. M., Moore, M. J. & Garber, M. DEBrowser: interactive differential expression analysis and visualization tool for count data. *BMC Genomics* **20**, 6 (2019). <https://doi.org:10.1186/s12864-018-5362-x>
- 112 Kuleshov, M. V. *et al.* Enrichr: a comprehensive gene set enrichment analysis web server 2016 update. *Nucleic Acids Res* **44**, W90-97 (2016). <https://doi.org:10.1093/nar/gkw377>
- 113 Lee, Y. R., Chen, M. & Pandolfi, P. P. The functions and regulation of the PTEN tumour suppressor: new modes and prospects. *Nat Rev Mol Cell Biol* **19**, 547-562 (2018). <https://doi.org:10.1038/s41580-018-0015-0>
- 114 Shankar, A. *et al.* Subcurative radiation significantly increases cell proliferation, invasion, and migration of primary glioblastoma multiforme in vivo. *Chin J Cancer* **33**, 148-158 (2014). <https://doi.org:10.5732/cjc.013.10095>
- 115 Medici, D., Hay, E. D. & Olsen, B. R. Snail and Slug promote epithelial-mesenchymal transition through beta-catenin-T-cell factor-4-dependent expression of transforming growth factor-beta3. *Mol Biol Cell* **19**, 4875-4887 (2008). <https://doi.org:10.1091/mbc.e08-05-0506>

- 116 Gladson, C. L. The extracellular matrix of gliomas: modulation of cell function. *J Neuropathol Exp Neurol* **58**, 1029-1040 (1999). <https://doi.org:10.1097/00005072-199910000-00001>
- 117 Wang, M., Wang, T., Liu, S., Yoshida, D. & Teramoto, A. The expression of matrix metalloproteinase-2 and -9 in human gliomas of different pathological grades. *Brain Tumor Pathol* **20**, 65-72 (2003). <https://doi.org:10.1007/BF02483449>
- 118 Forsyth, P. A. *et al.* Gelatinase-A (MMP-2), gelatinase-B (MMP-9) and membrane type matrix metalloproteinase-1 (MT1-MMP) are involved in different aspects of the pathophysiology of malignant gliomas. *Br J Cancer* **79**, 1828-1835 (1999). <https://doi.org:10.1038/sj.bjc.6690291>
- 119 Nager, M. *et al.* β -Catenin Signalling in Glioblastoma Multiforme and Glioma-Initiating Cells. *Chemother Res Pract* **2012**, 192362 (2012). <https://doi.org:10.1155/2012/192362>
- 120 Mehta, S. & Lo Cascio, C. Developmentally regulated signaling pathways in glioma invasion. *Cell Mol Life Sci* **75**, 385-402 (2018). <https://doi.org:10.1007/s00018-017-2608-8>
- 121 Ramaswamy, P., Nanjiah, N. D. & Borkotokey, M. Role of MEK-ERK signaling mediated adhesion of glioma cells to extra-cellular matrix: Possible implication on migration and proliferation. *Ann Neurosci* **26**, 52-56 (2019). <https://doi.org:10.5214/ans.0972.7531.260203>
- 122 Park, J. *et al.* STAT3 is a key molecule in the oncogenic behavior of diffuse intrinsic pontine glioma. *Oncol Lett* **20**, 1989-1998 (2020). <https://doi.org:10.3892/ol.2020.11699>
- 123 Wirsching, H. G., Galanis, E. & Weller, M. Glioblastoma. *Handb Clin Neurol* **134**, 381-397 (2016). <https://doi.org:10.1016/B978-0-12-802997-8.00023-2>
- 124 Gargini, R. *et al.* The IDH-TAU-EGFR triad defines the neovascular landscape of diffuse gliomas. *Sci Transl Med* **12** (2020). <https://doi.org:10.1126/scitranslmed.aax1501>
- 125 Carlsson, E. *et al.* Neuron navigator 3 alterations in nervous system tumors associate with tumor malignancy grade and prognosis. *Genes Chromosomes Cancer* **52**, 191-201 (2013). <https://doi.org:10.1002/gcc.22019>
- 126 Mills, B. N., Albert, G. P. & Halterman, M. W. Expression Profiling of the MAP Kinase Phosphatase Family Reveals a Role for DUSP1 in the Glioblastoma Stem Cell Niche. *Cancer Microenviron* **10**, 57-68 (2017). <https://doi.org:10.1007/s12307-017-0197-6>
- 127 Liu, C. A. *et al.* Migration/Invasion of Malignant Gliomas and Implications for Therapeutic Treatment. *Int J Mol Sci* **19** (2018). <https://doi.org:10.3390/ijms19041115>
- 128 Shin, K. J. *et al.* Phospholipase C γ 1 represses colorectal cancer growth by inhibiting the Wnt/ β -catenin signaling axis. *Biochem Biophys Res Commun* **577**, 103-109 (2021). <https://doi.org:10.1016/j.bbrc.2021.09.012>
- 129 Behjati, S. *et al.* Recurrent PTPRB and PLCG1 mutations in angiosarcoma. *Nat Genet* **46**, 376-379 (2014). <https://doi.org:10.1038/ng.2921>
- 130 Xie, Z. *et al.* Phospholipase C-gamma1 is required for the epidermal growth factor receptor-induced squamous cell carcinoma cell mitogenesis. *Biochem Biophys Res Commun* **397**, 296-300 (2010). <https://doi.org:10.1016/j.bbrc.2010.05.103>

- 131 Li, X. *et al.* NF-kappaB and Hsp70 are involved in the phospholipase Cgamma1 signaling pathway in colorectal cancer cells. *Life Sci* **77**, 2794-2803 (2005). <https://doi.org:10.1016/j.lfs.2005.05.025>
- 132 Piperigkou, Z., Kyriakopoulou, K., Koutsakis, C., Mastronikolis, S. & Karamanos, N. K. Key Matrix Remodeling Enzymes: Functions and Targeting in Cancer. *Cancers (Basel)* **13** (2021). <https://doi.org:10.3390/cancers13061441>
- 133 Jin, Q. *et al.* Gene expression profiling reveals Ki-67 associated proliferation signature in human glioblastoma. *Chin Med J (Engl)* **124**, 2584-2588 (2011).
- 134 Saini, K. S. *et al.* Targeting the PI3K/AKT/mTOR and Raf/MEK/ERK pathways in the treatment of breast cancer. *Cancer Treat Rev* **39**, 935-946 (2013). <https://doi.org:10.1016/j.ctrv.2013.03.009>
- 135 Ji, H. *et al.* EGF-induced ERK activation promotes CK2-mediated disassociation of alpha-Catenin from beta-Catenin and transactivation of beta-Catenin. *Mol Cell* **36**, 547-559 (2009). <https://doi.org:10.1016/j.molcel.2009.09.034>
- 136 Zolezzi, J. M. *et al.* PPARs in the central nervous system: roles in neurodegeneration and neuroinflammation. *Biol Rev Camb Philos Soc* **92**, 2046-2069 (2017). <https://doi.org:10.1111/brv.12320>
- 137 Vallée, A. & Lecarpentier, Y. Crosstalk Between Peroxisome Proliferator-Activated Receptor Gamma and the Canonical WNT/ β -Catenin Pathway in Chronic Inflammation and Oxidative Stress During Carcinogenesis. *Front Immunol* **9**, 745 (2018). <https://doi.org:10.3389/fimmu.2018.00745>
- 138 Xie, B. *et al.* Dual blockage of STAT3 and ERK1/2 eliminates radioresistant GBM cells. *Redox Biol* **24**, 101189 (2019). <https://doi.org:10.1016/j.redox.2019.101189>
- 139 Zepecki, J. P. *et al.* Regulation of human glioma cell migration, tumor growth, and stemness gene expression using a Lck targeted inhibitor. *Oncogene* **38**, 1734-1750 (2019). <https://doi.org:10.1038/s41388-018-0546-z>